

International Doctorate Program in Molecular
Oncology and Endocrinology
Doctorate School in Molecular Medicine

XXII cycle - 2006–2009
Coordinator: Prof. Giancarlo Vecchio

“The CBX7 protein, whose expression is decreased in human carcinomas, positively regulates E-cadherin expression by interacting with the HDAC2 protein.”

Mimma Bianco

University of Naples Federico II
Dipartimento di Biologia e Patologia Cellulare e Molecolare
“L. Califano”

Administrative Location

Dipartimento di Biologia e Patologia Cellulare e Molecolare “L. Califano”
Università degli Studi di Napoli Federico II

Partner Institutions

Italian Institutions

Università degli Studi di Napoli “Federico II”, Naples, Italy
Istituto di Endocrinologia ed Oncologia Sperimentale “G. Salvatore”, CNR, Naples, Italy
Seconda Università di Napoli, Naples, Italy
Università degli Studi di Napoli “Parthenope”, Naples, Italy
Università del Sannio, Benevento, Italy
Università di Genova, Genoa, Italy
Università di Padova, Padua, Italy
Università degli Studi “Magna Graecia”, Catanzaro, Italy
Università degli Studi di Firenze, Florence, Italy
Università degli Studi di Bologna, Bologna, Italy
Università degli Studi del Molise, Campobasso, Italy
Università degli Studi di Torino, Turin, Italy
Università di Udine, Udine, Italy

Foreign Institutions

Université Libre de Bruxelles, Brussels, Belgium
Universidade Federal de Sao Paulo, Brazil
University of Turku, Turku, Finland
Université Paris Sud XI, Paris, France
University of Madras, Chennai, India
University Pavol Jozef Šafárik, Kosice, Slovakia
Universidad Autonoma de Madrid, Centro de Investigaciones Oncologicas (CNIO), Spain
Johns Hopkins School of Medicine, Baltimore, MD, USA
Johns Hopkins Krieger School of Arts and Sciences, Baltimore, MD, USA
National Institutes of Health, Bethesda, MD, USA
Ohio State University, Columbus, OH, USA
Albert Einstein College of Medicine of Yeshiwa University, N.Y., USA

Supporting Institutions

Ministero dell’Università e della Ricerca
Associazione Leonardo di Capua, Naples, Italy
Dipartimento di Biologia e Patologia Cellulare e Molecolare “L. Califano”, Università degli Studi di Napoli “Federico II”, Naples, Italy
Istituto Superiore di Oncologia (ISO), Genoa, Italy
Università Italo-Francese, Torino, Naples, Italy
Università degli Studi di Udine, Udine, Italy
Agenzia Spaziale Italiana
Istituto di Endocrinologia ed Oncologia Sperimentale “G. Salvatore”, CNR, Naples, Italy

Italian Faculty

Giancarlo Vecchio, MD, Co-ordinator
Salvatore Maria Aloj, MD
Francesco Saverio Ambesi Impiombato, MD
Francesco Beguinot, MD
Maria Teresa Berlingieri, MD
Angelo Raffaele Bianco, MD
Bernadette Biondi, MD
Francesca Carlomagno, MD
Gabriella Castoria, MD
Angela Celetti, MD
Mario Chiariello, MD
Lorenzo Chiariotti, MD
Vincenzo Ciminale, MD
Annamaria Cirafici, PhD
Annamaria Colao, MD
Alma Contegiacomo, MD
Sabino De Placido, MD
Gabriella De Vita, MD
Monica Fedele, PhD
Pietro Formisano, MD
Alfredo Fusco, MD
Michele Grieco, MD
Massimo Imbriaco, MD
Paolo Laccetti, PhD
Antonio Leonardi, MD
Paolo Emidio Macchia, MD
Barbara Majello, PhD
Rosa Marina Melillo, MD
Claudia Miele, PhD
Francesco Oriente, MD
Roberto Pacelli, MD
Giuseppe Palumbo, PhD
Silvio Parodi, MD
Nicola Perrotti, MD
Giuseppe Portella, MD
Giorgio Punzo, MD
Antonio Rosato, MD
Guido Rossi, MD
Giuliana Salvatore, MD
Massimo Santoro, MD
Giampaolo Tortora, MD
Donatella Tramontano, PhD
Giancarlo Troncone, MD
Giuseppe Viglietto, MD
Roberta Visconti, MD
Mario Vitale, MD

Foreign Faculty

Université Libre de Bruxelles, Belgium

Gilbert Vassart, MD
Jacques E. Dumont, MD

Universidade Federal de Sao Paulo, Brazil

Janete Maria Cerutti, PhD
Rui Monteiro de Barros Maciel, MD PhD

University of Turku, Turku, Finland

Mikko Laukkanen, PhD

Université Paris Sud XI, Paris, France

Martin Schlumberger, MD
Jean Michel Bidart, MD

University of Madras, Chennai, India

Arasambattu K. Munirajan, PhD

University Pavol Jozef Šafàrik, Kosice, Slovakia

Eva Cellárová, PhD
Peter Fedoročko, PhD

Universidad Autonoma de Madrid - Instituto de Investigaciones Biomedicas, Spain

Juan Bernal, MD, PhD
Pilar Santisteban, PhD

Centro de Investigaciones Oncologicas, Spain

Mariano Barbacid, MD

Johns Hopkins School of Medicine, USA

Vincenzo Casolaro, MD
Pierre A. Coulombe, PhD
James G. Herman MD
Robert P. Schleimer, PhD

Johns Hopkins Krieger School of Arts and Sciences, USA

Eaton E. Lattman, MD

National Institutes of Health, Bethesda, MD, USA

Michael M. Gottesman, MD
J. Silvio Gutkind, PhD

Genoveffa Franchini, MD
Stephen J. Marx, MD
Ira Pastan, MD
Phillip Gorden, MD

Ohio State University, Columbus, OH, USA

Carlo M. Croce, MD
Ginny L. Bumgardner, MD PhD

Albert Einstein College of Medicine of Yeshiwa University, N.Y., USA

Luciano D'Adamio, MD
Nancy Carrasco, MD

“The CBX7 protein, whose expression is decreased in human carcinomas, positively regulates E-cadherin expression by interacting with the HDAC2 protein.”

TABLE OF CONTENTS

LIST OF PUBLICATIONS.....	4
ABSTRACT	5
1. BACKGROUND	6
1.1 CBX7 and thyroid carcinogenesis.....	6
1.2 CBX7, a novel Polycomb protein	7
1.3 CBX7 and Polycomb Group proteins	10
1.4 Epithelial–Mesenchymal Transition	12
1.5 E-cadherin	15
1.5.1 <i>E-cadherin implication in tumor progression.....</i>	<i>18</i>
1.5.2 <i>Mechanisms of E-cadherin repression: potential co-operation with epigenetic modifications.....</i>	<i>20</i>
1.6 Epigenetic control of gene expression	22
2. AIMS OF THE STUDY.....	24
3. MATERIALS AND METHODS	25
3.1 Cell culture and transfections.....	25
3.2 Plasmid constructs.....	25
3.3 Protein extraction	26
3.4 Western blotting and immunoprecipitation assay	27
3.5 Samples preparation and immunoprecipitation for proteomic assay	27
3.6 Electrophoresis fractionation and in situ digestion	28
3.7 Liquid Chromatography/Mass Spectrometry/Mass Spectrometry (LCMSMS) analysis	28
3.8 Expression and purification of recombinant proteins/GST pull-down experiments	28
3.9 HDAC activity assay.....	29
3.10 Chromatin immunoprecipitation (ChIP) and Re-ChIP assays	29
3.11 Electrophoretic mobility shift assay (EMSA) and supershift assay.....	30
3.12 ImmunoFRET	31
3.13 Transactivation assay	32
3.14 DNA extraction and methylation analysis	32
3.15 Fresh human thyroid tissue samples	33

3.16 RNA extraction, reverse transcription, and PCR analysis	33
3.17 Selection of primers, probes and qRT-PCR.....	33
3.18 Immunohistochemistry.....	34
3.19 Statistical analysis	35
4. RESULTS AND DISCUSSION	36
4.1 Proteomic analysis of CBX7 interacting proteins.....	36
4.2 <i>In vitro</i> characterization of CBX7 and HDAC2 interaction	38
4.3 CBX7 physically interacts with HDAC2 protein.....	38
4.4 CBX7 inhibits HDAC activity	39
4.5 CBX7 and HDAC activity in tumors	41
4.6 CBX7 binds to the E-cadherin gene promoter	42
4.7 CBX7 occupies the <i>E-cadherin</i> promoter with HDAC2.....	44
4.8 CBX7 colocalize with HDAC2.....	44
4.9 CBX7 positively regulates the <i>E-cadherin</i> promoter.....	45
4.10 CBX7 expression results in increased histone acetylation of the E-cadherin promoter	48
4.11 Increased methylation of H3K4 and decreased methylation of H3K9 and H4K20 in CBX7-transfected cells.....	50
4.12 CBX7 and E-cadherin expression levels are correlated in human thyroid carcinomas.....	51
5. CONCLUSIONS	53
7. REFERENCES.....	55
8. Table CBX7 interacting proteins.	

LIST OF PUBLICATIONS

This dissertation is based upon the following publications:

Chromobox Protein Homologue 7 Protein, with Decreased Expression in Human Carcinomas, Positively Regulates E-Cadherin Expression by Interacting with the Histone Deacetylase 2 Protein. Federico A, Pallante P, Bianco M, Ferraro A, Esposito F, Monti M, Cozzolino M, Keller S, Fedele M, Leone V, Troncone G, Chiariotti L, Pucci P, Fusco A. *Cancer Res.* 2009 Sep 1;69(17):7079-87.

Loss of the CBX7 gene expression correlates with a highly malignant phenotype in thyroid cancer. Pallante P, Federico A, Berlingieri MT, Bianco M, Ferraro A, Forzati F, Iaccarino A, Russo M, Pierantoni GM, Leone V, Sacchetti S, Troncone G, Santoro M, Fusco A. *Cancer Res.* 2008 Aug 15;68(16):6770-8.

UbcH10 is overexpressed in malignant breast carcinomas. Berlingieri MT, Pallante P, Sboner A, Barbareschi M, Bianco M, Ferraro A, Mansueto G, Borbone E, Guerriero E, Troncone G, Fusco A. *Eur J Cancer.* 2007 Dec;43(18):2729-35.

ABSTRACT

CBX7, chromobox homolog 7, is a chromobox family protein encoding a novel Polycomb protein, component of the Polycomb repressive complex 1 (PRC1). The Polycomb group (PcG) proteins are epigenetic transcriptional repressors involved in the control of cellular proliferation and oncogenesis. CBX7 protein levels show a progressive reduction, well related with the malignant grade of the thyroid neoplasias. Indeed, its expression decreased in an increasing percentage of cases going from benign adenomas to papillary, follicular and anaplastic thyroid carcinomas.

To elucidate the function of CBX7 in carcinogenesis, we searched for CBX7 interacting proteins by a proteomic analysis. By this approach, we identified several proteins among which we selected Histone Deacetylase 2 (HDAC2) that is well known to play a key role in neoplastic cell transformation and to downregulate E-cadherin expression, whose loss is a critical event in the Epithelial-Mesenchymal Transition, and therefore emerging as one of the caretakers of the epithelial phenotype.

We confirmed by co-immunoprecipitation that CBX7 physically interacts with the HDAC2 and demonstrated that is able to inhibit its activity. Then, we showed that both these proteins bind the *E-cadherin* promoter, and that CBX7 is able to upregulate E-cadherin expression. Consistent with these data we found a positive statistical correlation between CBX7 and E-cadherin expression in human thyroid carcinomas. Finally, we demonstrated that the expression of CBX7 increases the acetylation status of the histones H3 and H4 on the *E-cadherin* promoter. Therefore, the ability of CBX7 to positively regulate E-cadherin expression, by interacting with HDAC2 and inhibiting its activity on the *E-cadherin* promoter, would account for the correlation between the loss of CBX7 expression and a highly malignant phenotype in thyroid cancer patients. Thus, several important interacting proteins of CBX7 and the pathways in which they are involved strongly suggest that CBX7 can be considered a very important regulator of thyroid malignant transformation.

1. BACKGROUND

1.1 CBX7 and thyroid carcinogenesis.

The thyroid gland is the largest endocrine organ in humans (Kondo et al. 2006) and regulates systemic metabolism through thyroid hormones. It is located in the neck region, on the anterior surface of the trachea, and is formed by two distinct cell types, the follicular cells and the parafollicular or C cells (De Felice and Di Lauro 2004). However, more than 95% of thyroid carcinomas are derived from follicular cells (Kondo et al. 2006) and are the most common endocrine malignancies, with an estimated 25000 new cases diagnosed annually in the United States. Conversely, only 3% of thyroid tumors, referred to as medullary thyroid carcinoma, are of parafollicular origin. Thyroid tumors result from the accumulation of different modifications in critical genes involved in the control of cell proliferation. Thyroid neoplasms represent a good model for studying the events involved in epithelial cell multistep carcinogenesis, because they comprise a broad spectrum of lesions with different degrees of malignancy, which are diagnosed on the basis of histological and clinical parameters. In fact, follicular cell-derived thyroid tumors include: 1) benign adenomas, which are not invasive and very well differentiated; 2) carcinomas, which are divided into well-differentiated, poorly differentiated (PDCT) and undifferentiated (ATC). Well-differentiated thyroid carcinomas are papillary (PTC) that represent more than 70% of thyroid malignant tumors and follicular (FTC) that represent 10% of thyroid carcinomas. These tumors, being differentiated, have a good prognosis (Kondo et al. 2006; Saltman et al. 2006). PDTC and ATC seem to derive from the progression of differentiated carcinomas (Van der Laan et al. 1993). Although the ATC represent 2-5% of thyroid malignant tumors, they are one of the most lethal human neoplasms being rapidly-growing, very aggressive and always fatal. Finally, PDTC, representing 7% of thyroid carcinomas, are morphologically and behaviourally intermediate between well-differentiated and undifferentiated thyroid carcinomas. Although various therapeutic approaches are followed in clinical practice, most of them are not life-saving. Hence, the discovery of new approach to diagnose cancer at an early stage and to establish more effective therapies is a critical and urgent issue. To achieve this goal, identification and characterization of key molecules that participate in carcinogenesis are essential steps.

Microarray studies are widely used to define diagnostic and prognostic signatures in cancers and they have led to the identification of a large list of carcinoma-regulated genes also in thyroid cancers (Delys et al. 2007). To identify the genes involved in the process of thyroid carcinogenesis we analysed the gene expression profiles using an Affymetrix HG_U95Av2 oligonucleotide array. This study led to the identification of genes whose expression was up- or down-regulated in the carcinoma cell lines compared

with the primary cell culture of normal thyroid origin, assuming that the genes altered in their expression in all of the thyroid carcinoma cell lines might represent candidate genes involved in thyroid cell transformation (Pallante et al. 2005). Among the down-regulated genes, we identified CBX7 that resulted down-regulated about 20 fold in all the carcinoma cell lines analysed and that could be actively involved in the process of thyroid carcinogenesis. CBX7 is a chromobox family protein encoding a novel polycomb protein and its expression shows a progressive reduction, well related with the malignant grade of the thyroid neoplasias. Indeed, CBX7 protein levels decreased in an increasing percentage of cases going from benign adenomas to PTC, FTC, ATC. Moreover, correlation between low CBX7 expression and a more aggressive histotype seems to apply also to breast, ovary, and lung carcinomas and seems to reduce survival in colon carcinoma (Pallante et al. 2008).

1.2 CBX7, a novel Polycomb protein.

CBX7, which is located on chromosome 22q13.1, encodes a novel Polycomb protein (Pc) of 28.4 kDa and 251 amino acids that contains a highly conserved "chromodomain" (**chromatin organisation modifier**, CD) at N-terminal, between amino acids 10 and 46. This domain was originally identified in *Drosophila melanogaster* as a 37-amino-acid region of homology shared by heterochromatin protein 1 (HP1) and Pc proteins (Paro and Hogness 1991). Phylogenetic and sequence analyses of the chromodomain (figure 1A and B) revealed that CBX7 has a great similarity to other known or putative Pc proteins like CBX2 (Pc1), CBX4 (Pc2), CBX6 and CBX8 (Pc3). This similarity is less pronounced respect to the HP1 proteins, such as CBX1 (HP1 β), CBX3 (HP1 γ), CBX5 (HP1 α) and, moreover, CBX7 does not contain the "chromo-shadow domain" that, instead, is a hallmark of HP1 proteins.

Despite a high degree of conservation, the CD display significant differences in binding histone H3 modification. Not all CDs in fact bind preferentially to trimethylated Lys 27 on histone H3 (H3K27me₃); rather, some (Cbx2 and Cbx7) display affinity towards both histone H3 tri-methylated at K9 (H3K9me₃) and H3K27me₃, one (Cbx4) binds K9me₃ and some (Cbx6 and Cbx8) do not bind significantly to either modification suggesting that these CDs may bind to another methylation site not yet identified or tested (Bernstein et al. 2006). CBX7, in particular, displays strong affinity for both H3K9me₃ and H3K27me₃ and is developmentally regulated in its association with chromatin. CBX7 chromodomain contains Pc-specific residues that have been shown to be necessary both for Pc dimerization and recognition of H3K27me₃ (Min et al. 2003). In addition to the high homology within the CD, CBX7 has also homology to Pc proteins in a carboxy-terminal region (figure 1C) previously defined as the Pc box or C-box (Jones et al. 2000).

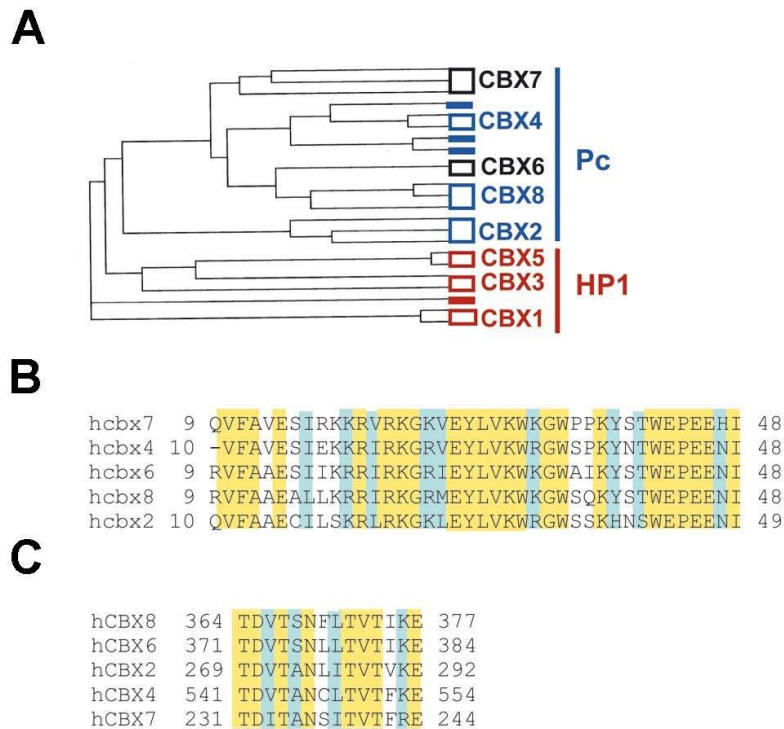


Figure 1. Identification of CBX7 as a Polycomb protein. A) Phylogenetic analysis of Chromobox (CBX) proteins. Lines grouped by open rectangles denote orthologs of a same CBX protein (name in the right). Full rectangles refer to proteins that cannot be considered purely orthologs of any of the CBX proteins. Pc proteins are shown in blue, and HP1 proteins in red. CBX7 and CBX6 are shown in black. **B)** Alignment of CBX7 chromodomain with that of other known and putative human Polycombs. Identical residues are shown in a yellow background, and similar residues are shown in a cyan background. **C)** Alignment of CBX7 Polycomb box with that of other known and putative human Polycombs. Background colours are as described in *B* (from Gil et al. 2004).

It is known that the Pc box (aminoacids 231–243) and the CD (Jones et al. 2000) are both necessary for CBX7 function. It was seen that a fusion protein between CBX7 and the DNA-binding domain of Gal4 is able to repress in a dose dependent manner, the transcription over a 4xGal4-tk-luc reporter, suggesting that CBX7 functions by repressing transcription (Gil et al. 2004). So, CBX7 seems to act like the others Pc proteins exerting its effect through transcriptional repression.

Mouse Cbx7 is, moreover, able to associate with facultative heterochromatin and with the inactive X chromosome, which indicates that CBX7 is really

involved in the repression of gene transcription (Bernstein et al. 2006). It has also been found *in vitro* that the CD of CBX7 can bind RNA and that, *in vivo*, the interaction of CBX7 with chromatin, and in particular with the inactive X chromosome, partially depends on its association with RNA (Bernstein et al. 2006). These data suggest that the capacity of this mouse Polycomb homolog to associate with the inactive X chromosome, or any other region of chromatin, depends not only on its chromodomain but also on the combination of histone modifications and RNA molecules present at its target sites (Bernstein et al. 2006). CBX7 has also been shown to initiate lymphomagenesis and cooperate with c-myc in tumor progression *in vivo* (Scott et al. 2007). Analysis of the CBX7 chromodomain showed that this protein can associate with repressive histone modifications, including dimethylated and trimethylated H3K9, as well as trimethylated H3K27 (Bernstein et al. 2006) suggesting that a CBX7-containing complex may possess the ability to read histone modifications found in promoters of key genes, including those susceptible to cancer-specific DNA methylation.

CBX7 is also capable to interact with different Pc group members. In fact, similarly to other Pc proteins, CBX7 is able to inter-functions with itself and with the ring-finger protein Ring1 (Gil et al. 2004), as reported by the mean of Glutathione S-transferase (GST) pull-down experiments (Satijn et al. 1997, Satijn and Otte 1999). In addition, within the nucleus, CBX7 co-localizes with Ring1 to distinct foci-like structures termed Pc-bodies as demonstrated, in several cell lines, with immunofluorescence microscopy studies (Saurin et al. 1998). However there is not association between CBX7 and other PcG proteins, such as Bmi1, EED or EHZ2 (Gil et al. 2004) so this let think that CBX7 is part of different complexes than Bmi1 and Pc2.

CBX7 is highly expressed in a number of different normal tissue types, including brain, kidney, heart and skeletal muscle and recent studies suggest that may play an important role in tumorigenesis. CBX7 was identified in a functional screen for genes involved in senescence bypass, at least partially via repression of expression of the tumor suppressor gene, p16, extending cellular life span in mouse embryonic fibroblasts and human prostate primary epithelial cell (Gil et al. 2004, Bernard et al. 2005).

However, another study on ependymoma (Suarez-Merino et al. 2005) reported a consistent down-regulation of CBX7 in the tumor samples, in fact in this study is suggested the presence of a microdeletion at this site of 22q. The abnormal expression of CBX7 was due to allelic loss in 55% of cases, where underexpression was due to loss of one allele in 46% of cases and both alleles in 9% of cases. Moreover, none sequence alteration of the CBX7 coding region was identified, suggesting that other mechanisms, such as promoter methylation or histone deacetylation, may be responsible for the silencing of this gene in ependymoma samples. Also in thyroid carcinomas was detected LOH in 36.8% of PTC and 68.7% of ATC and no mutations were found (Pallante et al. 2008). Therefore, other epigenetic mechanisms associated with

an allelic loss might account for the reduced CBX7 expression in human thyroid carcinomas.

1.3 CBX7 and Polycomb Group proteins.

CBX7 is a part of the Polycomb Group proteins (PcG) (Gil et al. 2006). PcG, so named because of mutations that affect the patterning of the male sex combs in *Drosophila*, are transcriptional repressors that participate in distinct multiprotein complexes, the best characterized being Polycomb repressive complexes 1 and 2 (PRC1 and PRC2) (Sparmann and van Lohuizen 2006, Schwartz and Pirrotta 2007). The PRC2 complex has associated histone deacetylase and histone methyl transferase activities specific for lysine of Histone H3, H3K27, thus contributing to the establishment of histone repressive marks (Kuzmichev et al. 2002, Kirmizis et al. 2007). Between the known mammalian components of this complex are Enhancer of Zeste (EZH2), Early embryonic deficient (EED), Suppressor of Zeste (SUZ12) and other associated proteins. The prototypic PRC1 complex comprises stoichiometric amounts of Polycomb (Pc), Posterior sex comb (Psc), Polyhomeotic (Ph) and Sex combs extra (Sce) (Shao et al. 1999, Saurin et al. 2001). PRC1 binds to the H3K27me3 mark via the chromodomain of the Pc protein (Fischle et al. 2003, Bernstein et al. 2006) and catalyzes the mono-ubiquitylation of histone H2A on lysine 119, thereby shutting down transcription (Wang et al. 2004, Cao et al. 2005, Sparmann and van Lohuizen 2006).

In mammalian cells, the formation of this complex is complicated by the presence of multiple orthologs of the archetypal PRC1 proteins. With five Pc proteins (CBX2, CBX4, CBX6, CBX7 and CBX8), six Psc proteins (BMI1, MEL18, MBLR, NSPC1, RNF159 and RNF3), three Ph proteins (HPH1, HPH2 and HPH3) and two Sce proteins (RING1 and RING2). There is enormous diversity for combinatorial association between these proteins (Gil and Peters 2006, Whitcomb et al. 2007) (figure 2). The reasons for such diversification and the interplay between the different family members remain unclear. Genetic ablation of specific PcG genes in mice has confirmed their role in embryonic patterning and *Hox* gene regulation but also pointed to more general effects on stem cell function. For example, *Bmi-1* null mice have hematological and neurological defects that are traceable to a failure in the self-renewal of the relevant stem cells (Lessard and Sauvageau 2003, Park et al. 2003).

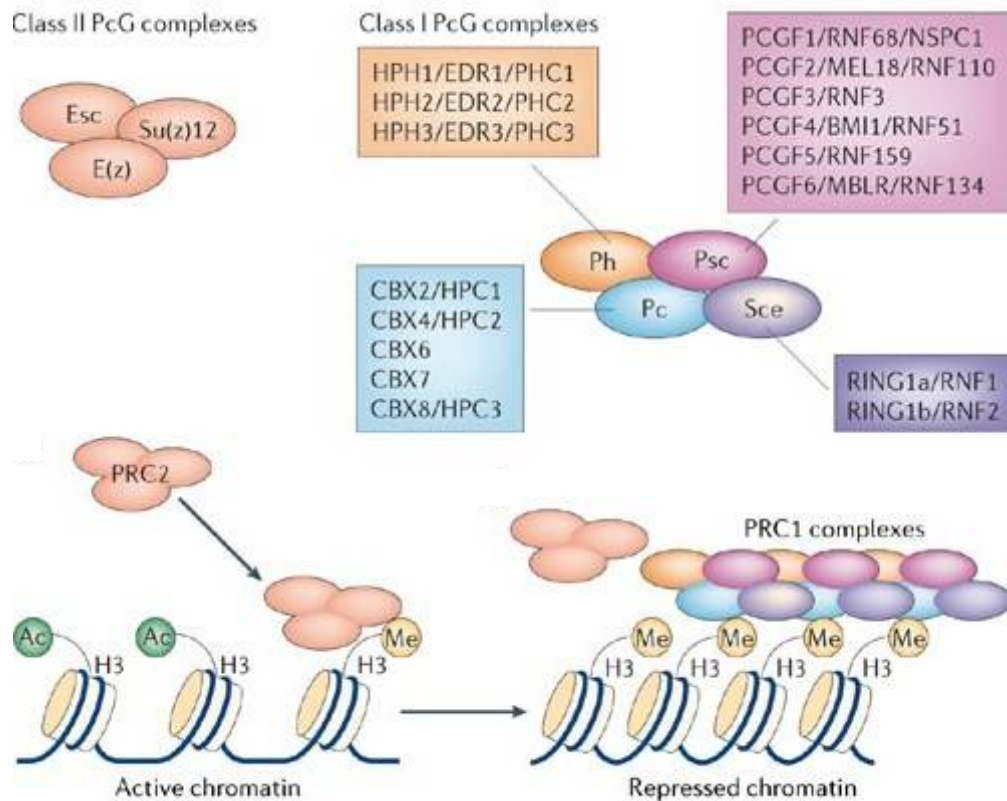


Figure 2. Transcriptional repression by the Polycomb group proteins. The PRC2 complex, comprising Ezh2, Eed and Su(z)12, binds to Polycomb responsive elements (PRE) and establishes epigenetic marks in chromatin by tri-methylating histone H3 on lysine 27 (H3K27). This mark is recognised by the PRC1 complex, which mono-ubiquitylates histone H2A on lysine 119, leading to transcriptional repression. Whereas the PRC1 complex in *Drosophila* comprises stoichiometric amounts of Pc, Psc, Ph and Sce, there are multiple orthologues of these proteins in mammalian cells, as indicated in the coloured boxes. (Gil et al. 2006).

More recently, genome-wide ChIP analyses have identified over 1000 genes that are potential targets of PcG-mediated repression, many of which are implicated in the maintenance of pluripotency (Bracken et al. 2006, Tolhuis et al. 2006). Evidence is rapidly increasing that PcG genes are a novel class of oncogenes and anti-oncogenes, which may in future years become central to the development of novel cancer therapies based on epigenetic gene silencing (Nakao et al. 2004, Egger et al. 2004). Not only PcG genes such as BMI-1 and EZH2 are capable of cellular transformation, but are also essential for cell survival. To date, abnormal PcG genes expression has been described in most human cancers. Moreover, the correlation between PcG expression and biological behavior of clinically defined cancer subtypes suggests that these

genes play a central role in oncogenesis, and holds a promise for discovery of novel diagnostic markers (Raaphorst et al. 2004). Recent studies have shown that a large group of genes silenced in association with aberrant promoter DNA hypermethylation in cancer are frequent targets of the PcG repressive complexes in normal and neoplastic embryonic cells (Ohm et al. 2007; Schlesinger et al. 2007). These studies suggest a stem cell origin for cancer in which silencing of genes in adult cancer are linked to the epigenetic control of stem/precursor cell gene expression patterns regulated by PcG proteins. However, a direct link has not yet been established.

CBX7, constituent of the PRC1 complex, has a direct association with gene repression and promoter DNA hypermethylation of genes frequently silenced in cancer (Mohammad et al. 2009). CBX7, in fact, is able to complex with DNA methyltransferase (DNMT) enzymes, which led to explore a role for CBX7 in maintenance and initiation of gene silencing. Knock-down of CBX7 was unable to relieve suppression of deeply silenced genes in cancer cells; however, in embryonal carcinoma (EC) cells, CBX7 can initiate stable repression of genes that are frequently silenced in adult cancers. Furthermore, it was observed the assembly of DNMTs at CBX7 target gene promoters. Sustained expression of CBX7 in EC cells confers a growth advantage and resistance to retinoic acid-induced differentiation. In this setting, especially, there is increased promoter DNA hypermethylation for many genes. Indeed, DNA methylation is another well studied epigenetic mechanism. Methylation at the C-5 position of cytosine residues present in CpG dinucleotides by DNA methyltransferases (DNMTs) is generally considered to facilitate static long-term gene silencing (Lund and van Lohuizen, 2004). Therefore CBX7 promote the initiation of epigenetic changes involving abnormal DNA hypermethylation of genes frequently silenced in adult cancers (Mohammad et al. 2009).

To elucidate the function of CBX7 in carcinogenesis, we searched for CBX7 interacting proteins by a proteomic analysis. By this approach, we identified several proteins among which we selected Histone Deacetylase 2 (HDAC2) that is well known to play a key role in neoplastic cell transformation and to downregulate E-cadherin expression, whose loss is a critical event in the Epithelial-Mesenchymal Transition.

1.4 Epithelial–Mesenchymal Transition.

Epithelial–Mesenchymal Transition (EMT) is an indispensable morphogenetic process which allows tissues and organs formation involving cell migration (Thiery and Sleeman 2006). This phenotypic change is known to take place, for example, in gastrulation, neural crest cell migration, and heart formation (Savagner 2001). EMT can be distinguished on the basis of morphological criteria including the loss of epithelial polarization and the acquisition of a flattened and elongated cell shape (Hay 1995). Cells that dissociate from primitive embryonic epithelia during tissue patterning often convert to a

migrating, mesenchymal cell type. Crucial to the EMT process is the down-regulation of cell-cell contacts, most notably E-cadherin-based adhesion (Savagner 2001). Epithelial and mesenchymal cells differ in various functional and phenotypic characteristics. Epithelial cells grow in layers and communicate through specialized membrane structures, such as tight junctions, adherens junctions, desmosomes and gap junctions. Epithelial cells are motile and can move away from their nearest neighbours, while remaining within the epithelial layer (Schock and Perrimon 2002). Mesenchymal cells, on the other hand, do not form an organized cell layer, nor do they have the same apical–basolateral organization and polarization of the cell-surface molecules and the actin cytoskeleton as epithelial cells.

Epithelial cells can convert into mesenchymal cells by a process known as the EMT. The precise spectrum of changes that occur during EMT is probably determined by the integration of extracellular signals that the cell receives, although this is still unclear. It has also been reported the reverse process, known as mesenchymal-epithelial transition (MET) (figure 3).

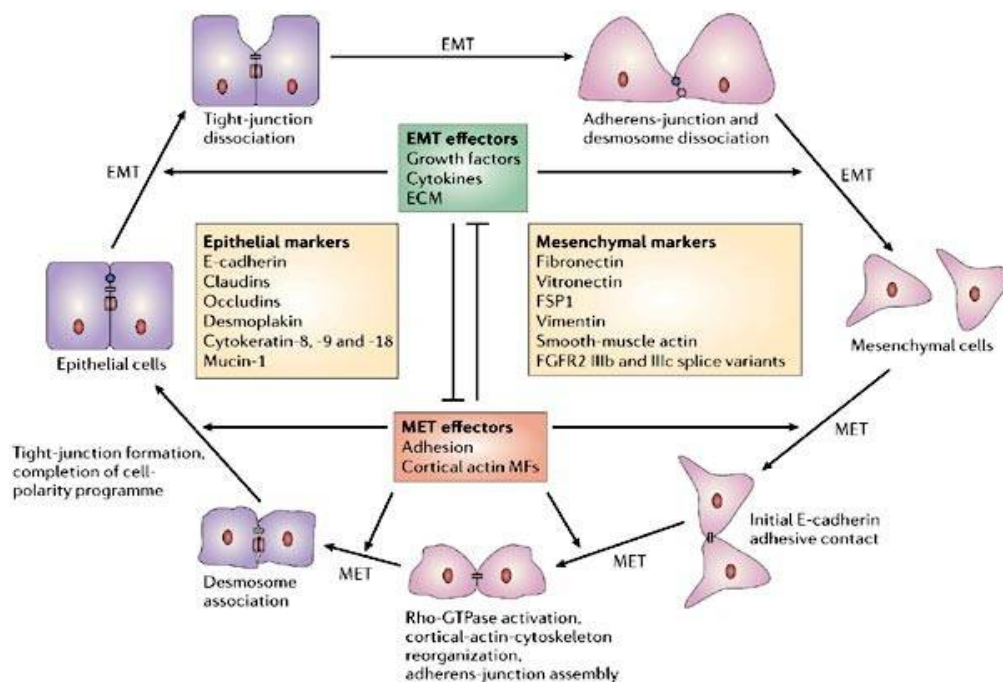


Figure 3. The cycle of epithelial-cell plasticity. The diagram shows the cycle of events during which epithelial cells are transformed into mesenchymal cells and vice versa. The different stages during EMT (Epithelial–Mesenchymal Transition) and the reverse process MET (Mesenchymal–Epithelial Transition) are regulated by effectors of EMT and MET, which influence each other. Important events during the progression of EMT and MET, including the regulation of the tight junctions and the adherens junctions, are indicated. (Thiery and Sleeman 2006)

The thyroid gland is unique among the endodermally derived organs that has no connection with the gut tube and is located rather distant from the site of embryological specification. The effector mechanisms regulating the dislocation of the thyroid anlage from the pharyngeal endoderm, its further migration, and the terminal differentiation of the follicular epithelium are largely unknown. Unexpectedly, during thyroid morphogenesis is not involved an EMT-like process, typically characterized by loss of E-cadherin and up-regulation of N-cadherin. The finding of continuous expression of E-cadherin in thyroid progenitor cells, in fact, demonstrates that the epithelial differentiation is maintained throughout the entire morphogenetic process. Conversely, N-Cadherin expression, often associated with increased migrating capacity, was not detected in the thyroid primordium, but was expressed in the surrounding mesenchyme. These findings indicate the lack of EMT because, in thyroid progenitor cells, the epithelial phenotype is maintained throughout organogenesis, and suggest that translocation of the developing thyroid does not involve active migration of individual cells, but rather is secondary to movements of surrounding tissues (Fagman et al. 2003). Another classical cadherins that influences thyroid development is the R-cadherin. Its expression in late thyroid development, in fact, proposes a functional role in folliculogenesis and was maintained in the adult thyroid along with E-cadherin (Fagman et al. 2003).

Modifications of cell-cell interactions similar to those observed during development also occur in some pathological situations, such as during carcinogenesis, where the disruption of cell-cell contact is one of key events in tumor progression. EMT provides a new basis for understanding cancer progression towards dedifferentiated and more malignant states. In fact, during recent years, EMT has emerged as a central process during cancer progression and metastasization. In this process, cancer cells acquire a fibroblastoid invasive phenotype, down-regulate epithelial-specific proteins, such as adherens and tight junction proteins, induce various mesenchymal markers, such as vimentin, and finally migrate through the extracellular matrix (Savagner 2001, Huber et al. 2005). This results in changed adhesive properties, and the activation of proteolysis and motility, which allows the tumour cells to metastasize and establish secondary tumours at distant sites (Sleeman 2000).

Many effectors orchestrate the disassembly of junctional complexes and the changes in cytoskeletal organization that occur during EMT. The activation of signalling pathways also results in the activation of transcriptional regulators such as Snail (now known as SNAI1) (Ballaro-Gimeto and Nieti 2005) and Slug (now known as SNAI2), which regulate the changes in gene-expression patterns that underlie EMT.

A central target of these transcriptional regulators is the repression of the E-cadherin gene, an important caretaker of the epithelial phenotype. Loss of E-cadherin protein and/or transcriptional repression of its mRNA are hallmarks of EMT (Cano et al. 2000, Batlle et al. 2000). Several studies indicated that

down-regulation of E-cadherin is accompanied by upregulation of the mesenchymal N-cadherin expression, which correlates with invasion, metastasis, and EMT (Cavallaro and Christofori 2004). This dynamic and reciprocal change in E- and N-cadherin expression is known as “cadherin switching”. The intracellular domain of E-cadherin interacts with catenin proteins, called α -, β -, γ -, and p120-catenin, which connect the adhesion complex to the actin cytoskeleton (Thiery 2002). The interaction between the cytoplasmic tail of cadherins with the catenins and the actin cytoskeleton is critical for the establishment of stable and functional adherens junction (Rosanò et al. 2006). However, signals generated by intracellular cadherin-binding proteins may also alter cellular behavior. This is most notable for β -catenin, which, apart from linking cadherins to the cytoskeleton, is able to enter the nucleus and trans-activate target genes (Fagman et al. 2003).

1.5 E-cadherin.

Cadherins constitute a major class of adhesion molecules that support calcium-dependent, homophilic cell-cell adhesion in all solid tissues of the body. The cadherins mediate cell-cell recognition events and, in association with the actin cytoskeleton, bring about morphological transitions that underlie tissue formation and maintain tissue architecture in the adult organism. In this way, five different sub-families can be considered: 1) type I, classical cadherins, mainly localised to adherens junctions; 2) Highly related type II cadherins; 3) Desmosomal cadherins (desmocollins and desmogleins) that form desmosomal junctions; 4) Protocadherins, mainly implicated in neural development; 5) Cadherin-related proteins, like the Flamingo (7Tm) and Fat-like cadherins (Peinado et al. 2004) (figure 4).

The classical cadherins typically consist of five tandemly repeated extracellular domains, approximately of 110 amino acids, single membrane-spanning segment and a cytoplasmic region. The N-terminal extracellular domains mediate cell-cell contact while the cytoplasmic region interacts with the cytoskeleton through the catenins. Specific adhesive binding is conferred by the cadherin ectodomain. Although the ectodomain alone possesses homophilic-binding properties (Brieher et al. 1996), stable cell adhesion requires the cadherin cytoplasmic tail and associated proteins (Nagafuchi and Takeichi 1988, Brieher et al. 1996). In the case of E-cadherin, specificity of the homophilic interactions was localized to the first N-terminal extracellular domains (Nose et al. 1990) (figure 4).

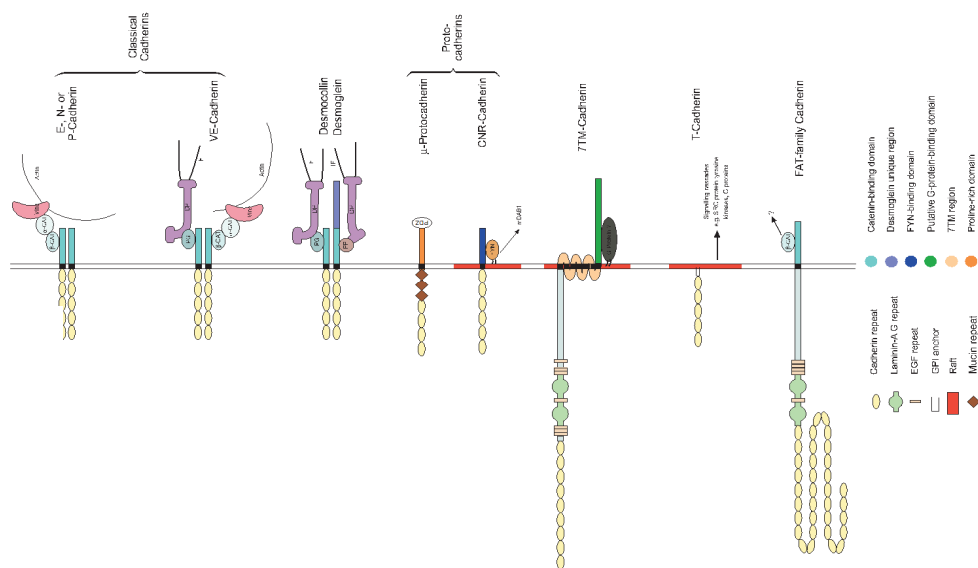


Figure 4. Schematic overview of the cadherin superfamily. The main structural domain and schematic structure of the different cadherin types are shown at the right.

The human E-cadherin gene (*CDH1*) is located at the 16q22.1 locus and is comprised of 16 exons, spanning 99 Kb of genomic DNA. The mouse E-cadherin gene (*cdh1*) has a similar exon-intron organization and is located on chromosome 8. The mouse *E-cadherin* promoter was first isolated in 1991. Its initial characterization showed that it was a TATA-less promoter containing several potential proximal regulatory elements, including a CCAAT box (-65), a GC-rich region (-30 to -58) and a palindromic element (-70 to -90) composed of two adjacent E-boxes flanked by four inverted nucleotides called E-pal (Faraldo et al. 1997) (figure 5). The proximal CCAAT box and GC-rich regions are required for basal E-cadherin expression and are recognized by CAAT-binding proteins and constitutive AP2 and Sp1 transcription factors, respectively (Behrens et al. 1991, Hennig et al. 1996, Faraldo et al. 1997).

The E-pal element was initially described as an epithelial-specific regulator (Behrens et al. 1991), but subsequent studies showed it to be an active repressor in E-cadherin deficient cells (Hennig et al. 1996, Faraldo et al. 1997, Rodrigo et al. 1999). Equally, the E-boxes in the proximal *E-cadherin* promoter repress its expression (Battle et al. 2000, Hajra et al. 2002).

A study based on the yeast one-hybrid system has led to identification of several E-cadherin repressors. More than 90% of these identified factors, that specifically bound to the E-boxes, corresponded to transcription factors, of which, two in particular were highly represented: 49% corresponded to the zinc finger factor Snail and 32% to the class I bHLH factors, E47 (Cano et al. 2000, Perez-Moreno et al. 2001). The remaining factors corresponded mainly to an

additional class I bHLH factor, mITF2 (also called E2-2), while a single clone corresponded to another member of the Snail family, Slug (Bolòs et al. 2003). Functional characterisation of Snail, bHLH E47 and Slug have confirmed their ability to behave as E-cadherin repressors and to induce EMT when over-expressed in epithelial cell line (Batlle et al. 2000, Cano et al. 2000). Other two factors have also been described as repressors of E-cadherin and are δ EF1 (Zeb1) and SIP1 (Zeb2) of homeodomain and zinc finger family. In all these instances, these repressors silence E-cadherin binding to the proximal E-boxes, although some differences are observed between the mouse and the human promoters. While the factors that act on the mouse promoter seem to preferentially interact with the E-pal element (including Snail, Slug and E47) (Cano et al. 2000, Perez-Moreno et al. 2001, Bolòs et al. 2003), in the human promoter all three E-boxes or E-box 1 and 3 appear to be required for the interaction of Snail/Slug or δ EF1/ SIP1, respectively (Batlle et al. 2000, Hajra et al. 2002) (figure 5). These observations suggest that at least two of the three proximal E-boxes in the mammalian *E-cadherin* promoter are functionally similar in terms of recruiting repressors, regardless of their relative location. Interestingly, all of the E-cadherin repressors identified exhibit expression patterns in developing embryos compatible with this function.

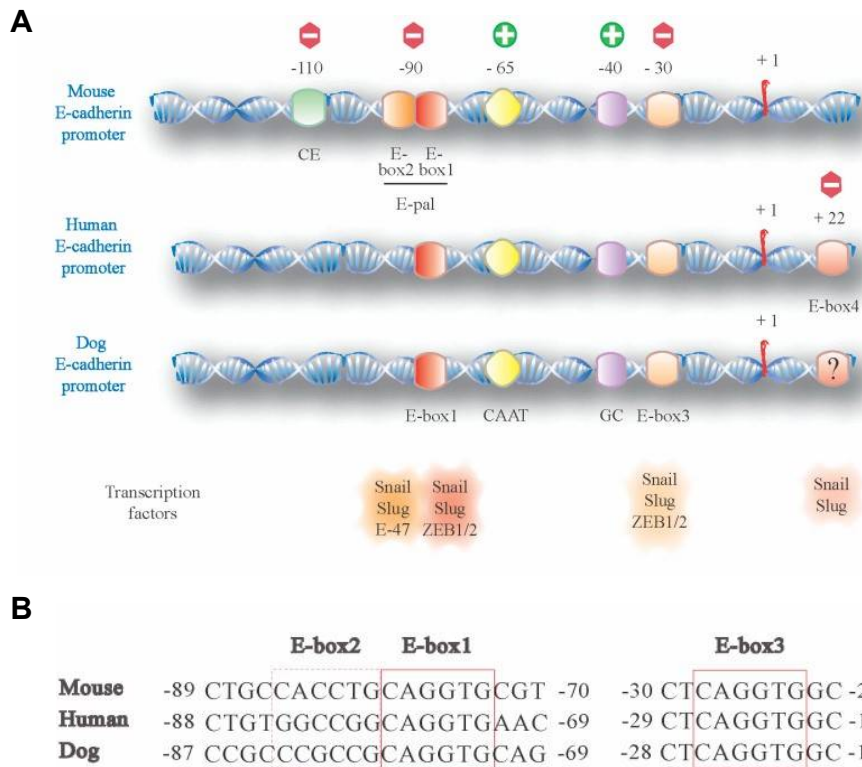


Figure 5. Schematic representation of the *E-cadherin* promoter region and E-box sequences in mouse, human and dog. **A) The *E-cadherin* promoter region is represented with its representative proximal control elements in the proximal region (exerting either a positive or negative effect on *E-cadherin* expression). The CAAT, GC and E-box1/E-box3 are conserved in all three promoters, while the E-box 2 is only present in the mouse promoter region. An additional E-box (E-box 4) downstream of the transcription initiation site is present in the human promoter, but is not conserved in the region encompassing the mouse promoter. Binding of identified factors to the different E-boxes is shown in the lower part. **B)** Sequence of the E-boxes present in the proximal region of the mouse, human and dog *E-cadherin* promoter. Observe the high degree of conservation of E-box 1 and E-box 3. (Peinado et al. 2004).**

1.5.1 E-cadherin implication in tumor progression.

The long-standing observation that tumor cells demonstrate decreased cellular adhesion, as well as the observation that *E-cadherin* expression is frequently lost in human cancers, led investigators to hypothesize that changes in the cadherin-catenin complex may play a causative role in cancer development and progression (Jiang 1996). In several cancer types, in fact, loss of either *E-cadherin* or β -catenin expression has been correlated with tumor

dedifferentiation, infiltrative growth, lymph node metastasis, and poorer patient prognosis. Immunohistochemical studies have demonstrated that loss of E-cadherin expression is a frequent event in many types of carcinomas (Jiang 1996, Papadavid and Katsambas 2001). Restoration of E-cadherin expression into highly invasive epithelial tumor cell lines of dog kidney or mouse mammary gland origin abrogates their invasive behavior, though reversion to the invasive phenotype is seen following treatment with anti-E-cadherin antibodies. Alternatively, a plasmid encoding E-cadherin-specific anti-sense RNA was introduced into noninvasive ras-transformed cells with high endogenous E-cadherin expression. The resulting down-regulation, albeit partial, rendered the cells invasive. These data have provided direct evidence that E-cadherin acts as an “invasion suppressor” (Vleminckx et al. 1991). Subsequent studies have shown that loss of E-cadherin expression is a common finding in a wide spectrum of human epithelial cancers (Birchmeier and Behrens 1994). Recent studies have provided more compelling evidence that E-cadherin inactivation does not simply reflect the cancer phenotype, but its inactivation has a causal role in the process (Gayther et al. 1998; Guilford et al. 1998).

Although somatic mutations in the *CDH1* gene have been identified in a small subset of tumors, in the majority of cancers the mechanisms underlying loss of E-cadherin expression are poorly understood. The *CDH1* gene is located on chromosome 16q in a region that is frequently affected by allelic loss in several cancer types (Risinger et al. 1994). Somatic mutations in the *CDH1* gene have been identified in more than 30% of gastric cancers of diffuse subtype, about 5-10% of endometrial and ovarian cancer. Moreover, in many cancer types where expression is frequently lost, *CDH1* mutations are rare or absent (Hirohashi 1998). Proposed epigenetic mechanisms for E-cadherin loss include alterations in the expression and/or function of the trans-acting factors that regulate *CDH1* gene transcription, hypermethylation of its promoter, and chromatin-mediated effects. In some cases, transcriptional mechanisms underlie loss of E-cadherin expression through its proximal promoter (Hajra et al. 1999), and E-box elements within this region have been proposed to be critical in the silencing of *CDH1* transcription in cancer (Girolodi et al. 1997).

Hypermethylation of the *CDH1* promoter has been postulated to play a critical role in the loss of E-cadherin expression observed in some primary tumors and in cell lines without identified *CDH1* mutations. Mechanisms other than repression by certain transcription factors and promoter hypermethylation have been suggested to inactivate *CDH1* expression in cancer. In particular, chromatin condensation has been proposed to play a role in the silencing of *CDH1* expression in carcinomas (Hennig et al. 1995). The various proposed mechanisms of *CDH1* silencing in cancer may not be mutually exclusive. For instance, *CDH1* promoter hypermethylation and chromatin remodeling may occur in concert with or as a specific consequence of the transcriptional repression effects of distinct trans-acting transcription factors targeted to the *CDH1* promoter (Hennig et al. 1995).

1.5.2 Mechanisms of E-cadherin repression: potential co-operation with epigenetic modifications.

The informations available regarding the different mechanisms involved in E-cadherin silencing make it difficult to define a simple model where E-cadherin expression is regulated by just a single genetic, epigenetic or transcriptional control mechanism. Probably it seems more that a combination of different mechanisms is responsible for defining the status of E-cadherin expression during tumour progression.

Current evidence indicates that silencing of E-cadherin transcription requires the participation of several repressor factors that interact with specific E-box elements in the proximal promoter. The repression of gene expression either involves the local modification of chromatin organization through the recruitment of specific co-repressor complexes (Snail, Slug and potentially δ -EF1/SIP1), or heterodimerization of repressors with specific partners (E47). The specific mechanisms by which Snail, and/or other repressors, mediates E-cadherin silencing are still largely unknown. The modification of chromatin by the co-ordinated action of DNA and/or histone methylation, and acetylation, has emerged as one of the major mechanisms for regulating the transcriptional activity of different regulatory genes (Peinado et al. 2004). Very recently, details of the mechanism underlying Snail repression of E-cadherin were revealed, providing a link between transcriptional control and the epigenetic modifications of the *E-cadherin* promoter (Peinado et al. 2004). Snail repression of the *E-cadherin* promoter involves the recruitment of a repressor complex formed, at least, by the co-repressor mSin3A, HDAC1 and HDAC2 (Peinado et al. 2004). The recruitment of this complex is mediated by the N-terminal SNAG domain of Snail, previously thought to act as the repressor domain. The presence of this complex results in a net decrease in the amount of acetylated histones H3/H4 and an increase in methylated K9 of histone H3 in the endogenous *E-cadherin* promoter. In turn, this leads to a compact organisation of the chromatin (Peinado et al. 2004). A preliminary analysis in the mouse skin carcinogenesis model indicates that Snail expression is also associated with the hypermethylation and silencing of the *E-cadherin* promoter, further supporting the notion of a connection between Snail and epigenetic modifications (figure 6). The molecular mechanisms involved in this link remain to be elucidated, but the implication of MBDs (methyl DNA binding protein) and HDACs is an interesting aspect of E-cadherin silencing for further study, since treatment with inhibitors of DNA methylation and HDACs promotes the re-expression of E-cadherin (Peinado et al. 2004).

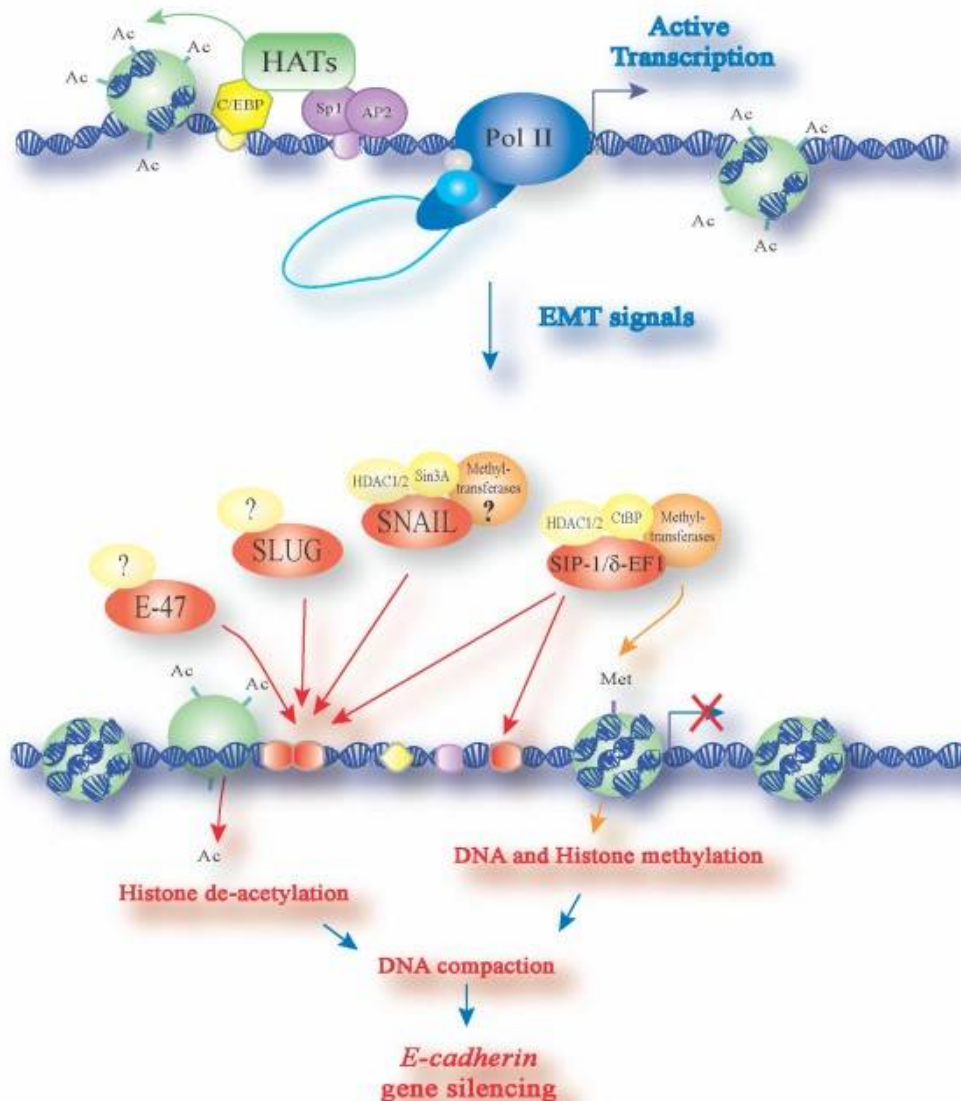


Figure 6. A model for the regulation of E-cadherin expression involving different repressors and epigenetic mechanisms

A schematic illustration of the putative epigenetic mechanisms involved in E-cadherin regulation is shown. In this model, active transcription is probably achieved through the interaction of several activators, and involves the acetylation of histone residues which promotes the chromatin to adopt an open conformation. Under the influence of the appropriate signals, several repressors and co-repressor molecules are recruited (depending on either the tissue or cellular context), attracting the repressor machinery which includes corepressor molecules, HDACs and methylases, and still unidentified molecules which will modify the acetylation and methylation status of chromatin, promoting E-cadherin silencing. (Peinado et al. 2004).

1.6 Epigenetic control of gene expression.

The term “epigenetics” refers to mitotically and meiotically heritable changes in gene expression that are not coded in the DNA sequence itself (Egger et al. 2004).

The DNA of eukaryotic cells is compacted by basic histone proteins in a highly organized structure called chromatin to achieve compaction, enabling the entire genome to fit into the nucleus, and allowing DNA transcription, replication, and repair, when necessary. The nucleosome, the basic unit of chromatin, consists of 147 base pairs of DNA wrapped around the histone octamer, composed of two copies of each of the four core histones, H2A, H2B, H3, and H4 (van Holde 1988). Although the structure of the core nucleosome is well defined, the basic N-terminal histone tails protrude from the core nucleosome and show no defined structure (Luger et al. 1997, Luger and Richmond 1998).

These histone tail domains are subject to post-translational modifications, such as acetylation, methylation, phosphorylation, and ubiquitination. Recent observations indicate that histone modifications occur interdependently and create a pattern that might modulate the affinity of histone-binding proteins. A correlation between histone acetylation and increased gene expression was discovered earlier on (Alfrey et al. 1964). According to the current model, the acetylation of lysine residues within the histone tails neutralizes the positive charge of ϵ -amino groups and thereby reduces the interaction between the N-terminal tails of histones and the negatively charged DNA. Acetylation at the N termini of core histones is therefore believed to induce the local opening of chromatin structures. Reversible histone acetylation is controlled by histone acetyltransferases (HAT), which usually act as transcriptional coactivators, and histone deacetylases (HDACs), which repress transcription. Activator complexes containing HAT activity have been shown to contribute to transcriptional activation by recruitment of general transcription factors and RNA polymerase II (Carrozza et al. 2003, Torok and Grant 2004). In contrast, recruitment of repressor complexes with HDAC activity is considered to lead to deacetylation of histones, stabilization of nucleosome structure, and formation of a repressive chromatin state. Strahl and Allis proposed that distinct histone modifications, on one or more tails, act sequentially or in combination to form a 'histone code' that is read by other proteins leading to distinct downstream events (Strahl and Allis 2000). This theory states that post-translational modifications can act through two mechanisms that are not mutually exclusive: 1) by structurally changing the chromatin fiber through internucleosomal contacts thus regulating the access of transcription factors to the DNA; 2) by generating docking sites for effector molecules that, in turn, initiate distinct biological processes. The histone code is part of the epigenetic information found into the cells.

All the core histones are acetylated *in vivo*; however, modifications of histones H3 and H4 are much more extensively characterized than those of H2A and H2B (Struhl 1998, Annunziato and Hansen 2000). Acetylation of histone H3 is

primarily associated with transcription whereas H4 acetylation is associated with both transcription and with chromatin assembly (Struhl 1998, Annunziato and Hansen 2000). Steady-state levels of acetylation in the core histones result from the balance of the antagonistic activities of histone acetyltransferases and histone deacetylases (Grunstein 1997, Struhl 1998). In general, increased levels of histone acetylation are associated with transcriptional activity whereas decreased acetylation levels are associated with repression (Grunstein 1997, Struhl 1998).

During the last decade, more than a dozen of histone deacetylases have been identified in mammalian cells. Based on sequence similarities, HDACs are divided into four functional classes: class I (HDAC1, HDAC2, HDAC3, and HDAC8), class II (HDAC4, HDAC5, HDAC6, HDAC7, HDAC9, and HDAC10), class III (SIRT1 to SIRT7), and the recently described class IV of HDACs, which consists of HDAC11-related enzymes (Grozingler and Schreiber 2002, Gregoretta et al. 2004).

HDAC inhibitors have been shown to induce cell cycle arrest, differentiation, or apoptosis in tumor cells, and some of these compounds are currently tested as antitumor drugs in clinical trials (Mei and Mahlknecht 2004, Dokmanovic and Marks 2005, Drummond et al. 2005). These inhibitors affect the catalytic activity of most class I and class II deacetylases. However, little is known about the individual roles of mammalian deacetylases in transcriptional control and the relevant target enzymes for HDAC inhibitors as antitumor drugs.

2. AIMS OF THE STUDY

Thyroid tumors are the result of the accumulation of different modifications in critical genes involved in the control of cell proliferation. Although various therapeutic approaches are followed in clinical practice, most of them are not life-saving. Hence, the discovery of new approach to diagnose cancer at an early stage and to establish more effective therapies is a critical and urgent issue. To achieve this goal, identification and characterization of key molecules that participate in carcinogenesis are essential steps.

CBX7 is a chromobox family protein encoding a novel polycomb protein, the expression of which shows a progressive reduction, well related with the malignant grade of thyroid neoplasias. The aim of this study has been to elucidate CBX7 function in normal cells and understand why it is drastically down-regulated in tumor thyroid cells. Thus, we investigated proteins interacting with CBX7, by a proteomic assay because the association of CBX7 with partners involved in a particular mechanism might strongly suggesting the biological function of the protein (Monti et al. 2005). Thus, we try to elucidate the mechanisms by which the loss of CBX7 expression contributes to cancer progression by the identification and characterization of proteins that interact with CBX7 and might contribute to the transformation process of the thyroid follicular cells.

3. MATERIALS AND METHODS

3.1 Cell culture and transfections.

In this study we have used HEK 293 cells (Human embryonal kidney), and HeLa cells maintained in Dulbecco's Modified Eagle's Medium (DMEM) and RPMI medium respectively, supplemented with 10% fetal calf serum, L-glutamine 10 mM, and penicillin/streptomycin 100 µg/ml. The human thyroid carcinoma cell lines TPC-1 and NPA were grown as described elsewhere (Pallante et al. 2005). Normal human thyroid primary culture cells have been established and grown as already described (Curcio et al. 1994). PC Cl3 cell lines was cultured in modified F12 medium supplemented with 5% calf serum (Gibco Laboratories) and six growth factors (thyrotropic hormone, hydrocortisone, insulin, transferrin, somatostatin and glycyl-histidyl-lysine) (Sigma, St. Louis, MO) (Fusco et al. 1987). All cell lines were maintained at 37°C under 5% CO₂ atmosphere.

Cells were transfected using Lipofectamine reagent (Invitrogen, Carlsbad, CA) according to the manufacturer's instructions. The transfected cells were selected in a medium containing geneticin (G418) (Gibco Laboratories, Carlsbad, CA). CBX7 inducible NPA cells were generated by trasfecting NPA cells with the pcDNATM6/TR regulatory vector (Invitrogen) that provides high level expression of the tetracycline repressor and with the expression vector which contains the *CBX7* gene under the control of a tetracycline-regulated promoter. Cells, plated at a density of 90% in 100 mm dishes, were co-transfected with pcDNATM6/TR and pCBX7-TetO2 and supplemented with Zeocin and Blasticidin (Invitrogen) 24 h later. Two weeks after the onset of drug selection, several resistant clones were picked, expanded and analysed for CBX7 expression after adding tetracycline to the medium.

In the experiments performed in presence of trichostatin A (TSA) (Sigma) the cells were treated 24 h after transfection. TSA was dissolved in ethanol and added to the culture medium at 300 nM and a corresponding volume of ethanol was added to untreated cells.

For the inhibition of CBX7 expression, rat *cbx7* siRNA (SI01495795 and SI01495802, Qiagen, Hilden, Germany) and Nonsilencing Control siRNA (1022076, Qiagen) were transfected using Oligofectamine (Invitrogen) according to the manufacturer's recommendations. siRNAs were used at a final concentration of 100 nM and 12x10⁵ PC Cl3 cells/well were plated in a six-well format plate. RNAs were extracted 48 h after siRNA treatment.

3.2 Plasmid constructs.

CBX7 expression plasmid was constructed by cloning the human cDNA sequence in a pCRTMII TA Cloning® vector (Invitrogen, Carlsbad, CA). The primers used were: CBX7 forward 5'-ATGGAGCTGTCAGCCATC-3' and

CBX7 reverse 5'-TCAGAACTTCCCCTGCG-3'. The inserted cDNA was then subcloned into the BamHI/XhoI sites of the mammalian expression vector pcDNA 3.1 (Invitrogen).

V5-tagged CBX7 expression plasmid was generated by the insertion of the PCR product into the Gateway entry vector pENTR/D-TOPO and subsequently cloned into the destination vector pcDNA-DEST-40 Gateway Vector (Invitrogen) by using the pENTR/D-TOPO Cloning Kit (Invitrogen) according to the manufacturer's instructions. Primers are as follows: CBX7-dest-forward 5'-CACCATGGAGCTGTCAGC-3' and CBX7-dest-reverse 5'-GAACTTCCCCTGCGGT-3'. The expression of CBX7 was assessed by Western blotting.

HA-tagged CBX7 expression plasmid containing the entire portion of the *CBX7* coding sequence was obtained by PCR amplification and subcloned into the pCEFL-HA expression vector. CBX7-deletion mutants were cloned in pCEFL-HA:

- for p-CEFL-HA-CBX7-CHROMO (1-100aa): CHROMO forward 5'-GAGCTGTCAGCCATCGGC-3' and CHROMO reverse 5'-TCACTTCTCCTTGCCCTTGGC-3';

- for pCefl-HA-CBX7-NOCHROMO (55-251aa): CBX7-NOCHROMO forward 5'-GCCAAGGGCAAGGAGAAGTGAC-3' and CBX7-NOCHROMO reverse 5'-GTCAGAACTTCCCCTGCGG-3'.

E-cadherin-luc reporter construct, in which the *luciferase* gene was driven by a fragment extending from -1359 bp 5' to +125 bp 3' of the human *E-cadherin* promoter and 5' UTR of *E-cadherin* gene, was kindly provided by Dr ER Fearon, University of Michigan Medical School (Hajra et al. 1999, Ji et al. 1997). Ather two reporter construct containing *E-cadherin* promoter sequence were generated by PCR and subcloned into pGL2-Basic vector (Promega) upstream of the firefly *luciferase* gene. The sequences subcloned cover *E-cadherin* promoter and 5' UTR of *E-cadherin* gene from -601 bp to +125 bp (*E-cadherin* 601) and from -211 bp to +125 bp (*E-cadherin* 211). Primers used were: 601 forward: 5'-TGGGCAATACAGGGAGACAC-3' and 601 reverse: 5'-TCACAGGTGCTTTGCAGTTC-3'; 211 forward: 5'-AACTCCAGGCTAGAGGGTCA-3' and 211 reverse: 5'-TCACAGGTGCTTTGCAGTTC-3'.

The identities of the sequences cloned for all constructs were confirmed by sequences analysis.

pEGFP expression vector (Clontech) was used as control in transfection experiments and as negative control in FRET experiment.

3.3 Protein extraction.

For total cell extract (TCE) preparation, cells were harvested 48 h after the onset of transfection. Cells were then lysed in RIPA buffer (20 mM Tris-HCl pH 7.5, 5 mM EDTA, 150 mM NaCl, 1% Nonidet P40, and a mix of protease inhibitors), and clarified by ultracentrifugation at 13000 rpm at 4°C for 30 min.

For nuclear extract (NE), cells were washed twice in phosphate-buffered saline and resuspended in 3 volumes of a solution containing 10 mM HEPES pH 7.9, 10 mM KCl, 1.5 mM MgCl₂, 0.1 mM EGTA, 0.5 mM DTT (homogenization solution). The cells were disrupted by passage through a 26-gauge needle. Nuclei were collected by centrifugation at 1500 rpm and resuspended in a 1.2-volume of extraction solution containing 10 mM HEPES pH 7.9, 0.4 M NaCl, 1.5 mM MgCl₂, 0.1 mM EGTA, 0.5 mM DTT, 5% glycerol, to allow elution of nuclear proteins by gentle shaking at 4°C for 30 min. Nuclei were pelleted again by centrifugation at 12000 rpm for 30 min and the supernatant was stored at -80°C until used. The protease inhibitors (leupeptin 5 mM, aprotinin 1.5 mM, phenylethylsulfonyl fluoride 2 mM, pepstatin A 3 mM, and benzamidine 1 mM) were added to both homogenization and extraction solutions. Protein concentration was determined by the Bradford protein assay (BioRad).

3.4 Western blotting and immunoprecipitation assay.

Protein extracts and immunoprecipitated pellets were separated by SDS-PAGE, and then transferred onto Immobilon-P Transfer membranes (Millipore). Membranes were blocked with 5% non-fat milk proteins and incubated with antibodies (Ab) at the appropriate dilutions. To ascertain that equal amounts of protein were loaded, the western blots were incubated with antibody against the α -tubulin protein (Santa Cruz Biotechnology Inc.). After the hybridization with primary antibody the filters were incubated with horseradish peroxidase-conjugated secondary antibody (1:3000) for 60 min at room temperature. The signals were detected by Western blotting detection system (ECL) (GE Healthcare).

For immunoprecipitation (IP) experiments, TCE was incubated for pre-clearing with protein A-sepharose or G-sepharose beads (Amersham) for 1 h at 4°C, then sample was centrifuged to 2000 rpm to eliminate beads and incubated overnight with antibody. The day after the IP was incubated again with protein A-sepharose or G-sepharose beads for 1 h at 4°C. The beads were collected and washed five times with lysis buffer, and boiled in Laemmli sample buffer for immunoblotting analysis. The Abs used for IP and Western blotting were: anti-CBX7 protein (Neosystem), anti-V5 (Sigma), anti-HDAC2 (Upstate), anti-HA (Roche), anti- α Tubulin (Santa Cruz Biotechnology Inc.).

3.5 Samples preparation and immunoprecipitation for proteomic assay.

For preparative gels, 8×10^7 cells were transfected with 10 μ g of empty vector or with CBX7-V5-His expression plasmid. The IP was performed with 1 mg of NE and the complex immunoprecipitated was recovered by competition with peptide V5 (Abcam). For immunoblotting analysis, 50 μ g of TCE or immunoprecipitated proteins were analysed by Western blotting.

3.6 Electrophoresis fractionation and *in situ* digestion.

The IP and the control were fractionated by SDS-PAGE on a 12% bis-acrylamide gel. The gel was stained by Colloidal Comassie (Pierce) and the corresponding protein bands were excised from both lanes and digested *in situ* with trypsin (Shevchenko et al. 1997). Peptide mixtures were extracted, freeze-dried and resuspended in 10 μ l of 0.2% trifluoroacetic acid (TFA) for the Liquid Chromatography/Mass Spectrometry/Mass Spectrometry (LCMSMS) analysis.

3.7 Liquid Chromatography/Mass Spectrometry/Mass Spectrometry (LCMSMS) analysis.

Each peptide mixture was directly analysed by LCMSMS using an Agilent ion trap mass spectrometer LC/MSD Trap XCT Ultra integrated with a new microfluidic chip-based technology for nanospray LC/MS (Agilent) and coupled on-line with a nano chromatography system Agilent 1100. After loading, the peptide mixture (8 μ l) was first concentrated and washed at 4 μ l/min onto a reverse-phase pre-column on the chip using 0.2% formic acid as eluent. The sample was then transferred and fractionated by reverse-phase chromatography onto a capillary column present on the chip at a flow rate of 300 nl/min using a linear gradient of eluent B (0.2% formic acid in 95% acetonitrile) in A (0.2% formic acid in 5% acetonitrile) from 7 to 60% in 50 min. The mass spectrometer was set up in a data-dependent MS/MS mode where a full scan spectrum (m/z acquisition range from 400 to 1600 Da/e) was followed by a tandem mass spectrum (m/z acquisition range until 1800 Da/e). The precursor ions were selected as the most intense peaks of the previous scan. LC/MSD Trap software, provided by the manufacturers, was used to analyse raw MS and MS/MS spectra and to generate a peak list which was introduced in the MASCOT MS/MS ion search software for protein identification.

3.8 Expression and purification of recombinant proteins/GST pull-down experiments.

GST fusion proteins were constructed by cloning the human cDNA sequence of CBX7 in a pGEX4T-1 (Promega). The primers used were:

- for GST-CBX7: CBX7 forward 5'-GAGCTGTCAGCCATCGGC-3' and CBX7 reverse 5'-GTCAGA AACTTCCC ACTGCGG-3';
- for GST-CBX7-CHROMO: CBX7-CHROMO forward 5'-GAGCTGTCAGCCATCGGC-3' and CBX7 reverse 5'-TCACTTCTCCTTGCCCTTGCC-3';

- for GST-CBX7-NOCHROMO: CBX7-NOCHROMO forward 5'-GCCAAGGGCAAGGAGAAGTGAC-3' and CBX7-NOCHROMO reverse 5'-GTCAGAACTTCCCACTGCGG-3'.

GST fusion proteins were produced in *Escherichia coli* BL21 cells. Stationary phase cultures of *E. coli* cells transformed with the plasmid of interest were diluted 1000 ml in LB with ampicillin (100 mg/ml), grown at 30°C to an OD 600 of 0.6 and induced with 1 mM IPTG. After an additional 2 h at 30°C, the cultures were harvested and resuspended in 10 ml of cold PBS, 140 mM NaCl, 20 mM sodium phosphate pH 7.4, 1 mM phenylmethylsulfonyl fluoride (PMSF) and protease inhibitors (Boehringer). The cells were broken by French Press. For the GST proteins, the supernatant was then incubated at 4°C for 1 h with 250 µl of glutathione-Sepharose beads (Amersham Pharmacia Biotech). The expression of recombinant protein of CBX7 was assessed by Coomassie. The recombinant proteins were eluted with a buffer containing PBS, 10mM reduced glutathione, and 10% (v/v) glycerol. For GST pull-down the fusion proteins were incubated with TCEs in NETN buffer (20 mM Tris-HCl, pH 8.0, 100 mM NaCl, 1 mM EDTA, and 0.5% Nonidet P-40) for 2 h at 4°C. The resins were then extensively washed in the same buffer and then resuspended in Laemmli buffer. The bound proteins were separated by SDS-PAGE and analysed by Western blotting.

3.9 HDAC activity assay.

HEK 293, HeLa and NPA cells were transfected with increasing amount of CBX7 expression vector and were used to assay the HDAC activity. 30 µg of TCE were incubated with 5 µl of [³H]acetate-labeled histone H4 (1.8 nCi/µg) in 200 µl of activity buffer (25 mM Tris-HCl [pH 7.5], 10% glycerol, 1 mM EDTA, 125 mM NaCl) overnight at 37°C. The reaction was stopped by the addition of 50 µl of 1 N HCl-0.4 M acetate and the released [³H]acetate was extracted with 600 µl of ethyl acetate (Upstate). After centrifugation, 100 µl of the supernatant was counted in 5 ml of scintillation cocktail. All experiments were carried out three times, and samples were assayed in duplicate. The same protocol was used to analyse HDAC activity in TCE from human tumor samples.

3.10 Chromatin immunoprecipitation (ChIP) and Re-ChIP assays.

ChIP and Re-ChIP experiments were performed as reported elsewhere (Pierantoni et al. 2006). Briefly, after transfection, 5x10⁶ HEK 293 and HeLa cells were cross-linked using 1% formaldehyde at room temperature for 10 min, reaction was terminated with glycine (final concentration, 0.125 mol/L). Cells were lysed in 200 µl of lysis buffer containing 10 mM EDTA, 50 mM Tris-HCl pH 8.0, 1% SDS and protease inhibitors and sonicated five times for 30 sec at maximum settings, obtaining fragments between 0.3 and 1.0 kb. The

samples were cleared by centrifugation at 14000 rpm for 15 min. After centrifugation, 3% of the supernatants were used as inputs, and the other part of the samples diluted 2.5-fold in Ip buffer (100 mM NaCl, 2 mM EDTA pH 8.0, 20 mM Tris-HCl pH 8.0, 0.5% Triton X-100 and protease inhibitors). After 2 h pre-clearing at 4°C with Protein A Sepharose or Protein G Sepharose/BSA/Salmon Sperm (Upstate), samples were subjected to IP with the following specific antibodies: anti-HA (Roche) and anti-HDAC2, anti-H3K4m2, anti-H3K4m3, anti-H3K9me, anti-H3K9m3, anti-H4K20 (Upstate) and with aspecific IgG (Upstate). After an over-night incubation with antibody, the proteins A/G were added again for the precipitation of chromatin complexes. The chromatin immunoprecipitated was removed from the beads through 15 min incubation with 250 µl of 1% SDS, 0.1 M NaHCO₃. For Re-ChIP assays, complexes from the primary ChIP were eluted with 10 mmol/L of DTT for 30 min at 37°C diluted in 250 µl of Re-ChIP buffer (20 mmol/L Tris-HCl (pH 8.1), 1% Triton X-100, 2 mmol/L EDTA, 150 mmol/L NaCl) followed by re-IP with the indicated second antibodies and were again subjected to the ChIP procedure. Crosslink was reversed by an overnight incubation at 65°C with 20 µl of 5 M NaCl. Then were added 10 µl 0.5 mM EDTA, 20 µl 1 M Tris-HCl pH 6.5 and 20 µg of Proteinase K, and incubated for 1 h at 45°C. DNA was purified by Phenol/CHCl₃, and precipitated by two volumes of ethanol and 0,1 M NaOAc.

Semi quantitative PCR was performed using specific primers:
 pE-cadherin-F(-300)-L, 5'-GAACTCAGCCAAGTGTAAGCC-3'
 pE-cadherin-R(+40)-R, 5'-GAGTCTGAACTGACTTCCGC-3'
 p16-F, 5'-GCAGTCCGACTCTCCAAAAG-3'
 p16-R, 5'-GGGTGTTTGGTGTTCATAGGG-3'
 pE2F1-F, 5'-CGTTGGCTGTTGGAGATTTT-3'
 pE2F1-R, 5'-TTGCCTCACCCATGACATTA-3'
 S100A4-ChIP-F, 5'-TCATCCAGTCCCCTGCTAGT-3'
 S100A4-ChIP-R, 5'-AGAGCGGATACTGCCTTCCT-3'
 GAPDH-F, 5'-TCCTGTTTCATCCAAGCGTG-3'
 GAPDH-R, 5'-GACTGTCTCGAACAGGAGGAG-3'

Quantitative PCR(qRT-PCR) was performed using specific primers:
 E-cadherin-F(-70), 5'-GAACCCTCAGCCAATCAGC -3'
 E-cadherin-R (+54), 5'-GAGTCTGAACTGACTTCCGC -3'

3.11 Electrophoretic mobility shift assay (EMSA) and supershift assay.

For gel shift analysis, NE were prepared following the method of Dignam (Dignam et al. 1983). The double-strand oligonucleotides covered a region spanning from nucleotide -70 to +54 of the human *E-cadherin* promoter with respect to the transcription start site (TSS), were ³²P labeled (TransCruz™ Gel

Shift Oligonucleotides) with $^{32}\text{[P]}$ -ATP to 50,000 cpm/ng by using polynucleotide kinase. Binding reaction mixtures (20 μl) were incubated for 20 min at room temperature in 10 mM Tris pH7.5, 50 mM NaCl 1 mM dithiothreitol (DTT), 1 mM EDTA, 5% glycerol. Binding reaction contained DNA probe (50000 cpm), 5 μg nuclear extract and 1 μg poly dI-dC to inhibit non specific binding of the labeled probe to nuclear extract protein. The protein-DNA complexes were resolved by native PAGE (6% gel) in 0.5xTris/borate/EDTA and visualized by autoradiography.

For supershift analysis, assay were performed as described above with the exception that antibody (2 μg) was normally added 4 h prior to addition of labelled oligonucleotide probe to NE.

3.12 ImmunoFRET.

HEK 293 cells were plated on a slide and transfected with pCDNA3.1-V5-CBX7. After 24 h from transfection the slides were incubated with RNase 10 $\mu\text{g}/\text{ml}$ in 1xPBS for 45 min at room temperature. For fixation, the slides were submerged in 4% paraformaldehyde solution for 20 min at room temperature and then washed twice for 5 min with NH_4Cl 50 mM in 1xPBS and then in 0,2% Triton X-100 in 1xPBS. After a wash in 1xPBS, 200 $\mu\text{l}/\text{slide}$ of Blocking solution (1% BSA in 1xPBS) was added for 30 min. The slides were washed again in 1xPBS and were incubated with DNAsi 1 $\mu\text{g}/\text{ml}$ for 15 min. The slides were washed again and were incubated with primary antibodies (anti-HDAC2, Upstate; anti-CBX7, Neosystem) diluted in blocking solution, (0,5% BSA in 1xPBS) for 45min-1hr at 37°C in the dark. Then the slides were incubated with the secondary antibody (Cy3-antiRabbit to CBX7 and Cy5-antimouse to HDAC2) diluted in blocking solution (0,5% BSA in 1xPBS) for 20 min at room temperature in the dark. After that, 30 μl of 0.1 $\mu\text{g}/\text{ml}$ DAPI in 1X PBS, 0,01% Tween20, were added and the slides were incubated at room temperature for 15 min. At the end the slides were washed in H_2O and shake off excess liquid from the slides and fixed upon cover glass with 2 μl of 50 % glycerol/PBS solution and seal with a nail polish.

Imaging was performed by a Zeiss LSM510 meta confocal microscope equipped with a plan-apochromat 63x/1.4 oil immersion objective. Excitation lasers HeNe 543nm and 633nm, respectively for Cy3 and Cy5, were used to performe the FRET assay by acceptor photobleaching (Kenworthy 2001; Piston 2007). Upon Cy5 photobleaching, Cy3 fluorescence was releved to measure FRET efficiency. HDAC2, indirectly immunostained by Cy3 and Cy5 was used as positive control while EGFP, indirectly immunostained by Cy3, was used as negative control.

3.13 Transactivation assay.

In the luciferase transactivation assay, HEK 293 and HeLa cells were transiently transfected with the reporter construct (kindly provided by Dr ER Fearon, University of Michigan Medical School) in which the luciferase gene was driven by a fragment extending from -1359 bp 5' to +125 bp 3' of the human E-cadherin transcription start site (Hajra et al. 1999, Ji et al.1997). Reporter constructs containing 211 or 601 bp of *E-cadherin* promoter were generated by PCR and subcloning into pGL2-basic vector (Promega). All transfections experiments were performed in duplicate and normalized with the use of a co-transfected β -galactosidase construct. Cell extracts were prepared 48h post-transfection using reporter lysis buffer (Promega), followed by determination of luciferase and β -galactosidase activities. Luciferase activity was analysed by Dual-Light System (Applied Biosystems, Massachusetts, USA).

3.14 DNA extraction and methylation analysis.

DNA was prepared using QIAamp DNA Mini Kit (Qiagen) following the instruction manual. PCR primers to analyse *E-cadherin* promoter were designed by using Methprimer (Li and Dahiya 2002). The MassCLEAVE biochemistry was done as described previously (Ehrich et al. 2005). Mass spectra were acquired by using a MassARRAY Compact matrix-assisted laser desorption/ionization-time-of-flight (Sequenom) and spectra methylation ratios were generated by the Epytyper software version 1.0 (Sequenom). SEQUENOM MassARRAY platform was used for DNA methylation quantitative analysis. This system utilizes MALDI-TOF mass spectrometry in combination with RNA base specific cleavage (MassCLEAVE). A detectable pattern was then analysed for methylation status. PCR primers to analyse CDH1 promoter designed by using Methprimer (www.urogene.org/methprimer), were cdh1-10F 5'-AGGAAGAGAGGATTTAGTAATTTAGGTTAGAGGGTT-3' (position from nucleotides -190 to nucleotides -163) and cdh1-T7R 5'-CAGTAATACGACTCACTATAGGGAGAAGGCTAAATACCTACAACAACAACAAC-3' (from nucleotides +154 to nucleotides +178). For reverse primer, an additional T7 promoter tag for *in vivo* transcription was added, as well as a 10-mer tag on the forward primer to adjust for melting-temperature differences. The MassCLEAVE biochemistry was performed as previously described (Ehrich et al. 2005). Mass spectra were acquired by using a MassARRAY Compact MALDI-TOF (Compact matrix-assisted laser desorption/ionization-time-of-flight Sequenom) and spectra's methylation ratios were generated by the Epytyper software v1.0 (Sequenom). The whole procedure was performed at Sequenom GmbH Laboratories (Hamburg, Germany). The amplicons contained 32 CpG sites of which 26 were successfully analysed by MassARRAY.

3.15 Fresh human thyroid tissue samples.

Neoplastic human thyroid tissues and normal adjacent tissue or the normal contralateral thyroid lobe were obtained from surgical specimens and immediately frozen in liquid nitrogen. Thyroid tumors were collected at the Service d'Anatomo-Pathologie, Centre Hospitalier Lyon Sud, Pierre Bénite, France. The tumor samples were stored frozen until required for RNA, DNA and protein extraction.

3.16 RNA extraction, reverse transcription, and PCR analysis.

Total RNA isolation from human tissues was performed with Trizol (Invitrogen) according to the manufacturer's instructions. RNA was extracted from fresh specimens after pulverizing the tumors with a stainless steel mortar and pestle was chilled on dry ice. The integrity of the RNA was assessed by denaturing agarose gel electrophoresis. 1 µg of total RNA of each sample was reverse-transcribed with the QuantiTect Reverse Transcription (QIAGEN group) using an optimized blend of oligo-dT and random primers according to the manufacturer's instructions. To ensure that RNA samples were not contaminated with DNA, negative controls were obtained by performing PCR on samples that were not reverse transcribed but identically processed. For semiquantitative PCR (Pallante et al. 2005) the reactions were optimized for the number of cycles to ensure product intensity within the linear phase of amplification. The PCR products were separated on a 2% agarose gel, stained with ethidium bromide, and scanned using a Typhoon 9200 scanner (GE Healthcare, Piscataway, NJ). Digitized data were analysed using Imagequant (Molecular Dynamics).

Primers used to semiquantitative analysis in ChIP and Re-Chip analysis are described in paragraph 3.10.

Primers used for siRNA experiments are:

Rat-Cbx7-F, 5'-GTCATGGCCTACGAGGAGAA-3',
Rat-Cbx7-R, 5'-CTTGGGTTTCGGACCTCTCT-3';
Rat-GAPDH-F, 5'-TGATTCTACCCACGGCAAGTT-3'
Rat-GAPDH-R, 5'-TGATGGGTTTCCCATTGATGA-3'
Rat-E-cadherin-F, 5'-CAAACACATCCCCCTTCACT-3'
Rat-E-cadherin-R, 5'-GTTGACGGTCCCTTCACAGT-3'

3.17 Selection of primers, probes and qRT-PCR.

Briefly, using locked nucleic acid (LNATM) technology (Obika et al. 1997, Koshkin et al. 1998), Exiqon (Exiqon, Vedbaek, Denmark) provides 90 human prevalidated TaqMan probes of only 8-9 nucleotides that recognize 99% of human transcripts in the RefSeq database at NCBI (Mouritzen et al. 2004,

2005). Using the ProbeFinder assay design software (freely accessed on the web site www.probelibrary.com) we chose the best probe and primers pair for each gene of interest. Real-Time Quantitative TaqMan PCR was carried out with the Chromo4 Detector (MJ Research, Waltham, MA) in 96-well plates using a final volume of 20 μ l. For PCR we used 8 μ l of 2.5x RealMasterMix™ Probe ROX (Eppendorf AG, Hamburg, Germany) 200 nM of each primer, 100 nM probe and cDNA generated from 50 ng of total RNA. The conditions used for PCR were 2 min at 95°C and then 45 cycles of 20 sec at 95°C and 1 min at 60°C.

We also carried out qRT-PCR reactions with chromatin of ChIP in a final volume of 20 μ l using 10 μ l of 2x Power SYBR Green PCR Master Mix (Applied Biosystems), 200 nM of each primer and cDNA generated from 50 ng of total RNA. The conditions used for PCR were 10 min at 95°C and then 45 cycles of 30 sec at 95°C and 1 min at 60°C. Each reaction was carried out in duplicate, and at the end of the PCR run, a dissociation curve was constructed using a ramping temperature of 0.2°C per sec from 65°C to 95°C. Each reaction was carried out in duplicate. We used the $2^{-\Delta\Delta CT}$ method to calculate relative expression levels (Livak 2001).

Primers used for quantitative analysis of ChIP and Re-Chip samples are described in paragraph 3.10.

Primers used for quantitative analysis of gene expression are:

CBX7-F, 5'-CGTCATGGCCTACGAGGA-3'

CBX7-R, 5'-TGGGTTTCGGACCTCTCTT-3'

G6PD-F, 5'-ACAGAGTGAGCCCTTCTTCAA-3'

G6PD-R, 5'-GGAGGCTGCATCATCGTACT-3'

E-cadherin-F, 5'-CCACCAAAGTCACGCTGAA-3'

E-cadherin-R, 5'-TGCTTGGATTCCAGAAACG-3'

N-cadherin-F, 5'-AGGGGACCTTTTCCTCAAGA-3'

N-cadherin-R, 5'-GGGGTTGAGAATGAAGATACCA-3'

3.18 Immunohistochemistry.

The cell distribution of the CBX7 protein was assessed by immunostaining of formalin-fixed, paraffin-embedded thyroid tumor blocks retrieved from the files of the Dipartimento di Scienze Biomorfologiche e Funzionali at the University of Naples Federico II and selected to represent a wide range of thyroid neoplastic diseases. Tissue sections were processed as reported elsewhere (Pallante et al. 2005). We scored paraffin-embedded stained slides from 20 cases of FTA, 30 cases of classical PTC, 6 cases of TCV PTC, 32 cases of FTC, 12 cases of PDC, and 12 cases of ATC. As controls, we selected areas of normal thyroid parenchyma from the lobe contralateral to the tumor in 20 surgical specimens of PTC. Individual cells were scored for the expression of CBX7 by quantitative analysis performed with a computerized analyser

system (Ibas 2000, Kontron, Zeiss, Munich, Germany), as described previously (Pallante et al. 2005).

3.19 Statistical analysis.

For the comparison between two groups of experiments, Student's t test was used. The statistical significant difference was considered when $P < 0.05$. A Pearson correlation coefficient (R^2) close to 1 was considered indicative of a significant direct correlation. All experiments were done in triplicate and the data are mean \pm SD of three independent experiments.

4. RESULTS AND DISCUSSION

4.1 Proteomic analysis of CBX7 interacting proteins.

To investigate the mechanisms by which the loss of CBX7 expression correlates with the highly malignant phenotype, we searched for CBX7 interacting proteins by performing a functional proteomic analysis. Therefore, we transiently transfected the HEK 293 cells with a V5-tagged CBX7 expression vector and empty vector. About 1 mg of nucleus extract (NE) was used for the proteomic analysis.

Preliminary SDS-PAGE experiments of immunoprecipitation (IP) showed a large number of protein bands, therefore, to avoid having many aspecific proteins in the loading buffer we eluted the IP by competition with peptide V5. Before performing the preparative assay we have confirmed the expression of the CBX7-V5 construct in transfected HEK 293 cells and the efficiency of the IP by Western blotting, using anti-V5 antibody (figure 7A). Then, the preparative immunoprecipitated material was fractionated on a 12% one-dimensional (1D) gel. Preparative gel was stained with Blue Coomassie as shown in figure 7B.

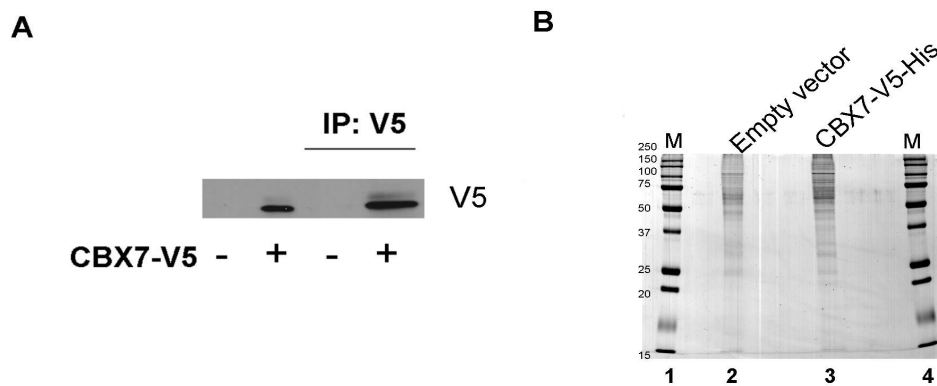


Figure 7. Proteomic analysis. **A)** A part of IP of empty vector and CBX7-V5 vector transfected HEK 293 cells were used to verify the expression of CBX7 in transfected cells and the efficiency of IP for proteomic assay. **B)** The preparative gel was stained with Blue coomassie (M:marker).

The comparison between the “empty-vector” lane, corresponding to the immunoprecipitated lysate from empty-vector transfected cells, and the “CBX7-V5” lane, which corresponds to that of CBX7 overexpressing cells,

allowed us to identify several bands that were present only in the “CBX7-V5” lane and absent in the control. Both gel lanes were sequentially cut in several fragments as shown in figure 8. Each protein band was digested *in situ* with trypsin (Shevchenko et al. 1997) and the peptide mixture obtained was directly analysed by Liquid chromatography tandem mass spectrometry (LCMSMS). The peak list of the peptides was introduced in the MASCOT MS/MS ion search software for protein identification. The final results are summarized in Table 1 (after the REFERENCES), where the names, accession numbers and function of the identified proteins are reported. It was not surprising that each excised band from 1-D gel separation contained more than one protein. We have also clustered CBX7 interacting proteins observing that there are many proteins involved in DNA regulation, export and metabolism. Generally, two peptide sequences are sufficient to identify a single protein, together with information about the score of peptides. In our proteomic experiment we identified the bait CBX7 on the basis of a single peptide sequence, because the protein was not abundant; for this reason after MASCOT we decided to take in consideration proteins present exclusively in the CBX7 IP even if identified by just a single peptide recognition.

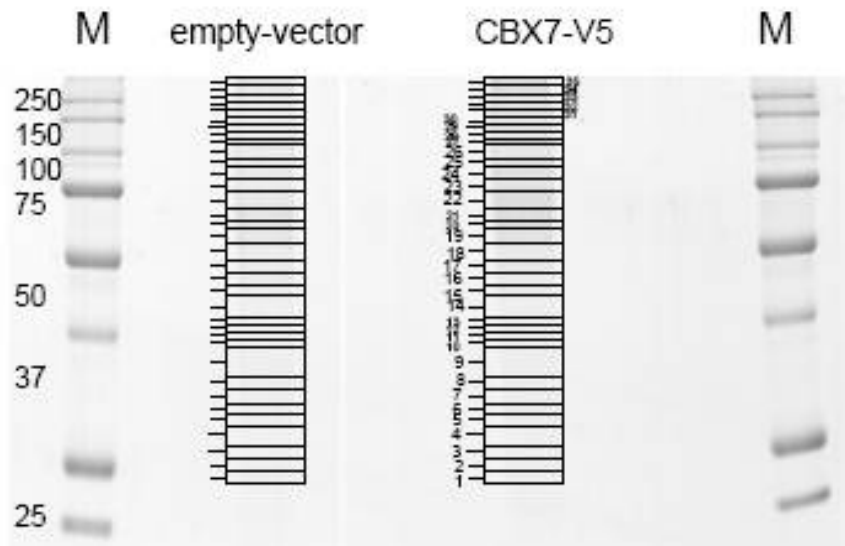


Figure 8. Proteomic analysis. IP of NE from cells transfected with empty and CBX7-V5 vectors were fractionated on one-dimensional gel. Preparative gel was stained with Blue coomassie and the gel was sequentially cut in several fragments covering all lane as shown in the figure (M:marker; number indicates a putative unique band).

4.2 *In vitro* characterization of CBX7 and HDAC2 interaction.

All CBX7 putative partners identified by the proteomic approach still needed to be confirmed by independent experiments, such as GST pull-down or co-IP. Among putative interactin protein we focused our attention on HDAC2 because of its relevance in tumor biology (Glozak and Seto 2007). HDACs catalyze the removal of acetyl groups from core histones and, because of their ability to induce local condensation of chromatin, are generally considered repressors of transcription.

To examine the specificity of this interactions and to map the regions of CBX7 proteins required for the binding to its molecular interactors, pull-down assays were performed incubating a total lysate deriving from HEK 293 cells with the CBX7 recombinant protein fused to GST (GST-CBX7), with two deletion mutants of CBX7: GST-CBX7-CHROMO (1-100 aminoacids) and GST-CBX7-NOCHROMO (55-251 aminoacids), and as negative control with GST protein (figure 9A).

First, we analysed the interaction between CBX7 and HDAC2. No associated proteins were detectable in the complexes obtained incubating TCE with the GST protein alone or with the GST-CBX7-CHROMO fusion protein. Instead there was interaction between GST-CBX7 and the GST-CBX7-NOCHROMO mutant with HDCA2. These results clearly show that the interaction between CBX7 and HDCA2 involves the region of CBX7 outside the Chromodomain. Gels were stained with Blue coomassie to show that equal amount of GST-fusion proteins were used for the pull-down assay (data not shown).

4.3 CBX7 physically interacts with HDAC2 protein.

To verify the CBX7/HDAC2 interaction *in vivo*, HEK 293 cells were transiently transfected with the V5-tagged CBX7 expression vector. Protein lysates were immunoprecipitated with either anti-V5 antibodies and immunoblotted with both anti-V5 and anti-HDAC2 antibodies (figure 9B). As shown in figure 9B, we detected the association between CBX7 and the endogenous HDAC2 protein, confirming that CBX7 and HDAC2 form complexes *in vivo*. The reciprocal experiment was performed immunoprecipitating with anti-HDAC2 and revealing with anti-V5 antibodies: it confirmed the interaction between the HDAC2 and CBX7 proteins (data not shown).

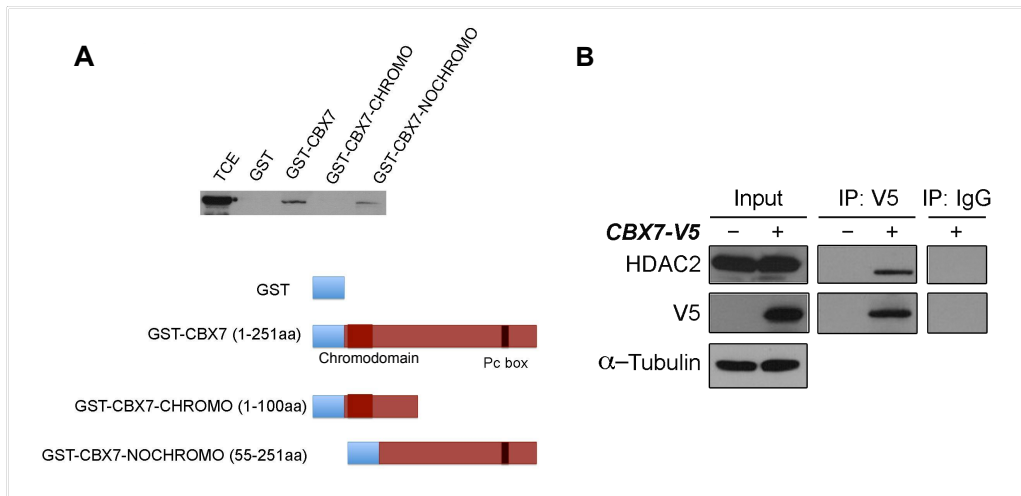


Figure 9. CBX7 interacts with HDAC2. A) GST pull-down assay with GST or recombinant GST-CBX7 proteins (wild-type and mutants as schematically reported below). The filter was incubated with an anti-HDAC2 antibody. **B)** Co-immunoprecipitation analysis. HEK 293 cells were transiently transfected with V5-tagged-CBX7 or empty vectors. After 48 h, TCE were prepared and equal amounts of proteins were immunoprecipitated with anti-HDAC2 antibodies. The immunocomplexes were analysed by Western blot analysis using anti-V5 and anti-HDAC2 antibodies. IgG antibodies indicate the negative control of immunoprecipitation using an unrelated antibody. The relative inputs deriving from empty vector or V5-tagged-CBX7 overexpressing cells were tested for α -tubulin expression.

4.4 CBX7 inhibits HDAC activity.

In order to evaluate the effects of the CBX7/HDAC2 interaction on the HDAC2 activity, we performed an HDAC activity assay on HEK 293 cells overexpressing CBX7. As shown in figure 10A, CBX7 inhibited HDAC activity, almost as strongly as 250 mmol/L sodium butyrate (NaB), a strong HDAC inhibitory compound (Kruh 1982, Rada-Iglesias et al. 2007), used as positive control. In figure 10B are shown the CBX7 expression levels in transfected cells.

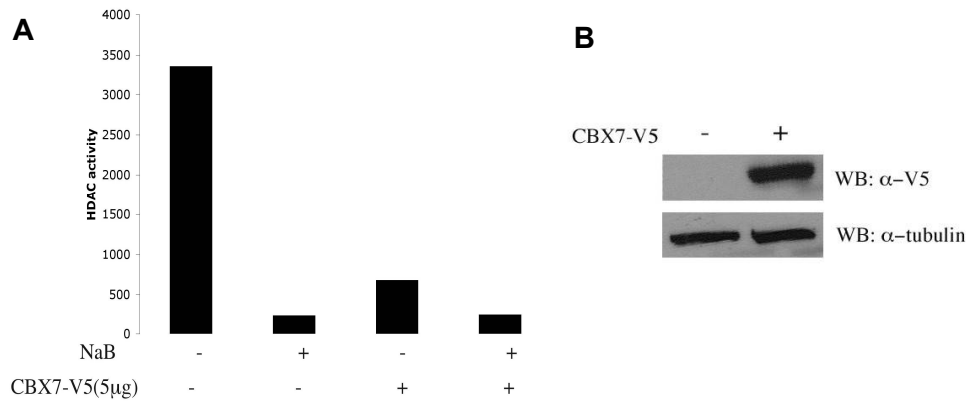


Figure 10. HDAC activity assay. **A)** HEK 293 cells were transfected with empty vector (-) and CBX7 expression vector (+). NE were assayed for HDAC activity after 48 h. Samples treated with sodium butyrate (NaB) were used as positive control. Values represent the average of three experiments +/- SD. **B)** Aliquots of the same lysates were resolved by SDS-PAGE, transferred to nitrocellulose membrane, and immunoblotted with the indicated antibodies.

To further confirm the effects of the CBX7/HDAC2 interaction on the HDAC2 activity, we transfected HeLa and NPA cells with increasing amount of transfected *CBX7*. These nuclear extracts were used to perform a HDAC activity assay. CBX7 expression significantly inhibited HDAC activity in a dose-dependent manner. The percentage of inhibition was 65.15% and 42.55% in HeLa and NPA cells, respectively, after the transfection of 10 μg *CBX7* expression vector (figure 11A and B). As positive control for HDAC inhibition, we used 250 mmol/L NaB. NE from NPA transfected with *CBX7* were immunoprecipitated with anti-HDAC2 antibodies. Then, immunoprecipitated material was tested using a HDAC activity assay. Thus we confirmed that the decreased HDAC activity detected in previously assays depends by specific HDAC2 inhibition induced by CBX7 expression. As shown in figure 10C, CBX7 specifically inhibited HDAC2 activity.

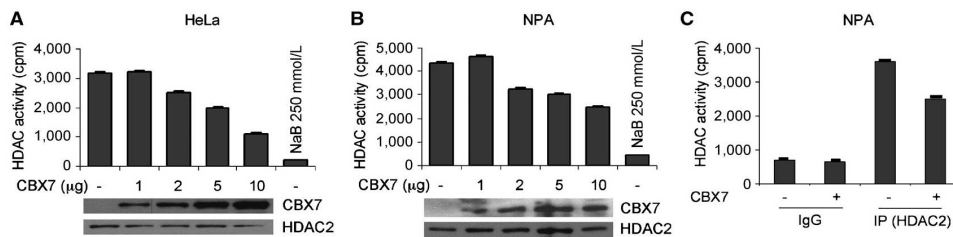


Figure 11. CBX7 inhibits HDAC activity. HeLa and NPA cells (**A** and **B**, respectively), transiently transfected with increasing amounts of CBX7 expression vector, were assayed for HDAC activity. Samples treated with NaB were used as positive control of HDAC activity inhibition. Aliquots of the same lysates were immunoblotted with the indicated antibodies. **C**) NPA cells were transiently transfected with the CBX7 expression vector or the empty vector. Nuclear extracts were immunoprecipitated using anti-HDAC2 antibodies and assayed for HDAC activity. Mean \pm SD of three independent experiments.

4.5 CBX7 and HDAC activity in tumors.

As previously shown by RT-PCR and immunohistochemistry (Pallante et al. 2008), CBX7 was strongly down-regulated in tumors. Therefore, we investigated HDAC activity in normal thyroid in comparison to ATC. As expected, in absence of CBX7 there was an increase in HDAC activity (figure 12).

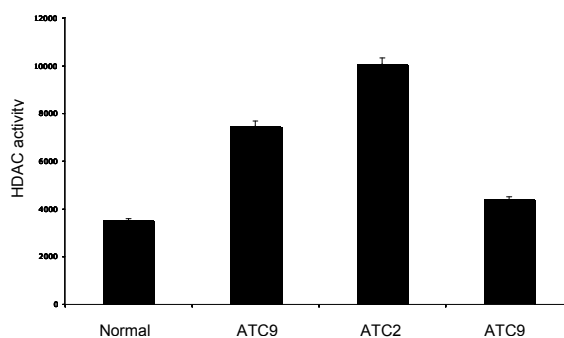


Figure 12. HDAC activity assay in anaplastic tumors (ATC). Normal thyroid and ATC sample were assayed for HDAC activity. Values represent the average of three experiments \pm SD.

4.6 CBX7 binds to the E-cadherin gene promoter.

HDACs catalyze the removal of acetyl groups from core histones (Marks et al. 2001). Because of their capacity to induce local condensation of chromatin, HDACs are generally considered repressors of transcription (Marks et al. 2001) and it is already known that HDAC2 is able to repress *E-cadherin* gene expression (Ou et al. 2007) during tumor progression. E-cadherin is one of the caretakers of the epithelial phenotype and the loss of its expression has been shown to be a critical event of Epithelial-to-Mesenchymal Transition (Thiery 2002, Thiery and Sleeman 2006). Given that CBX7 is a protein that probably binds chromatin, we asked whether the physical interaction between CBX7 and HDAC2 takes place on the human *E-cadherin* promoter. Therefore, to evaluate whether CBX7 protein was able to bind the *E-cadherin* promoter *in vivo* we performed ChIP assays. HEK 293 and HeLa cells were transfected with HA-tagged-CBX7 expression vector, tested by Western blotting for protein expression, crosslinked, and immunoprecipitated with anti-HA or anti-IgG antibodies. Immunoprecipitation of chromatin was subsequently analysed by semiquantitative PCR, using primers spanning the region of the *E-cadherin* promoter (-300 bp upstream to +40 bp downstream to the transcription start site). Anti-HA antibodies precipitated this *E-cadherin* promoter region from HEK 293 and HeLa cells transfected with HA-tagged-CBX7 protein (figure 13). No immunoprecipitation was observed with IgG antibodies and with primers for the *GAPDH* control promoter (figure 13A) indicating that the binding is specific for the *E-cadherin* promoter. We performed also PCR amplification of the immunoprecipitated DNA using primers for *p16*, *E2F1* and *SI00A4* gene promoter to validate the presence of the CBX7 on the promoters of other genes. Similar results were obtained when the NPA cells were used (data not shown). These results indicate that CBX7 protein binds the *E-cadherin* promoter region *in vivo*.

We also evaluated whether CBX7 protein binds the *E-cadherin* promoter *in vitro*, by performing an electrophoretic mobility shift assay (EMSA).

Nuclear extracts from HEK 293 cells, transiently transfected with either V5-tagged CBX7 or empty vectors, were incubated with a radiolabeled oligonucleotide corresponding to the *E-cadherin* promoter. In this way we identified a fragment of *E-cadherin* promoter containing an E-box. As shown in figure 13B, the *E-cadherin* oligonucleotide forms a specific complex (indicated in the figure as A) with nuclear proteins of cells transfected with V5-tagged CBX7, which was not present in mock-transfected cells (compare lanes 1 and 2). Binding specificity was shown by incubating the nuclear extract with a 100-fold molar excess of unlabeled *E-cadherin* oligonucleotide (lanes 3 and 4).

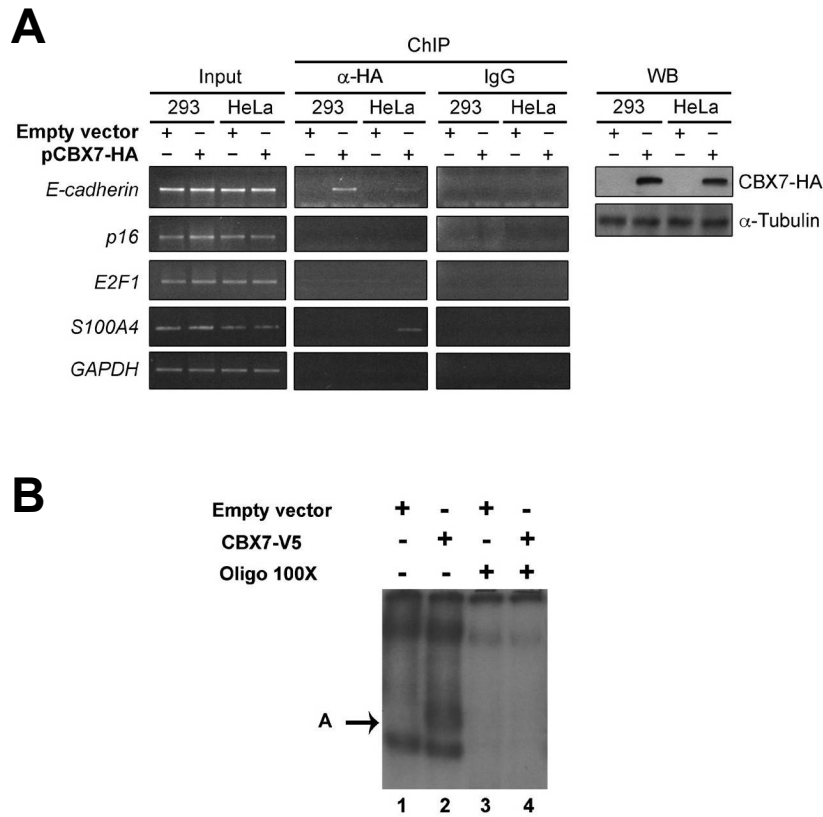


Figure 13. CBX7 binds the *E-cadherin* promoter region. **A) Chromatin immunoprecipitation (*ChIP*) assay using anti-HA antibodies in HEK 293 and HeLa cells transiently transfected with HA-tagged CBX7 or the empty vector. The associated DNA was amplified by PCR using primers specific for the human gene promoters (*left*). For the *E-cadherin* promoter, a region spanning from nucleotide –300 to +40 of the gene with respect to the TSS was used. IgG antibodies were used as an immunoprecipitation control. **B)** Electrophoretic mobility shift assay with nuclear extracts from HEK 293 cells transiently transfected with the V5-tagged CBX7 expression vector or the empty vector using the oligonucleotide spanning from nucleotide –70 to +54 of the human *E-cadherin* promoter as a probe. To assess the specificity of the binding, nuclear extracts were incubated in the presence of a 100-fold excess of unlabeled oligonucleotide used as competitor.**

4.7 CBX7 occupies the *E-cadherin* promoter with HDAC2.

Then, to investigate whether the physical interaction between CBX7 and HDAC2 takes place on the human *E-cadherin* promoter, we performed re-chromatin immunoprecipitation analysis (Re-ChIP). HEK 293 cells transiently transfected with HA-tagged CBX7 and empty vectors were crosslinked and immunoprecipitated with anti-HDAC2 antibodies. The anti-HDAC2 complexes were released, re-immunoprecipitated with anti-HA antibodies, and then analysed by PCR. The results shown in figure 14A reveal that the antibodies against HA precipitate the *E-cadherin* promoter after their release from anti-HDAC2, indicating that CBX7 occupies this promoter region together with HDAC2. The reciprocal experiment provided comparable results (figure 14B). Taken together, these results indicate that CBX7 binds the human *E-cadherin* promoter *in vivo* and participates in the same DNA-bound complexes that contain HDAC2.

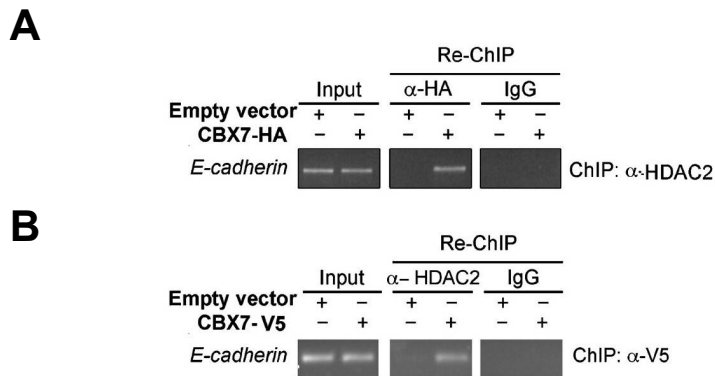


Figure 14. CBX7 binds *E-cadherin* promoter together to HDAC2. **A)** Re-ChIP experiments in which soluble chromatin immunoprecipitated with anti-HDAC2 was re-immunoprecipitated with anti-HA. IgG antibodies control refers to Re-ChIP with anti-HA. **B)** Re-ChIP experiments in which soluble chromatin immunoprecipitated with anti-V5 was re-immunoprecipitated with anti-HDAC2. IgG antibodies control refers to re-chromatin immunoprecipitation with anti-HDAC2.

4.8 CBX7 colocalize with HDAC2.

Indirect immunoFRET assay was used to further confirm the interaction between CBX7 and HDAC2 in HEK 293 cells. HEK 293 cells were transfected with pCDNA3.1-V5-CBX7. Upon fixation, cells were immunostained with anti-Cy3, that recognize anti-CBX7, and anti-Cy5, that recognize anti-HDAC2. As shown in figure 15A, CBX7 and HDAC2 perfectly colocalized in the

nucleus. Subsequently, we performed the FRET assay by acceptor photobleaching (Kenworthy 2001, Piston 2007). Upon Cy5 photobleaching, Cy3 fluorescence increased by 15% of its final value (figure 15B), which corresponds to 15% Cy3-Cy5 FRET efficiency. EGFP, the negative control, indirectly immunostained by Cy3, showed a negligible increase in Cy3 fluorescence upon Cy5 bleaching. On the contrary, HDAC2 indirectly immunostained by Cy3 and Cy5 was the positive control and showed a remarkable increase in Cy3 fluorescence upon Cy5 bleaching. Therefore, the FRET assay succeeded in distinguishing CBX7/HDAC2 colocalization and in confirming CBX7/HDCA2 interaction.

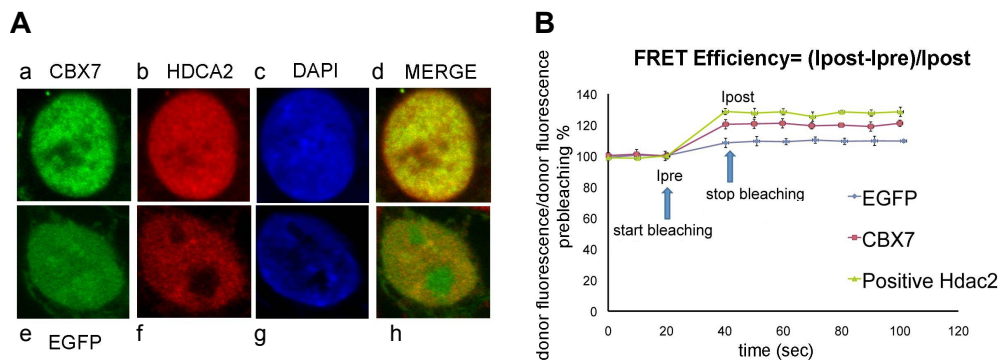


Figure 15. CBX7/HDAC2 colocalization. **A)** (a-c) Immunostaining of a CBX7-transfected HEK 293 cell with anti-CBX7 (green), anti-HDAC2(red) and DAPI (blue); (d) merging image of a, b and c; (e-g) immunostaining of a EGFP-transfected HEK 293 cell with anti-EGFP (green), anti-HDAC2 (red) and DAPI (blue); (h) merging image of e, f and g. **B)** Summary of FRET acceptor photobleaching.

4.9 CBX7 positively regulates the *E-cadherin* promoter.

To evaluate the effect of CBX7 expression on *E-cadherin* transcription, HEK 293 cells were transiently cotransfected with an expression vector encoding *CBX7* and with a reporter vector carrying the *luciferase* gene under the control of the *E-cadherin* promoter. As shown in figure 16A, CBX7 increases the transcriptional activity of the *E-cadherin* promoter in a dose-dependent manner. The same results were obtained on the NPA and TPC1 cell lines (data not show). The treatment of cells with trichostatin A (TSA), a potent inhibitor of HDAC activity (Ou et al. 2007), cooperates with CBX7 to induce *E-cadherin* gene transcription (figure 16B). These results strongly suggest that CBX7 protein is involved in the *E-cadherin* gene transcription likely counteracting with the already known inhibitory effect of HDAC2 on this gene promoter.

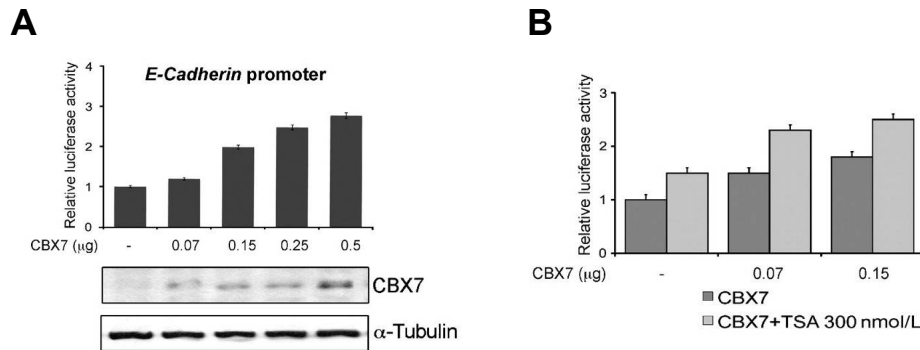


Figure 16. CBX7 enhances *E-cadherin* promoter activity. **A)** Dose-response analysis of increasing amounts of *CBX7* on the *E-cadherin* luciferase-reporter vector transiently transfected into HEK 293 cells. Western blot analysis confirmed the increasing amounts of *CBX7* expression. α -Tubulin expression served as a control of equal protein loading. **B)** Dose-response analysis of increasing amounts of *CBX7* on the *E-cadherin* luciferase-reporter vector transiently transfected into HEK 293 cells treated or not with 300 nmol/L of HDAC inhibitor *TSA*.

To identify the region of *CBX7* required for *E-cadherin* promoter activation, we constructed two *CBX7* deletion mutants in the expression vector pCefl-HA: pCefl-HA-*CBX7*-CHROMO (1-100 amino acids) and pCefl-HA-*CBX7*-NOCHROMO (55-251 amino acids). Transfection of the mutant pCefl-HA-*CBX7*-CHROMO, containing only the chromodomain, did not induce transcriptional activation of the *E-cadherin* promoter. Conversely, the mutant lacking the chromodomain, pCefl-HA-*CBX7*-NOCHROMO, induced a moderate activation of the *E-cadherin* promoter. Thus, these data indicate that chromodomain is not essential for the *CBX7* transcriptional activity on the *E-cadherin* promoter (figure 17A).

To identify the regulatory elements essential for the activity of *CBX7* on the *E-cadherin* promoter, we also tested some deletion mutants of the *E-cadherin* promoter: *E-cadherin* 601 and *E-cadherin* 211. Activation of *E-cadherin* promoter by *CBX7* protein was maintained on full-length and 601 mutants of *E-cadherin* promoter. Conversely, the 211 mutant, which lacks a portion of -70/+54 sequence (able to bind *CBX7*), was not activated by *CBX7* protein (figure 17B). In fact sequence elements within the proximal 108 bp of *E-cadherin* promoter include the CCAAT-box, two E-box elements that may bind basic helix-loop-helix protein, and a consensus sequence for binding zinc-finger proteins such as Sp1 and WT1 (Ji et al. 1997, Hajra et al. 1999).

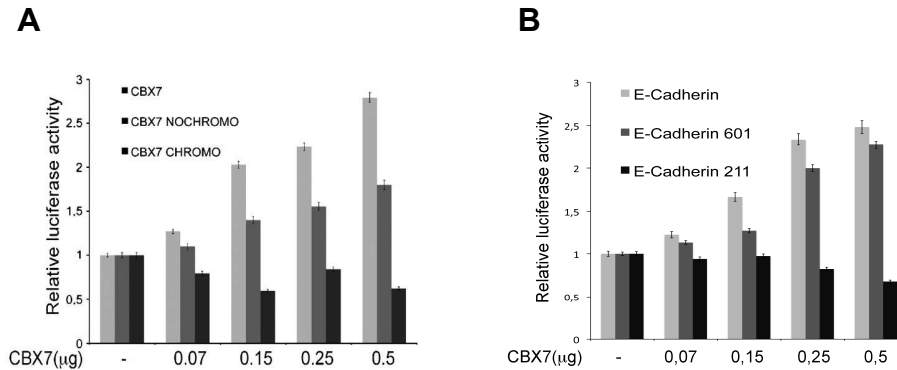


Figure 17. Identification of essential elements for the activity of CBX7 on *E-cadherin* promoter. **A) Dose-response analysis of increasing amounts of *CBX7* and the two *CBX7*-deletion mutants (schematically illustrated in figure 9A) on the *E-cadherin* luciferase-reporter vector transiently transfected into HEK 293 cells. **B)** Dose response analysis of increasing amounts of *CBX7* on the two deletion mutant of *E-cadherin* promoter cloned in luciferase-reporter vector.**

Moreover, to show that the expression of *E-cadherin* is directly regulated by *CBX7*, we generated some clones of NPA cells (NPA 4-11 and NPA 5-11) in which *CBX7* cDNA was under the control of a tetracycline-regulated promoter. Western blot analysis (figure 18A, top) and quantitative RT-PCR experiment (figure 18A bottom) show that the expression of *CBX7* increases the levels of *E-cadherin* only after treatment with tetracycline.

To further confirm the role of *CBX7* in the modulation of the *E-cadherin* gene, we evaluated the expression of the *E-cadherin* gene in the normal rat thyroid cell line PC C13 in which the synthesis of *Cbx7* was suppressed by RNA interference. The knockdown of the *Cbx7* mRNA levels, observed at 48 h after treatment, resulted in the reduction of *E-cadherin* mRNA levels in comparison with the untreated cells or those treated with the nonsilencing control small interfering RNA (figure 18B).

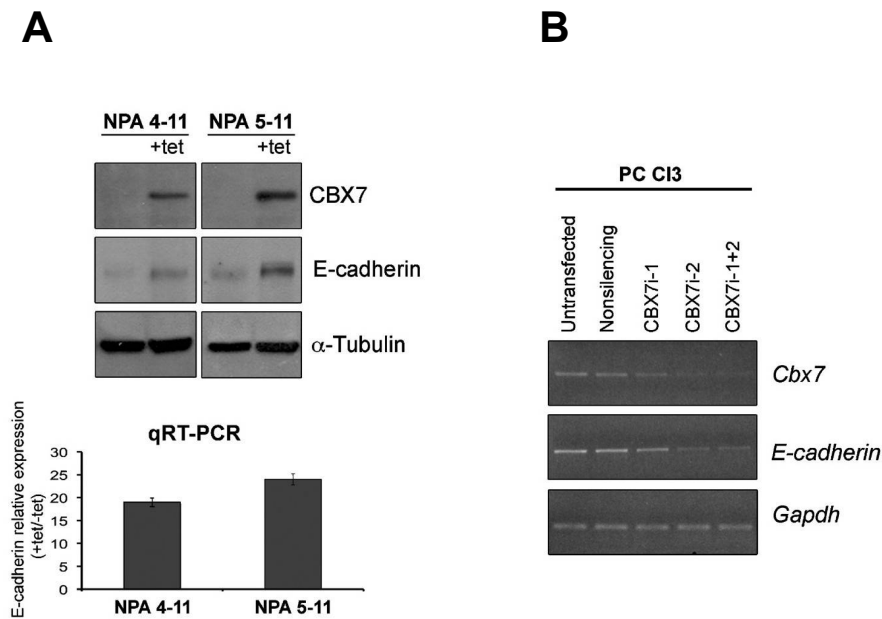


Figure 18. CBX7 modulates E-cadherin expression. A) top, Western blot analysis of CBX7 and E-cadherin expression in the NPA cell clones 4-11 and 5-11 treated or not with tetracycline. The treatment with tetracycline (+tet) was indicated on the top. α -Tubulin expression served as a control of equal protein loading. **Bottom**, quantitative RT-PCR (qRT-PCR) analysis of E-cadherin expression in the same NPA cell clones. The relative expression indicates the relative change in E-cadherin expression levels between treated cells versus the untreated ones, assuming that the value of E-cadherin expression in the untreated cells is equal to 1. **B)** *Cbx7* and *E-cadherin* gene expression was evaluated by RT-PCR in rat PC C13 cells after treatment with small interfering RNA against rat *Cbx7*. The expression of *GAPDH* was used to normalize the amounts of RNAs used in the experiment.

4.10 CBX7 expression results in increased histone acetylation of the E-cadherin promoter.

During the last years, chromatin remodeling and histone modifications have emerged as the main mechanisms in the control of gene expression and the connection between DNA methylation and histone deacetylation in the silencing of genes has been established (Marks et al. 2001, van Leeuwen and van Steensel 2005). Because we have shown previously that CBX7 (a) interacts with HDAC2 on the human *E-cadherin* promoter, (b) reduces the activity of HDACs, (c) increases the transcriptional activity of the *E-cadherin* promoter in

a dose-dependent manner, we hypothesized that the positive effect on *E-cadherin* activation by CBX7 may be due to its ability to reduce the HDAC activity on the *E-cadherin* promoter. Therefore, we have evaluated the lysine acetylation of histone tails at the *E-cadherin* promoter.

HEK 293 cells were transiently transfected with V5-tagged CBX7 expression vector or empty vector. Then, the cells were crosslinked and DNA-chromatin was immunoprecipitated with anti-H3 or anti-H4 acetylated or IgG antibodies. The immunoprecipitated chromatin was subsequently analysed by quantitative PCR using primers spanning the region of the *E-cadherin* promoter (−70 bp upstream to +54 bp downstream to the TSS; ref. Li et al. 2007). As shown in figure 19, higher amounts of H3 and H4 acetylated tails were detected in the *E-cadherin* promoter in the cells transfected with CBX7, with respect to those detected in mock-transfected cells, indicating an increased histone acetylation in CBX7-transfected cells, likely due to the ability of CBX7 to reduce HDAC activity. We also treated the cells, transfected or not with CBX7, with TSA to verify the HDAC activity on H3 and H4 tails. As shown in the same figure, there were higher amounts of H3 and H4 acetylated tails in CBX7-transfected samples treated with TSA than in untreated cells. These results indicate that CBX7 protein regulates the *E-cadherin* expression by modifying histone acetylation at its promoter, likely reducing HDAC activity.

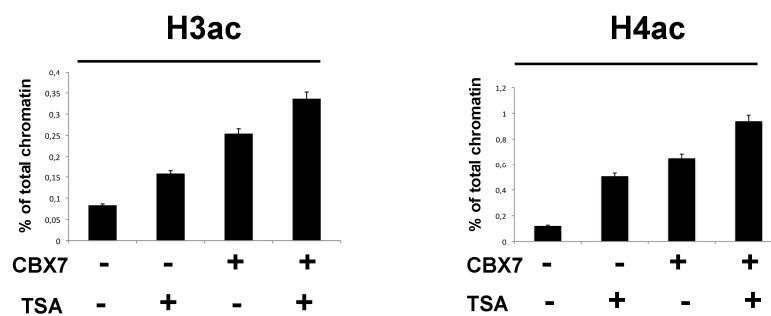


Figure 19. Analysis of the histone acetylation of the human *E-cadherin* promoter. HEK 293 cells transiently transfected with V5-tagged CBX7 expression or empty vectors, and treated or not with TSA for 24 h, were subjected to chromatin immunoprecipitation using anti-acetyl histone H3 (*H3ac*; left) and anti-acetyl histone H4 (*H4ac*; right) and analysed by quantitative RT-PCR for the *E-cadherin* promoter.

4.11 Increased methylation of H3K4 and decreased methylation of H3K9 and H4K20 in CBX7-transfected cells.

Lysine methylation can have different effects depending on which residue is modified: methylation of H3K4 and H3K36 is generally associated with transcribed chromatin; in contrast, methylation of H3K9, H3K27, and H4K20 generally correlates with gene repression (Li et al. 2007). Therefore, we have evaluated the lysine methylation status of histone tails of *E-cadherin* promoter in presence or absence of CBX7.

HEK 293 cells were transiently transfected with V5-tagged CBX7 or empty vectors and crosslinked, and DNA-chromatin was immunoprecipitated with anti-H3K4m2, anti-H3K4m3, anti-H3K9m2, anti-H3K9m3, and anti-H4K20m3 or IgG antibodies. The immunoprecipitated chromatin was subjected to PCR with specific primers for the *E-cadherin* promoter region (-70/+54).

Higher amounts of chromatin immunoprecipitated for H3K4m2 and H3K4m3 were observed in the CBX7-transfected cells compared with the control ones, indicating that this lysine is methylated in a higher proportion in CBX7-transfected cells with respect to that observed in control cells. Conversely, in the case of chromatin immunoprecipitated for the H3K9m2, H3K9m3, and H4K20m3, higher amounts of chromatin were detected in control cells, indicating that these sites were methylated at a higher level in the control cells versus CBX7-transfected cells (figure 20). These data indicate that CBX7 is able to alter the methylation status of specific lysines of *E-cadherin* promoter, promoting the transcriptional activity of *E-cadherin* promoter.

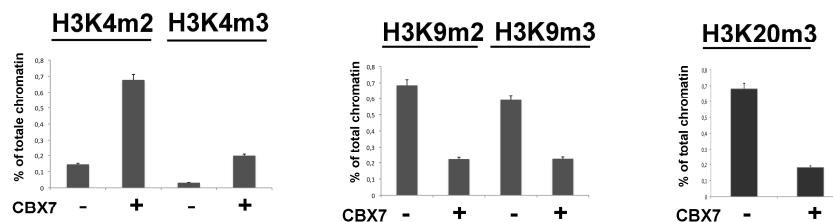


Figure 20. Analysis of the histone methylation of the human *E-cadherin* promoter. HEK 293 cells transiently transfected with V5-tagged CBX7 expression or empty vectors were subjected to chromatin immunoprecipitation using anti-H3K4m2 and anti-H3K4m3 (*left*), anti-H3K9m2 and anti-H3K9m3 (*middle*), and anti-H4K20m3 (*right*) and analysed by quantitative RT-PCR for the *E-cadherin* promoter.

4.12 CBX7 and E-cadherin expression levels are correlated in human thyroid carcinomas.

E-cadherin down-regulation, due to epigenetic mechanisms, including transcriptional repression, also mediated by HDAC activity, and promoter hypermethylation is a frequent event during human cancer progression (Koizume et al. 2002, Peinado et al. 2004). Because previous experiments showed that CBX7 expression was lost in most advanced thyroid cancers, we hypothesized the down-regulation of E-cadherin as a possible mechanism by which loss of CBX7 is involved in advanced stages of thyroid carcinogenesis. This hypothesis was also supported by recent results showing a role of polycomb repressive complex 1/2 in the regulation of E-cadherin expression (Cao et al. 2008).

Therefore, we analysed *CBX7* and *E-cadherin* mRNA levels in human thyroid carcinomas of different histotypes (Figure 21A). *CBX7* and *E-cadherin* mRNA levels were drastically reduced in anaplastic thyroid carcinoma, whereas just a weak decrease was observed for both genes in papillary thyroid carcinoma. The Epithelial-to-Mesenchymal Transition in our tumor samples was also confirmed by the increased N-cadherin expression (figure 21A).

We found a positive statistical correlation between CBX7 and E-cadherin expression in human thyroid carcinomas as shown in figure 21B. We also compared CBX7 and E-cadherin at protein level, by immunohistochemical analysis, confirming that E-cadherin protein expression parallels that of CBX7 (figure 21C).

Because hypermethylation of the *E-cadherin* promoter has been postulated to play a critical role in the loss of E-cadherin expression and has been reported previously in other cancers, we decided to investigate the DNA methylation status of *E-cadherin* promoter (Hajra and Fearon 2002). We analysed DNA methylation status of 26 CpG sites located in a 368-bp region spanning the *E-cadherin* gene TSS (figure 21D, *inset*) on 16 papillary thyroid carcinomas, 15 follicular variants of papillary thyroid carcinomas, 4 anaplastic thyroid carcinomas, and 4 normal thyroid tissue samples. A very low level of methylation was present in both normal and tumor samples, with the exception of only one anaplastic thyroid carcinoma sample in which a high degree of methylation was detected (figure 21D).

Therefore, epigenetic mechanisms, other than hypermethylation of the *E-cadherin* promoter, have a critical role in the down-regulation of E-cadherin expression.

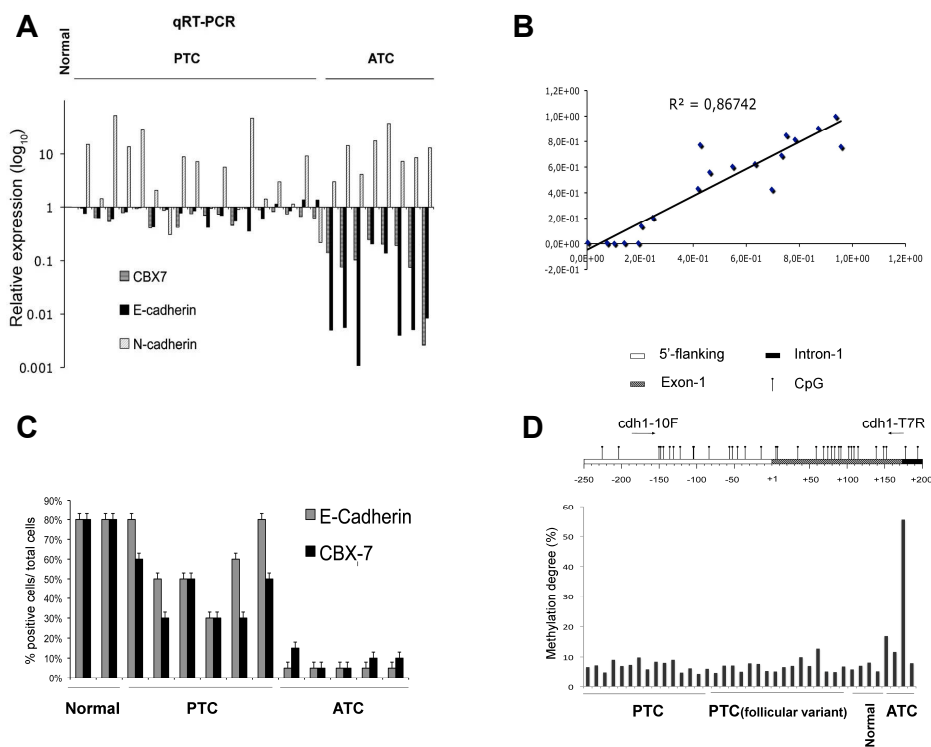


Figure 21. *CBX7* and *E-cadherin* gene expression levels are correlated in human thyroid carcinomas. **A)** *CBX7*, *E-cadherin*, and *N-cadherin* gene expression in thyroid tumor samples was analysed by quantitative RT-PCR. Relative expression indicates the change in expression levels between tumor and normal samples, assuming that the value of each normal sample is equal to 1. **B)** Positive statistical correlation between *CBX7* and *E-cadherin* expression in human thyroid carcinomas analysed in **A**. R^2 , Pearson correlation coefficient. **C)** Immunohistochemical analysis of normal and tumor samples stained with anti-*CBX7* and anti-*E-cadherin* antibodies. The percentage of positive cells for the staining/total number of cells was reported. **D) top**, positions of the primers used for amplifications of the region spanning from nucleotide -200 to $+200$ of *E-cadherin* with respect to the TSS; **bottom**, average methylation degree of 26 CpG sites at *E-cadherin* promoter in human thyroid carcinomas. *PTC*, papillary thyroid carcinoma; *ATC*, anaplastic thyroid carcinoma.

5. CONCLUSIONS

In a previous study our group has reported that *CBX7* gene expression was drastically down-regulated in thyroid carcinomas and progressively decreased with malignant grade and neoplastic stage (Pallante et al. 2008).

Thus, to elucidate the mechanism by which the loss of *CBX7* expression is involved in cancer progression, we investigated, by proteomic approach, proteins interacting with *CBX7*. Among the *CBX7* interacting proteins, we selected the *HDAC2* because of its relevance in tumor biology. *HDACs* regulate the expression and activity of numerous proteins involved in both cancer initiation and cancer progression, inducing a nonpermissive chromatin conformation that prevents the transcription of genes involved in tumorigenesis such as *E-cadherin* (Glozak and Seto 2007). In addition to histone, *HDACs* bind to and deacetylate a variety of protein targets including transcription factors and other abundant cellular proteins implicated in the control of cell growth, differentiation and apoptosis (Smith 2008). Therefore *HDAC* can alter the expression and function of cancer associated proteins by both transcriptional and post-translational mechanisms. *HDACs*, in fact, are often overexpressed in many tumors: for example, prostate cancer cells overexpress *HDAC1*, whereas gastric carcinomas, colorectal carcinomas, cervical dysplasias and endometrial stromal sarcomas all overexpress *HDAC2* (Glozak and Seto 2007).

In this study, we show that *CBX7* physically interacts with *HDAC2* protein and is able to inhibit its activity. It is known that *HDAC2* represses *E-cadherin* expression during tumor progression therefore we investigated whether the physical interaction between *CBX7* and *HDAC2* takes place on the human *E-cadherin* promoter. This evidence aimed us to hypothesize a role for *CBX7* as a transcriptional regulator of *E-cadherin* expression. Our data, in fact, suggested that the loss of *CBX7* expression is strictly correlated with the acquisition of malignant phenotype, often, accompanied by the loss of the epithelial features and the gain of a mesenchymal phenotype, a process known as Epithelial-to-Mesenchymal Transition (EMT). One of the caretakers of the epithelial phenotype is *E-cadherin*, which loss leads to disruption of cell junctions and consequent gain of cell mobility. In fact, a direct correlation between lack of *E-cadherin* expression and loss of the epithelial phenotype has been demonstrated (Thiery 2002). In most cancers, *E-cadherin* down-regulation during neoplastic progression occurs by epigenetic mechanisms, including transcriptional repression, in some cases mediated by *HDAC* activity (Peinado et al. 2004), and hypermethylation of the promoter (Hajra and Fearon 2002). Only in a few cases mutations have been found in the *E-cadherin* gene leading to the absence or the expression of a nonfunctional protein (Thiery 2002). For this reason, we evaluated *E-cadherin* expression in human thyroid carcinomas of different histotypes: an evident correlation was found between *CBX7* and *E-cadherin* expression levels in human thyroid carcinomas, both being drastically down-

regulated in anaplastic thyroid carcinomas in comparison with the normal thyroid tissue. Interestingly, no hypermethylation of *E-cadherin* promoter was observed in thyroid carcinomas. Our hypothesis about the role of CBX7 as a transcriptional regulator of E-cadherin seems also supported by recent results showing the involvement of PRC1/PRC2 complexes in the regulation of E-cadherin expression (Cao et al. 2008).

We confirmed, by ChIP, that both HDAC2 and CBX7 bind the *E-cadherin* promoter. We also showed the ability of CBX7 to positively regulate E-cadherin expression by interacting with HDAC2 and inhibiting its activity on the *E-cadherin* promoter. Further, we demonstrated that, in the presence of the CBX7 protein, there is an increased histone acetylation of the *E-cadherin* promoter, validating our hypothesis that CBX7 recruits HDCA2 on the *E-cadherin* promoter. Moreover, we show modifications in the histone methylation state on the *E-cadherin* promoter in the cells transfected with CBX7 confirming a relationship between acetylation and DNA methylation (Kouzarides 2007).

Finally, here we propose a novel pathway regulating the progression step of carcinogenesis in which the CBX7 protein, whose loss of expression correlates with a highly malignant phenotype, is a key molecule. Indeed, our results indicate that the loss of CBX7 expression contributes to cancer progression allowing the down-regulation of E-cadherin expression because of the lack of its inhibitory effect on HDAC activity on the *E-cadherin* promoter.

7. REFERENCES

1. Allfrey VG, Faulkner R and Mirsky AE. Acetylation and methylation of histones and their possible role in the regulation of RNA synthesis. *Proc. Natl. Acad. Sci. U S A* 1964;51:786-794.
2. Annunziato AT and Hansen JC. Role of histone acetylation in the assembly and modulation of chromatin structures. *Gene Expr* 2000;9, 37–61.
3. Barallo-Gimeto A, Nieti MA. The Snail genes as inducers of cell movement and survival: implications in development and cancer. *Development* 2005;132:3151-3161.
4. Batlle E, Sancho E, Francí C, Domínguez D, Monfar M, Baulida J, García De Herreros A. The transcription factor snail is a repressor of E-cadherin gene expression in epithelial tumour cells. *Nat Cell Biol* 2000;2:84-9.
5. Behrens J, Lowrick O, Klein-Hitpass L, Birchmeier W. The E-Cadherin Promoter: Functional Analysis Of A G.C-Rich Region And An Epithelial Cellspecific Palindromic Regulatory Element. *Proc Natl Acad Sci Usa* 1991;88:11495-11499.
6. Bernard D, Martinez-Leal JF, Rizzo S, Martinez D, Hudson D, Visakorpi T, Peters G, Carnero A, Beach D, Gil J. CBX7 controls the growth of normal and tumor-derived prostate cells by repressing the Ink4a/Arf locus. *Oncogene* 2005;24(36):5543-51.
7. Bernstein E, Duncan EM, Masui O, Gil J, Heard E, et al. Mouse polycomb proteins bind differentially to methylated histone H3 and RNA and are enriched in facultative heterochromatin. *Mol Cell Biol* 2006;26:2560–2569.
8. Birchmeier W, Behrens J. Cadherin expression in carcinomas: role in the formation of cell junctions and the prevention of invasiveness. *Biochim Biophys Acta* 1994;27;1198(1):11-26. Review.
9. Bolós V, Peinado H, Perez-Moreno MA, Fraga MF, Esteller M, Cano A. The Transcription Factor Slug Represses E-Cadherin Expression And Induces Epithelial To Mesenchymal Transitions: A Comparison With Snail And E47 Repressors. *J Cell Sci* 2003;116:499-511.
10. Bracken AP, Dietrich N, Pasini D, Hansen KH, Helin K. Genome-wide mapping of Polycomb target genes unravels their roles in cell fate transitions. *Genes Dev* 2006;20:1123–1136.
11. Briehner WM, Yap AS, Gumbiner BM. Lateral dimerization is required for the homophilic binding activity of C-cadherin. *J Cell Biol* 1996;135(2):487-96.
12. Cano A, Perez-Moreno MA, Rodrigo I, Locascio A, Blanco MJ, del Barrio MG, Portillo F, Nieto MA. The transcription factor Snail controls epithelial-mesenchymal transitions by repressing E-cadherin expression. *Nat Cell Biol* 2000;2:76–83.

13. Cao Q, Yu J, Dhanasekaran SM, et al. Repression of E-cadherin by the polycomb group protein EZH2 in cancer. *Oncogene* 2008;27:7274–84.
14. Cao R, Tsukada Y, Zhang Y. Role of Bmi-1 and Ring1A in H2A ubiquitylation and Hox gene silencing. *Mol Cell* 2005;20:845–854.
15. Carrozza MJ, Utley RT, Workman JL and Cote J. The diverse functions of histone acetyltransferase complexes. *Trends Genet* 2003;19:321-329.
16. Cavallaro U, Christofori G. Cell adhesion and signalling by cadherins and Ig-CAMs in cancer. *Nat Rev Cancer* 2004;4:118–132.
17. Curcio F, Ambesi-Impimombato FS, Perrella G, Coon HG. Long-term culture and functional characterization of follicular cells from adult normal human thyroids. *Proc Natl Acad Sci U S A* 1994;91:9004-8.
18. De Felice M, Di Lauro R. Thyroid Development and Its Disorders: Genetics and Molecular Mechanisms. *Endocrine Reviews* 2004;25:722–46.
19. Delys L, Detours V, Franc B, et al. Gene expression and the biological phenotype of papillary thyroid carcinomas. *Oncogene* 2007;26:7894–903.
20. Dignam JD, Lebovitz RM, Roeder RG. Accurate transcription initiation by RNA polymerase II in a soluble extract from isolated mammalian nuclei. *Nucleic Acids Res* 1983;11(5):1475-89.
21. Dokmanovic, M, and Marks PA. Prospects: histone deacetylase inhibitors. *J Cell Biochem* 2005;96:293-304.
22. Drummond DC, Noble CO, Kirpotin DB, Guo Z, Scott GK, and Benz CC. Clinical development of histone deacetylase inhibitors as anticancer agents. *Annu Rev Pharmacol Toxicol* 2005;45:495-528.
23. Egger G, Liang G, Aparicio A, Jones PA. Epigenetics in human disease and prospects for epigenetic therapy. *Nature* 2004;429(6990):457-63. Review.
24. Ehrich M, Nelson M, Stanssens P, Zabeau M, Liloglou T, Xinarianos G, Cantor CR, Field JK, van den Boom D. Quantitative high-throughput analysis of DNA methylation patterns by base-specific cleavage and mass spectrometry. *Proc Natl Acad Sci U S A* 2005;102:15785-90.
25. Fagman H, Grände M, Edsbacke J, Semb H, Nilsson M. Expression of classical cadherins in thyroid development: maintenance of an epithelial phenotype throughout organogenesis. *Endocrinology* 2003;144(8):3618-24.
26. Faraldo ML, Rodrigo I, Behrens J, Birchmeier W, Cano A. Analysis Of The E-Cadherin And P-Cadherin Promoters In Murine Keratinocyte Cell Lines From Different Stages Of Mouse Skin Carcinogenesis. *Mol Carcinog* 1997;20:33-47.
27. Fischle W, Wang Y, Jacobs SA, Kim Y, Allis CD, et al. Molecular basis for the discrimination of repressive methyl-lysine marks in histone H3 by Polycomb and HP1 chromodomains. *Genes Dev* 2003;17:1870–1881.

28. Fusco A, Berlingieri M, Di Fiore PP, Portella G, Grieco M, Vecchio G. One- and two-step transformations of rat thyroid epithelial cells by retroviral oncogenes. *Mol Cell Biol* 1987;7:3365-70.
29. Gayther SA, Goringe KL, Ramus SJ, Huntsman D, Roviello F, Grehan N, Machado JC, Pinto E, Seruca R, Halling K, MacLeod P, Powell SM, Jackson CE, Ponder BA, Caldas C. Identification of germ-line E-cadherin mutations in gastric cancer families of European origin. *Cancer Res* 1998;15;58(18):4086-9.
30. Gil J, Bernard D, Martínez D, Beach D. Polycomb CBX7 has a unifying role in cellular lifespan. *Nat Cell Biol* 2004;6(1):67-72.
31. Gil J, Peters G. Regulation of the INK4b-ARF-INK4a tumour suppressor locus: all for one or one for all. *Nat Rev Mol Cell Biol* 2006;7:667-677.
32. Giroldi LA, Bringuier PP, de Weijert M, Jansen C, van Bokhoven A, Schalken JA. Role of E boxes in the repression of E-cadherin expression. *Biochem Biophys Res Commun* 1997;241(2):453-8.
33. Glozak MA, Seto E. Histone deacetylases and cancer. *Oncogene* 2007;26:5420-32.
34. Gregoret IV, Lee YM and Goodson HV. Molecular evolution of the histone deacetylase family: functional implications of phylogenetic analysis. *J Mol Biol* 2004;338:17-31.
35. Grozinger CM and Schreiber SL. Deacetylase enzymes: biological functions and the use of small-molecule inhibitors. *Chem Biol* 2002;9:3-16.
36. Grunstein M. Histone acetylation in chromatin structure and transcription. *Nature* 1997;389:349-352.
37. Guilford P, Hopkins J, Harraway J, McLeod M, McLeod N, Harawira P, Taite H, Scoular R, Miller A, Reeve AE. E-cadherin germline mutations in familial gastric cancer. *Nature* 1998;392(6674):402-5.
38. Hajra KM, Fearon E. Cadherin and catenin alterations in human cancer. *Genes Chromosomes Cancer* 2002;34:255-68.
39. Hajra KM, Ji X, Fearon ER. Extinction of E-cadherin expression in breast cancer via a dominant repression pathway acting on proximal promoter elements. *Oncogene* 1999;51:7274-9.
40. Hay ED. An overview of epithelio-mesenchymal transformation. *Acta Anat* 1995;154:8-20.
41. Hennig G, Behrens J, Truss M, Frisch S, Reichmann E, Birchmeier W. Progression of carcinoma cells is associated with alterations in chromatin structure and factor binding at the E-cadherin promoter in vivo. *Oncogene* 1995;11(3):475-84.
42. Hennig G, Lowrick O, Birchmeier W, Behrens J. Mechanisms identified in the transcriptional control of epithelial gene expression. *J Biol Chem* 1996;271:595-602.
43. Hirohashi S. Inactivation of the E-cadherin-mediated cell adhesion system in human cancers. *Am J Pathol* 1998;153(2):333-9. Review.

44. Huber MA, Kraut N, Beug H. Molecular requirements for epithelial-mesenchymal transition during tumor progression. *Curr Opin Cell Biol* 2005;17:548–558.
45. Ji X, Woodard AS, Rimm DL, Fearon ER. Transcriptional defects underlie loss of E-cadherin expression in breast cancer. *Cell Growth Differ* 1997;8:773–8.
46. Jiang WG. E-cadherin and its associated protein catenins, cancer invasion and metastasis. *Br J Surg* 1996;83(4):437-46.
47. Jones DO, Cowell IG, Singh PB. Mammalian chromodomain proteins: their role in genome organisation and expression. *Bioessays* 2000;22(2):124-37. Review.
48. Kenworthy A. Imaging protein-protein interactions using fluorescence resonance energy transfer microscopy. *Methods* 2001;24:289-96.
49. Kirmizis A, Santos-Rosa H, Penkett CJ, et al. Arginine methylation at histone H3R2 controls deposition of H3K4 trimethylation. *Nature* 2007;449:928–32.
50. Kondo T, Ezzat S, Asa SL. Pathogenetic mechanisms in thyroid follicular-cell neoplasia. *Nat Rev Cancer* 2006;6:292–306.
51. Koizume S, Tachibana K, Sekiya T, Hirohashi S, Shiraishi M. Heterogeneity in the modification and involvement of chromatin components of the CpG island of the silenced human CDH1 gene in cancer cells. *Nucleic Acids Res* 2002;30:4770–80.
52. Koshkin AA, Nielsen P, Rajwanshi VK, Kumar R, Meldgaard M, Olsen CE, Wengel J. LNA (Locked nucleic acids): synthesis of the adenine, cytosine, guanine, 5-methylcytosine, thymine and uracil biocyclonucleoside monomers, oligomerisation and unprecedented nucleic acid recognition. *Tetrahedron* 1998; 54: 3607-30.
53. Kouzarides T. Chromatin modifications and their function. *Cell* 2007;128:693–705.
54. Kruh J. Effects of sodium butyrate, a new pharmacological agent, on cells in culture. *Mol Cell Biochem* 1982;42:65–82.
55. Kuzmichev A, Nishioka K, Erdjument-Bromage H, Tempst P, Reinberg D. Histone methyltransferase activity associated with a human multiprotein complex containing the Enhancer of Zeste protein. *Genes Dev* 2002;16(22):2893-905.
56. Lessard J, Sauvageau G. Bmi-1 determines the proliferative capacity of normal and leukaemic stem cells. *Nature* 2003;423:255–260.
57. Li B, Gogol M, Carey M, Lee D, Seidel C, Workman JL. The role of chromatin during transcription. *Science* 2007;316:1050–4.
58. Li LC, Dahiya R. MethPrimer: designing primers for methylation PCRs. *Bioinformatics* 2002;18:1427–31.
59. Livak KJ ST. Analysis of relative gene expression data using real-time quantitative PCR and the 2(-Delta Delta C(T)) Method. *Methods* 2001;25:402-8.

60. Luger K, Mader AW, Richmond RK, Sargent DF and Richmond TJ. Crystal structure of the nucleosome core particle at 2.8 Å resolution. *Nature* 1997;389:251-260.
61. Luger, K., and T. J. Richmond. The histone tails of the nucleosome. *Curr Opin Genet Dev* 1998;8:140-146.
62. Marks P, Rifkind RA, Richon VM, et al. Histone deacetylases and cancer: causes and therapies. *Nat Rev Cancer* 2001;1:194–202.
63. Mei S, Ho AD and Mahlknecht U. Role of histone deacetylase inhibitors in the treatment of cancer (review). *Int J Oncol* 2004;25:1509-1519.
64. Min J, Zhang Y, Xu RM. Structural basis for specific binding of Polycomb chromodomain to histone H3 methylated at Lys 27. *Genes Dev* 2003;17(15):1823-8.
65. Mohammad HP, Cai Y, McGarvey KM, Easwaran H, Van Neste L, Ohm JE, O'Hagan HM, Baylin SB. Polycomb CBX7 promotes initiation of heritable repression of genes frequently silenced with cancer-specific DNA hypermethylation. *Cancer Res* 2009;69(15):6322-30.
66. Monti M, Orrù S, Pagnozzi D, Pucci P. Interaction proteomics. *Biosci Rep* 2005;25(1-2):45-56. Review.
67. Mouritzen P, Nielsen PS, Jacobsen N, Noerholm M, Lomholt C, Pfundheller HM, Ramsing NB, Kauppinen S, Tolstrup N. The ProbeLibrary™ - Expression profiling 99% of all human genes using only 90 dual-labeled real-time PCR Probes. *Biotechniques* 2004;37:492-5.
68. Mouritzen P, Noerholm M, Nielsen PS, Jacobsen N, Lomholt C, Pfundheller HM, Tolstrup N. ProbeLibrary™ - Expression profiling 99% of all human genes using only 90 dual-labeled 2005. ProbeLibrary: A new method for faster design and execution of quantitative real-time PCR. *Nat Methods* 2005;2:313–7.
69. Nagafuchi A, Takeichi M. Cell binding function of E-cadherin is regulated by the cytoplasmic domain. *EMBO J* 1988;7(12):3679-84.
70. Nakao M, Minami T, Ueda Y, Sakamoto Y, Ichimura T. Epigenetic system: a pathway to malignancies and a therapeutic target. *Int J Hematol* 2004;80(2):103-7.
71. Nose A, Tsuji K, Takeichi M. Localization of specificity determining sites in cadherin cell adhesion molecules. *Cell* 1990;61(1):147-55.
72. Obika S ND, Hari Y, Morio K, In Y, Ishii JK, Imanishi T. Synthesis of 2'-O, 4'-C methyleneuridine and cytidine. Novel bicyclic Nucleosides Having a Fixed C3-endo Sugar Puckering. *Tetrahedron Lett* 1997;38:8735-8.
73. Ohm JE, McGarvey KM, Yu X, et al. A stem cell-like chromatin pattern may predispose tumor suppressor genes to DNA hypermethylation and heritable silencing. *Nat Genet* 2007;39:237–42.

74. Ou JN, Torrisani J, Unterberger A, et al. Histone deacetylase inhibitor trichostatin A induces global and gene-specific DNA demethylation in human cancer cell lines. *Biochem Pharmacol* 2007;73:1297–307.
75. Pallante P, Berlingieri MT, Troncone G, Kruhoffer M, Orntoft TF, Viglietto G, Caleo A, Migliaccio I, Decaussin-Petrucci M, Santoro M, et al. . UbcH10 overexpression may represent a marker of anaplastic thyroid carcinomas. . *Br J Cancer* 2005;93: 464-71.
76. Pallante P, Federico A, Berlingieri MT, Bianco M, Ferraro A, Forzati F, Iaccarino A, Russo M, Pierantoni GM, Leone V, Sacchetti S, Troncone G, Santoro M, Fusco A. Loss of the CBX7 gene expression correlates with a highly malignant phenotype in thyroid cancer. *Cancer Res* 2008;68(16):6770-8.
77. Papadavid E, Katsambas A. The interactions and role of epithelial cadherin and catenins in tumorigenicity. *Int J Dermatol* 2001;40(4):254-7.
78. Park IK, Qian D, Kiel M, Becker MW, Pihalja M, et al. Bmi-1 is required for maintenance of adult self-renewing haematopoietic stem cells. *Nature* 2003;423:302–305.
79. Paro R, Hogness DS. The Polycomb protein shares a homologous domain with a heterochromatin-associated protein of *Drosophila*. *Proc Natl Acad Sci U S A*. 1991;88(1):263-7.
80. Peinado H, Ballestar E, Esteller M, Cano A. Snail mediates E-cadherin repression by the recruitment of the Sin3A/histone deacetylase 1 (HDAC1)/HDAC2 complex. *Mol Cell Biol* 2004;24:306–19.
81. Peinado H, Portillo F, Cano A. Transcriptional regulation of cadherins during development and carcinogenesis. *Int J Dev Biol* 2004;48:365–75.
82. Pérez-Moreno MA, Locascio A, Rodrigo I, Dhondt G, Portillo F, Nieto MA, Cano A. A New Role For E12/E47 In The Repression Of E-Cadherin Expression And Epithelial-Mesenchymal Transitions. *J Biol Chem* 2001;276:27424-27431.
83. Pierantoni GM, Rinaldo C, Esposito F, Mottolese M, Soddu S, Fusco A. High Mobility Group A1 (HMGA1) proteins interact with p53 and inhibit its apoptotic activity. *Cell Death Differ* 2006;13(9):1554-63.
84. Piston DW KG. Fluorescent protein FRET: the good, the bad and the ugly. *Trends Biochem Sci* 2007;32:407-14.
85. Raaphorst FM, van Kemenade FJ, Blokzijl T, Fieret E, Hamer KM, Satijn DP, Otte AP, Meijer CJ. Coexpression of BMI-1 and EZH2 polycomb group genes in Reed-Sternberg cells of Hodgkin's disease. *Am J Pathol* 2000;157(3):709-15.
86. Rada-Iglesias A, Enroth S, Ameer A, et al. Butyrate mediates decrease of histone acetylation centered on transcription start sites and down-regulation of associated genes. *Genome Res* 2007;17:708–19.

87. Risinger JI, Berchuck A, Kohler MF, Boyd J. Mutations of the E-cadherin gene in human gynecologic cancers. *Nature Genet* 1994;7:98–102.
88. Rodrigo I, Cato AC, Cano A. Regulation of E-cadherin gene expression during tumor progression: the role of a new Ets-binding site and the E-pal element. *Exp Cell Res* 1999;248:358–371.
89. Rosanò L, Spinella F, Di Castro V, Decandia S, Nicotra MR, Natali PG, Bagnato A. Endothelin-1 is required during epithelial to mesenchymal transition in ovarian cancer progression. *Exp Biol Med (Maywood)* 2006;231(6):1128-31.
90. Saltman B, Singh B, Hedvat CV, Wreesmann VB, and Ghossein R. Patterns of expression of cell cycle/apoptosis genes along the spectrum of thyroid carcinoma progression. *Surgery* 2006;140:899-905.
91. Satijn DP, Otte AP. Polycomb group protein complexes: do different complexes regulate distinct target genes? *Biochim Biophys Acta* 1999;1447(1):1-16. Review.
92. Satijn DP, Gunster MJ, van der Vlag J, Hamer KM, Schul W, Alkema MJ, Saurin AJ, Freemont PS, van Driel R, Otte AP. RING1 is associated with the polycomb group protein complex and acts as a transcriptional repressor. *Mol Cell Biol* 1997;17(7):4105-13.
93. Saurin AJ, Shao Z, Erdjument-Bromage H, Tempst P, Kingston RE. A Drosophila Polycomb group complex includes Zeste and dTAFII proteins. *Nature* 2001;412:655–660.
94. Savagner P. Leaving the neighborhood: molecular mechanisms involved during epithelial-mesenchymal transitions. *BioEssays*;23:912–923.
95. Schlesinger Y, Straussman R, Keshet I, et al. Polycomb-mediated methylation on Lys27 of histone H3 pre-marks genes for de novo methylation in cancer. *Nat Genet* 2007;39:232–6.
96. Schock F, Perrimon N. Molecular mechanisms of epithelial morphogenesis. *Annu Rev Cell Dev Biol* 2002;18:463–493.
97. Schwartz YB, Pirrotta V. Polycomb silencing mechanisms and the management of genomic programmes. *Nat Rev Genet* 2007;8:9–22.
98. Scott CL, Gil J, Hernando E, et al. Role of the chromobox protein CBX7 in lymphomagenesis. *Proc Natl Acad Sci U S A* 2007;104:5389–94.
99. Shao Z, Raible F, Mollaaghababa R, Guyon JR, Wu CT, et al. Stabilization of chromatin structure by PRC1, a Polycomb complex. *Cell* 1999;98:37–46.
100. Shevchenko A, Keller P, Scheiffele P, Mann M, Simons K. Identification of components of trans-Golgi network-derived transport vesicles and detergent-insoluble complexes by nanoelectrospray tandem mass spectrometry. *Electrophoresis* 1997;18:2591–600.
101. Smith CL. A shifting paradigm: histone deacetylases and transcriptional activation. *Bioessays* 2008;30(1):15-24.

102. Sparmann A, van Lohuizen M. Polycomb silencers control cell fate, development and cancer. *Nat Rev Cancer* 2006;6:846–856.
103. Strahl BD, Allis CD. The language of covalent histone modifications. *Nature* 2000;403(6765):41-5.
104. Struhl, K. Histone acetylation and transcriptional regulatory mechanisms. *Genes Dev* 1998;12:599–606.
105. Suarez-Merino B, Hubank M, Revesz T, Harkness W, Hayward R, Thompson D, Darling JL, Thomas DG, Warr TJ. Microarray analysis of pediatric ependymoma identifies a cluster of 112 candidate genes including four transcripts at 22q12.1-q13.3. *Neuro Oncol* 2005;7(1):20-31.
106. Thiery JP. Epithelial-mesenchymal transitions in tumour progression. *Nat Rev Cancer* 2002;2:442–54.
107. Thiery JP, Sleeman J. Complex networks orchestrate epithelial-mesenchymal transitions. *Nat Rev Mol Cell Biol* 2006;7:131–42.
108. Tolhuis B, Muijters I, de Wit E, Teunissen H, Talhout W, et al. Genome-wide profiling of PRC1 and PRC2 Polycomb chromatin binding in *Drosophila melanogaster*. *Nat Genet.* 2006
109. Torok MS, and Grant PA. Histone acetyltransferase proteins contribute to transcriptional processes at multiple levels. *Adv Protein Chem* 2004;67:181-199.
110. Van der Laan BF et al. The association of well-differentiated thyroid carcinoma with insular or anaplastic thyroid carcinoma: evidence for dedifferentiation in tumor progression. *Endocr Pathol* 1993;4:215-221.
111. van Holde KE. *Chromatin*. Springer, New York, N.Y. 1988.
112. van Leeuwen F, van Steensel B. Histone modifications: from genome-wide maps to functional insights. *Genome Biol* 2005;6:113.
113. Vleminckx K, Vakaet L Jr, Mareel M, Fiers W, van Roy F. Genetic manipulation of E-cadherin expression by epithelial tumor cells reveals an invasion suppressor role. *Cell* 1991;66(1):107-19.
114. Wang H, Wang L, Erdjument-Bromage H, Vidal M, Tempst P, et al. Role of histone H2A ubiquitination in Polycomb silencing. *Nature* 2004;431:873–878.
115. Whitcomb SJ, Basu A, Allis CD, Bernstein E. Polycomb Group proteins: an evolutionary perspective. *Trends Genet* 2007;23:494–502.

TABLE CBX7 interacting proteins						
BAND	PROTEIN ID	score	N° peptidi	MW	Function	Process
T1	(P62826) GTP-binding nuclear protein Ran (GTPase Ran) (Ras-like protein TC4)	27	2	25	GTP-binding protein involved in nucleocytoplasmic transport. Required for the import of protein into the nucleus and also for RNA export. Involved in chromatin condensation and control of cell cycle. Nuclear; becomes dispersed throughout the cytoplasm during mitosis. Interact with RANGAP1	GTPase activity/ Signal transduction ; Cell communication
T4	(P61981) 14-3-3 protein gamma (Protein kinase C inhibitor protein 1)	88	1	28	Adapter protein implicated in the regulation of a large spectrum of both general and specialized signaling pathway. Binds to a large number of partners, usually by recognition of a phosphoserine or phosphothreonine motif. Binding generally results in the modulation of the activity of the binding partner. Interacts with RAF1 and SSH1. Cytoplasm.	Receptor signaling complex scaffold activity/ Signal transduction; cell communication
T5	(O95931) Chromobox protein homolog 7	40	1	28	BAIT	
T7	(P04083) Annexin A1 (Annexin I) (Lipocortin I) (Calpactin II) (Chromobindin-9)	785	19	39	Calcium/phospholipid-binding protein which promotes membrane fusion and is involved in exocytosis. This protein regulates phospholipase A2 activity. It seems to bind from two to four calcium ions with high affinity. Phosphorylated by protein kinase C, epidermal growth factor receptor/kinase and TRPM7. Phosphorylation results in loss of the inhibitory activity.	Calcium ion binding/Signal transduction ; Cell communication
	(P07355) Annexin A2 (Annexin II) (Lipocortin II) (Calpactin I heavy chain) (Chromobindin-8)	284	5	39	Calcium-regulated membrane-binding protein whose affinity for calcium is greatly enhanced by anionic phospholipids. It binds two calcium ions with high affinity	Calcium ion binding/Signal transduction ; Cell communication
	(Q08188) Protein-glutamine gamma-glutamyltransferase E precursor	231	6	77	Catalyzes the cross-linking of proteins and the conjugation of polyamines to proteins. It is responsible for the later stages of cell envelope formation in the epidermis and the hair follicle	Transaminase activity/ Metabolism; Cell growth and/or maintenance

gi 37183160 HRPE773 [Homo sapiens]	215	7	20	Q96DA0 HUMAN Similar to common salivary protein 1	Unknown
gi 662841 heat shock protein 27	147	5	22	Involved in stress resistance and actin organization. Associates with alpha- and beta-tubulin and microtubules. Interacts with HSPB8. Cytoplasm. Nucleus. Cytoplasmic in interphase cells. Colocalizes with mitotic spindles in mitotic cells. Translocates to the nucleus during heat shock.	Chaperone activity/Cell proliferation
gi 20334354 S100 calcium binding protein A14	144	2	12	Cytoplasm.	Calcium ion binding/Biological Process Unknown
gi 4885607 small proline-rich protein 3 [Homo sapiens]	132	3	19	Cross-linked envelope protein of keratinocytes. Cytoplasm.	Structural molecule activity/ Cell growth and/or maintenance
gi 31645 glyceraldehyde-3-phosphate dehydrogenase [Homo sapiens]	110	4	36	It has been suggested that glyceraldehyde-3-phosphate dehydrogenase (GAPDH) play a role in nuclear tRNA export	Catalytic activity/ Nuclear export
gi 187302 epithelial cell marker protein 1 (14-3-3 sigma)	90	2	28	Adapter protein implicated in the regulation of a large spectrum of both general and specialized signaling pathway. Binds to a large number of partners, usually by recognition of a phosphoserine or phosphothreonine motif. Binding generally results in the modulation of the activity of the binding partner. p53-regulated inhibitor of G2/M progression. Cytoplasm. Or: Secreted protein. May be secreted by a non-classical secretory pathway. Belongs to the 14-3-3 family.	Receptor signaling complex scaffold activity /Signal transduction ; Cell communication
gi 45592961 chromosome 20 open reading frame 70 [Homo sapiens]	76	2	27	containing a lipid binding domain - similar to short palate, lung and nasal epithelium carcinoma-associated protein 2	Unknown/Biological Process Unknown
gi 18204442 Ribosomal protein L18	64	1	22	Ribosomal protein	Ribosomal subunit/ Protein metabolism

	gi 895845 p64 CLCP	62	1	24	Seems to act as a chloride ion channel.. Mostly in the nucleus including in the nuclear membrane. Cytoplasm. Cell membrane. Small amount in the cytoplasm and the plasma membrane.SIMILARITY: Belongs to the chloride channel CLIC family. SUBCELLULAR LOCATION: Nucleus; nuclear membrane	Transmembrane receptor activity/ receptor
T8	(P09651) Heterogeneous nuclear ribonucleoprotein A1 (Helix-destabilizing protein)	58	1	39	Involved in the packaging of pre-mRNA into hnRNP particles, transport of poly(A) mRNA from the nucleus to the cytoplasm and may modulate splice site selection. Nucleus. Cytoplasm. Shuttles continuously between the nucleus and the cytoplasm along with mRNA. Component of ribonucleosomes.	Ribonucleoprotein/ Regulation of nucleobase, nucleoside, nucleotide and nucleic acid metabolism/ Nucleus export
	gi 627650 transcription factor BTF2 chain p34 - human	56	1	35	FUNCTION: Component of the core-TFIIF basal transcription factor involved in nucleotide excision repair (NER) of DNA and, when complexed to CAK, in RNA transcription by RNA polymerase II. Anchors XPB.SUBUNIT: One of the six subunits forming the core-TFIIF basal transcription factor.SUBCELLULAR LOCATION: Nucleus.SIMILARITY: Belongs to the TFB4 family.	nucleotide-excision repair/ regulation of transcription, DNA-dependent
T9	(P29692) Elongation factor 1-delta (EF-1-delta)	171	3	31	EF-1-beta and EF-1-delta stimulate the exchange of GDP bound to EF-1-alpha to GTP	Guanyl-nucleotide exchange factor activity/ Translation regulator activity
	(Q15024) Exosome complex exonuclease RRP42 (Ribosomal RNA-processing protein 42)	73	1	32	Component of the exosome 3'->5' exoribonuclease complex. Required for the 3' processing of the 7S pre-rRNA to the mature 5.8S rRNA. associated with the GTPase Ran. Interacts directly with CSL4. Nucleus; nucleolus	DNA binding/ Cell growth and/or maintenance
	gi 34335134 SEC13-like 1 isoform b	45	1	36	Molecular function unknown (Putative nucleoporin interacting protein)	unknown
T10	gi 12654583 Ribosomal protein P0	236	5	34	Localization: Citoplasm, nucleus, nucleolus	Ribosomal subunit/ Protein metabolism

T14	(O43684) Mitotic checkpoint protein BUB3	137	4	38	Required for kinetochore localization of BUB1. Nucleus.	protein serine/threonine kinase activity/Signal transduction; Cell communication
T15	(P68400) Casein kinase II subunit alpha	124	5	45	Casein kinases are operationally defined by their preferential utilization of acidic proteins such as caseins as substrates. The alpha and alpha' chains contain the catalytic site. Participates in Wnt signaling. Subunit alpha 1 e 2 interact with HISTONE DEACETILASE 2 (HDAC2)	Protein serine/threonine kinase activity/ Signal transduction ; Cell communication
	(Q01085) Nucleolysin TIAR	118	3	42	RNA-binding protein. Possesses nucleolytic activity against cytotoxic lymphocyte target cells. May be involved in apoptosis. Nuclear localization	RNA binding/Regulation of nucleobase, nucleoside, nucleotide and nucleic acid metabolism
	(Q15366) Poly(rC)-binding protein 2	84	2	39	Major cellular poly(rC)-binding protein. Binds also poly(rU). Nucleus. Cytoplasm. Loosely bound in the nucleus. May shuttle between the nucleus and the cytoplasm	RNA binding/Regulation of nucleobase, nucleoside, nucleotide and nucleic acid metabolism
	(Q14103) Heterogeneous nuclear ribonucleoprotein D0 (hnRNP D0)	76	3	38	Binds with high affinity to RNA molecules that contain AU-rich elements (AREs) found within the 3-prime untranslated regions of many protooncogenes and cytokine mRNAs. Also binds to double- and single-stranded DNA sequences in a specific manner and functions a transcription factor. Binding of RRM1 to DNA inhibits the formation of DNA quadruplex structure which may play a role in telomere elongation. May be involved in translationally coupled mRNA turnover. Implicated with other RNA-binding proteins in the cytoplasmic deadenylation/translational and decay interplay of the FOS mRNA mediated by the major coding-region determinant of instability (mCRD) domain. Nuclear; component of ribonucleosomes.	Ribonucleoprotein/Regulation of nucleobase, nucleoside, nucleotide and nucleic acid metabolism
	gi 1808644 arginine methyltransferase	64	2	40	Protein arginine methyltransferase that functions as a histone methyltransferase specific for H4	Methyltransferase activity/ Histone modifying protein

	gi 4758158 Septin 2	50	1	42	Septins may form a mitotic scaffold for CENP-E and other effectors to coordinate cytokinesis with chromosome congression and segregation Interact with S100 calcium-binding protein A4 . Nucleus.	Receptor signaling complex scaffold activity/ Signal transduction ; Cell communication
T16	(O00303) Eukaryotic translation initiation factor 3 subunit 5 (eIF-3 epsilon)	108	2	38	Binds to the 40S ribosome and promotes the binding of methionyl-tRNAi and mRNA. Associates with the complex p170-eIF3.	Translation regulator activity/ Protein metabolism
	(Q12905) Interleukin enhancer-binding factor 2	80	3	43	Appears to function predominantly as a heterodimeric complex with ILF3. This complex may regulate transcription of the IL2 gene during T-cell activation. It can also promote the formation of stable DNA-dependent protein kinase holoenzyme complexes on DNA. Nucleus; nucleolus.	Transcription factor activity/ Regulation of nucleobase, nucleoside, nucleotide and nucleic acid metabolism
T17	(Q86U42) Polyadenylate-binding protein 2 (Poly(A)-binding protein 2)	57	1	33	Involved in the 3'end formation of mRNA precursors (pre-mRNA) by the addition of a poly(A) tail of 200-250 nt to the upstream cleavage product. Stimulates poly(A) polymerase (PAPOLA) conferring processivity on the poly(A) tail elongation reaction and controls also the poly(A) tail length. Increases the affinity of poly(A) polymerase for RNA. Is also present at various stages of mRNA metabolism including nucleocytoplasmic trafficking and nonsense-mediated decay (NMD) of mRNA. Cooperates with SKIP to synergistically activate E-box-mediated transcription through MYOD1 and may regulate the expression of muscle-specific genes. Binds to poly(A) and to poly(G) with high affinity. May protect the poly(A) tail from degradation. Shuttles between the nucleus and the cytoplasm but predominantly found in the nucleus. Its nuclear import may involve the nucleocytoplasmic transport receptor transportin and a RAN-GTP-sensitive import mechanism. Is exported to the cytoplasm by a carrier-mediated pathway that is independent of mRNA traffic. Nucleus; nucleoplasm; nuclear speckle.	RNA binding/Regulation of nucleobase, nucleoside, nucleotide and nucleic acid metabolism/ Nuclear export/import

	(Q8NFW8) N-acylneuraminate cytidyltransferase	53	2	49	Catalyzes the activation of N-acetylneuraminic acid (NeuNAc) to cytidine 5'-monophosphate N-acetylneuraminic acid (CMP-NeuNAc), a substrate required for the addition of sialic acid. Has some activity toward NeuNAc, N-glycolylneuraminic acid (Neu5Gc) or 2-keto-3-deoxy-D-glycero-D-galacto-nononic acid (KDN). Nucleus. The BC2 (basic cluster 2) motif is necessary and sufficient for the nuclear localization and contains the catalytic active site. The localization in the nucleus is however not required for the enzyme activity	Ligase activity /Metabolism ; Energy pathways
	(P60842) Eukaryotic initiation factor 4A-1	47	1	46	ATP-dependent RNA helicase which is a subunit of the eIF4F complex involved in cap recognition and is required for mRNA binding to ribosome. Belongs to the DEAD box helicase family. eIF4A subfamily.	Translation regulator activity/ Protein metabolism
T18	(P68104) Elongation factor 1-alpha 1 (EF-1-alpha-1)	245	7	50	This protein promotes the GTP-dependent binding of aminoacyl-tRNA to the A-site of ribosomes during protein biosynthesis. Found in a nuclear export complex with XPO5, EEF1A1, Ran and aminoacylated tRNA. Interacts with XPO5.	Translation regulator activity/ Protein metabolism
T20	gi 33327055 DERPC [Homo sapiens]	71	2	51	nuclear, strong basic protein; decreased expression in renal and prostate tumors; has cell growth inhibiting function	DNA binding/ Regulation of nucleobase, nucleoside, nucleotide and nucleic acid metabolism/ Cell proliferation
	gi 8922679 smu-1 suppressor of mec-8 and unc-52 homolog	47	1	58	unknown	unknown

T21	gi 48146467 HSPC117 [Homo sapiens]	108	3	56	unknown	unknown
	gi 5901990 katanin p60 subunit A 1 [Homo sapiens]	51	2	56	Microtubules, polymers of alpha and beta tubulin subunits, form the mitotic spindle of a dividing cell and help to organize membranous organelles during interphase. Katanin is a heterodimer that consists of a 60 kDa ATPase (p60 subunit A 1) and an 80 kDa accessory protein (p80 subunit B 1). The p60 subunit acts to sever and disassemble microtubules, while the p80 subunit targets the enzyme to the centrosome. This gene encodes the p80 subunit. This protein is a member of the AAA family of ATPases.	ATPase activity/Metabolism; Cell maintenance
T22	gi 47940653 Chaperonin containing TCP1, subunit 8 (theta)	68	2	60		Chaperone activity/ Cell maintenance
	gi 56789228 Chaperonin containing TCP1, subunit 7 (eta) [Homo sapiens]	53	1	60		Chaperone activity/ Cell maintenance
	gi 71051977 HDAC2 protein [Homo sapiens]	65	2	45	Histone deacetylase family. Deacetylase activity. Interact with casein kinase 2, alpha 1 polypeptide	Histone modifying protein
T23	(P14866) Heterogeneous nuclear ribonucleoprotein L (hnRNP L)	267	11	61	This protein is a component of the heterogeneous nuclear ribonucleoprotein (hnRNP) complexes which provide the substrate for the processing events that pre-mRNAs undergo before becoming functional, translatable mRNAs in the cytoplasm. L is associated with most nascent transcripts including those of the landmark giant loops of amphibian lampbrush chromosomes. Nucleus; nucleoplasm	Ribonucleoprotein/ Regulation of nucleobase, nucleoside, nucleotide and nucleic acid metabolism

	(Q13283) Ras-GTPase-activating protein-binding protein 1 (ATP-dependent DNA helicase V)	180	4	52	May be a regulated effector of stress granule assembly. Phosphorylation-dependent sequence-specific endoribonuclease in vitro. Binds to the SH3 domain of Ras-GTPase-activating protein (RASA1) in proliferating cells. No interaction in quiescent cells. Interacts with USP10, and may regulate it. Forms homodimers and oligomers. Cytoplasm. Cytoplasm; cytosol. Cell membrane. Nucleus. Cytoplasmic in proliferating cells, can be recruited to the plasma membrane in exponentially growing cells. Cytosolic and partially nuclear in resting cells. Recruited to stress granules (SGs) upon either arsenite or high temperature treatment. Recruitment to SGs is influenced by HRAS.	Ribonuclease activity/ Regulation of nucleobase, nucleoside, nucleotide and nucleic acid metabolism
	(Q12800) Alpha-globin transcription factor CP2 (Transcription factor LSF)	166	3	58	Binds a variety of cellular and viral promoters including fibrinogen, alpha-globin, SV40 and HIV-1 promoters. Activation of the alpha-globin promoter in erythroid cells is via synergistic interaction with UBP1. Functions as part of the SSP (stage selector protein) complex. Facilitates the interaction of the gamma-globin genes with enhancer elements contained in the locus control region in fetal erythroid cells. Interacts by binding to the stage selector element (SSE) in the proximal gamma-globin promoter.	Transcription factor activity/ Regulation of nucleobase, nucleoside, nucleotide and nucleic acid metabolism
	gi 1809248 siah binding protein 1 [Homo sapiens]	107	2	58	Hypotetical Ribonucleoprotei/ RNA binding protein	RNA binding/ Regulation of nucleobase, nucleoside, nucleotide and nucleic acid metabolism
	gi 14124984 Chaperonin containing TCP1, subunit 3 (gamma) [Homo sapiens]	61	1	60		Chaperone activity/ Cell maintenance
T24	(P33240) Cleavage stimulation factor, 64 kDa subunit (CSTF 64 kDa subunit)	324	8	61	One of the multiple factors required for polyadenylation and 3'-end cleavage of mammalian pre-mRNAs. This subunit is directly involved in the binding to pre-mRNAs. Nucleus.	RNA binding/ Regulation of nucleobase, nucleoside, nucleotide and nucleic acid metabolism

	gi 57209129 paraspeckle component 1	199	5	59	Putative RNA binding protein	RNA binding/ Regulation of nucleobase, nucleoside, nucleotide and nucleic acid metabolism
T25	gi 23398584 Interferon regulatory factor 2 binding protein 1	80	1	62		Transcription regulator activity/ Regulation of nucleobase, nucleoside, nucleotide and nucleic acid metabolism
	gi 8923040 collaborates/cooperates with ARF (alternate reading frame) protein	74	1	61		RNA binding/ Regulation of nucleobase, nucleoside, nucleotide and nucleic acid metabolism
	(Q8WXI9) Transcriptional repressor p66 beta (p66/p68) (GATA zinc finger domain-containing protein 2)	47	1	66	Has transcriptional repressor activity. Targets MBD3 to discrete loci in the nucleus. Nucleus. Nuclear, in discrete foci.	Transcription regulator activity/ Regulation of nucleobase, nucleoside, nucleotide and nucleic acid metabolism
T26c	gi 178027 alpha-actin	258	9	42		Cell maintenance
	(P11940) Polyadenylate-binding protein 1 (Poly(A)-binding protein 1) (PABP 1)	48	1	71	Binds the poly(A) tail of mRNA. May be involved in cytoplasmic regulatory processes of mRNA metabolism. Its function in translational initiation regulation can either be enhanced by PAIP1 or repressed by PAIP2. Can probably bind to cytoplasmic RNA sequences other than poly(A) in vivo. May be involved in translationally coupled mRNA turnover. Implicated with other RNA-binding proteins in the cytoplasmic deadenylation/translational and decay interplay of the FOS mRNA mediated by the major coding-region determinant of instability (mCRD) domain. Cytoplasm. Nucleus. Shuttles between the cytoplasm and the nucleus.	RNA binding/Regulation of nucleobase, nucleoside, nucleotide and nucleic acid metabolism

	(Q9BTC8) Metastasis-associated protein MTA3	58	2	68	Plays a role in maintenance of the normal epithelial architecture through the repression of SNAI1 transcription in a histone deacetylase-dependent manner, and thus the regulation of E-cadherin levels. Nucleus. Interact with histone deacetylase 2 non directly	Transcription regulator activity/ Regulation of nucleobase, nucleoside, nucleotide and nucleic acid metabolism
	(Q9UBU9) Nuclear RNA export factor 1 (Tip-associating protein)	56	1	71	Involved in the nuclear export of mRNA species bearing retroviral constitutive transport elements (CTE) and in the export of mRNA from the nucleus to the cytoplasm. Nuclear; localized predominantly in the nucleoplasm and at both the nucleoplasmic and cytoplasmic faces of the nuclear pore complex. Shuttles between the nucleus and the cytoplasm.	RNA binding/Regulation of nucleobase, nucleoside, nucleotide and nucleic acid metabolism
	gi 57165052 Thyroid autoantigen 70kDa	53	1	70	Single stranded DNA-dependent ATP-dependent helicase. Has a role in chromosome translocation. The DNA helicase II complex binds preferentially to fork-like ends of double-stranded DNA in a cell cycle-dependent manner. It works in the 3'-5' direction. Binding to DNA may be mediated by p70. Involved in DNA nonhomologous end joining (NHEJ) required for double-strand break repair and V(D)J recombination. The Ku p70/p86 dimer acts as regulatory subunit of the DNA-dependent protein kinase complex DNA-PK by increasing the affinity of the catalytic subunit PRKDC to DNA by 100-fold. The Ku p70/p86 dimer is probably involved in stabilizing broken DNA ends and bringing them together. The assembly of the DNA-PK complex to DNA ends is required for the NHEJ ligation step. Required for osteocalcin gene expression	DNA repair protein/Regulation of nucleobase, nucleoside, nucleotide and nucleic acid metabolism
T27	gi 15530265 Eukaryotic translation elongation factor 1 gamma	320	8	50		Translation regulator activity/ Protein metabolism
T28	gi 34783356 RANGAP1 protein	99	2	64	GTPase activator for the nuclear Ras-related regulatory protein Ran, converting it to the putatively inactive GDP-bound state.	GTPase activator activity/ Signal transduction ; Cell communication

	gi 14250668 Cortactin, isoform b	106	3	58		Cytoskeletal protein binding/Cell growth and/or maintenance
	gi 82546879 GTP binding protein 1	106	2	73	FUNCTION: Not known, the C-terminus can act as an allosteric activator of the cholera toxin catalytic subunit.	GTPase activity/ Signal transduction ; Cell communication
T30	(Q14157) Ubiquitin-associated protein 2-like	97	3	104	Unclassified	Unknown/Biological_process unknown
	(P19447) TFIIH basal transcription factor complex helicase XPB subunit	97	2	90	ATP-dependent 3'-5' DNA helicase, component of the core-TFIIH basal transcription factor, involved in nucleotide excision repair (NER) of DNA and, when complexed to CAK, in RNA transcription by RNA polymerase II. Acts by opening DNA either around the RNA transcription start site or the DNA damage.	DNA repair protein/ Regulation of nucleobase, nucleoside, nucleotide and nucleic acid metabolism
	(Q9BSJ2) Gamma-tubulin complex component 2	69	1	104	Gamma-tubulin complex is necessary for microtubule nucleation at the centrosome. Centrosome.	Cytoskeletal protein binding/ Cell growth and/or maintenance
	(Q12906) Interleukin enhancer-binding factor 3 (Nuclear factor of activated T-cells 90 kDa)	64	1	96	May facilitate double-stranded RNA-regulated gene expression at the level of post-transcription. Can act as a translation inhibitory protein which binds to coding sequences of acid beta-glucosidase (GCase) and other mRNAs and functions at the initiation phase of GCase mRNA translation, probably by inhibiting its binding to polysomes. Can regulate protein arginine N-methyltransferase 1 activity. May regulate transcription of the IL2 gene during T-cell activation. Can promote the formation of stable DNA-dependent protein kinase holoenzyme complexes on DNA. Nucleus; nucleolus.	Transcription factor activity/Regulation of nucleobase, nucleoside, nucleotide and nucleic acid metabolism

	(Q01826) DNA-binding protein SATB1 (Special AT-rich sequence-binding protein 1)	60	1	86	Binds to DNA at special AT-rich sequences at nuclear matrix- or scaffold-associated regions. Thought to recognize the sugar-phosphate structure of double-stranded DNA. Nucleus.	Transcription factor activity/ Regulation of nucleobase, nucleoside, nucleotide and nucleic acid metabolism
	(P33992) DNA replication licensing factor MCM5 (CDC46 homolog) (P1-CDC46)	46	2	83		DNA binding /Regulation of nucleobase, nucleoside, nucleotide and nucleic acid metabolism
T31	gi 2494898 Periodic tryptophan protein 2 homolog	68	2	103	Nucleus; nucleolus. PWP2 is essential for viability and may play a role in the early G1 phase of the cell cycle.(La prot. Possiede diversi domini WD40)	Regulation of cell cycle/ Signal transduction ; Cell communication
	(Q02779) Mitogen-activated protein kinase kinase kinase 10	40	2	104	Activates the JUN N-terminal pathway	Protein serine-threonine kinase activity/ Signal transduction ; Cell communication
T32	(P43243) Matrin-3	160	6	95	May play a role in transcription or may interact with other nuclear matrix proteins to form the internal fibrogranular network. In association with the SFPQ-NONO heteromer may play a role in nuclear retention of defective RNAs. Nucleus; nucleoplasm; nuclear matrix.	RNA binding/Regulation of nucleobase, nucleoside, nucleotide and nucleic acid metabolism
	(P11586) C-1-tetrahydrofolate synthase, cytoplasmic (C1-THF synthase)	110	2	102	Cytoplasm	Catalytic activity/ Metabolism; Energy pathways

	(P55884) Eukaryotic translation initiation factor 3 subunit 9	62	2	93	Binds to the 40S ribosome and promotes the binding of methionyl-tRNA _i and mRNA	Translation regulator activity/ Protein metabolism
	(Q9H0D6) 5'-3' exoribonuclease 2 (EC 3.1.11.-) (DHM1-like protein)	61	1	109	Possesses 5'->3' exoribonuclease activity and may be involved in homologous recombination and RNA metabolism, such as RNA synthesis and RNA trafficking .Nucleus; nucleolus.	Ribonuclease activity/ Regulation of nucleobase, nucleoside, nucleotide and nucleic acid metabolism
	(Q99613) Eukaryotic translation initiation factor 3 subunit 8 (eIF3 p110)	57	1	106	Binds to the 40S ribosome and promotes the binding of methionyl-tRNA _i and mRNA	Translation regulator activity/ Protein metabolism
T33	(Q9ULK4) CRSP complex subunit 3 (Cofactor required for Sp1 transcriptional activation subunit 3)	102	2	158	Plays a role in transcriptional coactivation.	Transcription regulator activity/ Regulation of nucleobase, nucleoside, nucleotide and nucleic acid metabolism
	(P26640) Valyl-tRNA synthetase (EC 6.1.1.9) (Valine--tRNA ligase)	88	2	142		Translation regulator activity/ Protein metabolism

	(Q92900) Regulator of nonsense transcripts 1 (EC 3.6.1.-) (ATP-dependent helicase RENT1)	70	2	126	Part of a post-splicing multiprotein complex. Involved in nonsense-mediated decay (NMD) of mRNAs containing premature stop codons. Essential for embryonic viability.	RNA binding/ Regulation of nucleobase, nucleoside, nucleotide and nucleic acid metabolism
	(O00267) Transcription elongation factor SPT5 (hSPT5)	56	2	121	Component of the DRB sensitivity-inducing factor complex (DSIF complex), which regulates mRNA processing and transcription elongation by RNA polymerase II. DSIF positively regulates mRNA capping by stimulating the mRNA guanylyltransferase activity of RNGTT/CAP1A. DSIF also acts cooperatively with the negative elongation factor complex (NELF complex) to enhance transcriptional pausing at sites proximal to the promoter. NUCLEO	transcription
	(Q13435) Splicing factor 3B subunit 2 (Spliceosome-associated protein 145)	56	1	98	Subunit of the splicing factor SF3B required for 'A' complex assembly formed by the stable binding of U2 snRNP to the branchpoint sequence (BPS) in pre-mRNA. Sequence independent binding of SF3A/SF3B complex upstream of the branch site is essential, it may anchor U2 snRNP to the pre-mRNA. May also be involved in the assembly of the 'E' complex. Belongs also to the minor U12-dependent spliceosome, which is involved in the splicing of rare class of nuclear pre-mRNA intron. Nucleus.	RNA binding/ Regulation of nucleobase, nucleoside, nucleotide and nucleic acid metabolism
	(O75533) Splicing factor 3B subunit 1 (Spliceosome-associated protein 155)	52	2	146	Subunit of the splicing factor SF3B required for 'A' complex assembly formed by the stable binding of U2 snRNP to the branchpoint sequence (BPS) in pre-mRNA. Sequence independent binding of SF3A/SF3B complex upstream of the branch site is essential, it may anchor U2 snRNP to the pre-mRNA. May also be involved in the assembly of the 'E' complex. Belongs also to the minor U12-dependent spliceosome, which is involved in the splicing of rare class of nuclear pre-mRNA intron.	RNA binding/ Regulation of nucleobase, nucleoside, nucleotide and nucleic acid metabolism

T34	gi 89047296 similar to SMC hinge domain containing 1	136	3	221		Unknown
	gi 33946327 nucleoporin 214kDa [Homo sapiens]	54	3	214	integral to membrane.Interact with con Nuclear RNA export factor 1	porin activity/ protein import/ export
T35	gi 71044479 death inducer-obliterator 1 isoform c	358	12	245	Apoptosis, a major form of cell death, is an efficient mechanism for eliminating unwanted cells and is of central importance for development and homeostasis in metazoan animals. In mice, the death inducer-obliterator-1 gene is upregulated by apoptotic signals and encodes a cytoplasmic protein that translocates to the nucleus upon apoptotic signal activation. When overexpressed, the mouse protein induced apoptosis in cell lines growing in vitro. This gene is similar to the mouse gene and therefore is thought to be involved in apoptosis. Alternatively spliced transcripts have been found for this gene, encoding multiple isoforms.	Putative DNA binding protein/ Cell proliferation/ Apoptosis/ Regulation of nucleobase, nucleoside, nucleotide and nucleic acid metabolism
	gi 13606056 DNA dependent protein kinase catalytic subunit [Homo sapiens]	106	4	470	Serine/threonine-protein kinase that acts as a molecular sensor for DNA damage. Involved in DNA nonhomologous end joining (NHEJ) required for double-strand break (DSB) repair and V(D)J recombination. Must be bound to DNA to express its catalytic properties. Promotes processing of hairpin DNA structures in V(D)J recombination by activation of the hairpin endonuclease artemis (DCLRE1C). The assembly of the DNA-PK complex at DNA ends is also required for the NHEJ ligation step. Required to protect and align broken ends of DNA. May also act as a scaffold protein to aid the localization of DNA repair proteins to the site of damage. Found at the ends of chromosomes, suggesting a further role in the maintenance of telomeric stability and the prevention of chromosomal end fusion. Also involved in modulation of transcription. Recognizes the substrate consensus sequence [S/T-Q]. Phosphorylates Ser-139 of histone variant H2AX/H2AFX, thereby regulating DNA damage response mechanism.	protein kinase activity/DNA REPAIR

UbcH10 overexpression may represent a marker of anaplastic thyroid carcinomas

P Pallante¹, MT Berlingieri¹, G Troncione², M Kruhoffer³, TF Orntoft³, G Viglietto¹, A Caleo², I Migliaccio², M Decaussin-Petrucci⁴, M Santoro¹, L Palombini² and A Fusco^{*,1,5}

¹Dipartimento di Biologia e Patologia Cellulare e Molecolare c/o Istituto di Endocrinologia ed Oncologia Sperimentale del CNR, Facoltà di Medicina e Chirurgia di Napoli, Università degli Studi di Napoli 'Federico II', via Pansini, 5, 80131 Naples, Italy; ²Dipartimento di Anatomia Patologica e Citopatologia, Facoltà di Medicina e Chirurgia di Napoli, Università di Napoli 'Federico II', via Pansini, 5, 80131 Naples, Italy; ³Department of Clinical Biochemistry, Aarhus University Hospital, Skejby DK 8200 Aarhus N, Denmark; ⁴Service d'Anatomo-Pathologie, Centre Hospitalier Lyon Sud, Pierre Bénite, France; ⁵NOGEC (Naples Oncogenomic Center)-CEINGE, Biotecnologie Avanzate, via Comunale Margherita, 80131 Naples, Italy

The hybridisation of an Affymetrix HG_U95Av2 oligonucleotide array with RNAs extracted from six human thyroid carcinoma cell lines and a normal human thyroid primary cell culture led us to the identification of the UbcH10 gene that was upregulated by 150-fold in all of the carcinoma cell lines in comparison to the primary culture cells of human normal thyroid origin. Immunohistochemical studies performed on paraffin-embedded tissue sections showed abundant UbcH10 levels in thyroid anaplastic carcinoma samples, whereas no detectable UbcH10 expression was observed in normal thyroid tissues, in adenomas and goiters. Papillary and follicular carcinomas were only weakly positive. These results were further confirmed by RT-PCR and Western blot analyses. The block of UbcH10 protein synthesis induced by RNA interference significantly reduced the growth rate of thyroid carcinoma cell lines. Taken together, these results would indicate that UbcH10 overexpression is involved in thyroid cell proliferation, and may represent a marker of thyroid anaplastic carcinomas.

British Journal of Cancer (2005) **93**, 464–471. doi:10.1038/sj.bjc.6602721 www.bjcancer.com

Published online 2 August 2005

© 2005 Cancer Research UK

Keywords: UbcH10; thyroid; carcinomas; immunohistochemistry

Tumours are the result of the accumulation of different modifications in critical genes involved in the control of cell proliferation. In a large number of carcinomas with worst prognosis, lesions are not diagnosed until the disease is at an advanced stage. Although various therapeutic approaches are followed in clinical practice, most of them are not life saving. Hence, the discovery of ways to diagnose cancer at an early stage and to establish more effective therapies is a critical and urgent issue. To achieve this goal, identification and characterisation of key molecules that participate in carcinogenesis are essential steps. Thyroid neoplasms represent a good model for studying the events involved in epithelial cell multistep carcinogenesis, because they comprise a broad spectrum of lesions with different degrees of malignancy from benign adenomas, which are not invasive and very well differentiated, to the undifferentiated anaplastic thyroid carcinomas, which are very aggressive and always fatal; papillary and follicular carcinomas, the most common forms of thyroid cancer, represent intermediate forms of neoplasia being differentiated and

having a good prognosis (Hedinger *et al*, 1989; Wynford-Thomas, 1997).

The involvement of several oncogenes has been demonstrated in papillary thyroid carcinomas. Activation of the RET/PTC oncogene, caused by rearrangements of the RET protooncogene, is detectable in about 30% of the cases (Grieco *et al*, 1990; Tallini *et al*, 1998). Mutations of the B-RAF gene have been demonstrated in almost 40% of papillary carcinomas (Fukushima *et al*, 2003). TRK gene rearrangements (Pierotti *et al*, 1995) and MET gene overexpression are often found in papillary carcinomas (Di Renzo *et al*, 1992). RAS gene mutations (Suarez *et al*, 1990) and PAX8-PPAR- γ rearrangements (Kroll *et al*, 2000) are frequently detected in tumours of the follicular type. Impairment of the p53 tumour suppressor gene function represents a typical feature of the anaplastic carcinomas (Ito *et al*, 1992; Dobashi *et al*, 1993; Donghi *et al*, 1993; Fagin *et al*, 1993; Matias-Guiu *et al*, 1994). Even though critical molecular mechanisms of thyroid carcinogenesis have been clarified, other molecular steps of neoplastic progression need to be investigated.

Therefore, to identify the genes regulated in the process of thyroid carcinogenesis, we analysed a microarray with RNAs extracted from normal human thyroid primary cell culture (NTPC), and six human thyroid carcinoma cell lines of different histotype (one from a follicular carcinoma, three derived from papillary carcinomas and two from anaplastic carcinomas). Our attention was focused on the UbcH10 gene that was upregulated

*Correspondence: Dr A Fusco, Dipartimento di Biologia e Patologia Cellulare e Molecolare, Facoltà di Medicina e Chirurgia di Napoli and, NOGEC (Naples Oncogenomic Center)-CEINGE, Biotecnologie Avanzate, via Pansini 5, 80131 Naples, Italy; E-mail: afusco@napoli.com
Received 2 March 2005; revised 16 June 2005; accepted 22 June 2005; published online 2 August 2005

about 150-fold in all of the cell lines tested by the cDNA microarray. The UbcH10 gene belongs to the E2 gene family and codes for a protein of 19.6 kDa that is involved in the ubiquitin-dependent proteolysis. In this pathway, ubiquitin-conjugating enzyme (E2), together with ubiquitin ligase (E3), transfers ubiquitin to specific substrate proteins (Hershko and Ciechanover, 1998; Joazeiro and Weissman, 2000).

The expression level of UbcH10 was extremely low in the normal thyroid primary culture cells, but strong in all the cancerous cell lines. Immunohistochemical and RT-PCR analyses on a large panel of thyroid neoplasms of different histotypes revealed an increased UbcH10 expression in anaplastic thyroid carcinomas, whereas follicular and papillary carcinomas were just weakly positive. The block of UbcH10 protein synthesis by RNA interference inhibited the growth of two thyroid carcinoma cell lines.

MATERIALS AND METHODS

Cell culture and transfections

The human thyroid carcinoma cell lines used in this study are: TPC-1 (Tanaka *et al*, 1987), WRO (Estour *et al*, 1989), NPA and ARO (Pang *et al*, 1989), FRO (Fagin *et al*, 1993), NIM 1 (Zeki *et al*, 1993), B-CPAP (Fabien *et al*, 1994), FB-1 (Fiore *et al*, 1997), FB-2 (Basolo *et al*, 2002), Kat-4 and Kat-18 (Ain *et al*, 1997). They were grown in DMEM (Gibco Laboratories, Carlsbad, CA, USA) containing 10% fetal calf serum (Gibco Laboratories), glutamine (Gibco Laboratories) and ampicillin/streptomycin (Gibco Laboratories) in a 5% CO₂ atmosphere. Normal human thyroid primary culture cells have been established and grown as already described (Curcio *et al*, 1994). PC Cl 3 cell line derived from Fischer rat thyroid (Fusco *et al*, 1987) was cultured in modified F12 medium supplemented with 5% calf serum (Gibco Laboratories) and six growth factors (thyrotropic hormone, hydrocortisone, insulin, transferrin, somatostatin and glycyl-histidyl-lysine; Sigma, St Louis, MO, USA). Thyroid cells were transfected using Lipofectamine reagent (Invitrogen, Carlsbad, CA, USA) according to the manufacturer's instructions. The transfected cells were selected in a medium containing geneticin (G418) (Life Technologies, Italy). For each transfection, several G418-resistant clones and the mass cell population were isolated and expanded for further analysis.

Human thyroid tissue samples

Neoplastic human thyroid tissues and normal adjacent tissue or the controlateral normal thyroid lobe were obtained from surgical specimens and immediately frozen in liquid nitrogen. Thyroid tumours were collected at the Service d'Anatomo-Pathologie, Centre Hospitalier Lyon Sud, Pierre Bénite, France. The tumour samples were stored frozen until RNA or protein extractions were performed.

RNA isolation

Total RNA was extracted from tissues and cell cultures using the RNeasy mini kit (Qiagen, Valencia, CA, USA) according to the manufacturer's instructions. The integrity of the RNA was assessed by denaturing agarose gel electrophoresis.

Reverse transcriptase-PCR analysis

In total, 5 µg of total RNA from each sample, digested with DNaseI (Invitrogen), were reverse transcribed using random hexanucleotides and MuLV reverse transcriptase (Applied Biosystems, Foster City, CA, USA). PCR was carried out on cDNA using the GeneAmp PCR System 9600 (Applied Biosystems). RNA PCR Core Kit (Applied Biosystems) was used to perform RT-PCR reactions.

For the UbcH10 gene, after a first denaturing step (94°C for 3 min), PCR amplification was performed for 25 cycles (94°C for 30 s, 57°C for 30 s, 72°C for 30 s). The sequences of forward and reverse primers, amplifying a fragment of 115 bp in the UbcH10 cDNA, were: forward 5'-GCCCGTAAAGGAGCTGAG-3' and reverse 5'-GGGAAGGCAGAAATCCCT-3'. The human β-actin gene primers, amplifying a 109 bp cDNA fragment, were used as control; amplification was performed for 25 cycles (94°C for 30 s, 55°C for 30 s, 72°C for 30 s). β-Actin-forward, 5'-TCGTGCGTGACATTAAGGAG-3'; β-actin-reverse, 5'-GTCAGGCAGCTCGTAGCTCT-3'. To ensure that RNA samples were not contaminated with DNA, negative controls were obtained by performing the PCR on samples that were not reverse-transcribed, but otherwise identically processed. The PCR products were separated on a 2% agarose gel, stained with ethidium bromide and scanned using a Typhoon 9200 scanner. Quantitative PCR was performed in triplicate using iCycler (Bio-Rad, Hercules, CA, USA) with SYBR[®] Green PCR Master Mix (Applied Biosystems) as follows: 95°C 10 min and 40 cycles (95°C 15 s and 60°C 1 min). Fold mRNA overexpression was calculated according to the formula $2^{(Rt-Et)}/2^{(Rn-En)}$ as described previously (El-Rifai *et al*, 2001), where Rt is the threshold cycle number for the reference gene in the tumour, Et for the experimental gene in the tumor, Rn for the reference gene in the normal sample and En for the experimental gene in the normal sample.

Protein extraction, Western blotting and antibodies

Cells were washed once in cold PBS and lysed in a lysis buffer containing 50 mM HEPES, 150 mM NaCl, 1 mM EDTA, 1 mM EGTA, 10% glycerol, 1% Triton-X-100, 1 mM phenylmethylsulphonyl fluoride, 1 µg aprotinin, 0.5 mM sodium orthovanadate, 20 mM sodium pyrophosphate. The lysates were clarified by centrifugation at 14 000 r.p.m. × 10 min. Protein concentrations were estimated by a Bio-Rad assay (Bio-Rad), and boiled in Laemmli buffer (Tris-HCl pH 6.8, 0.125 M, SDS 4%, glycerol 20%, 2-mercaptoethanol 10%, bromophenol blue 0.002%) for 5 min before electrophoresis. Proteins were subjected to SDS-PAGE (15% polyacrylamide) under reducing condition. After electrophoresis, proteins were transferred to nitrocellulose membranes (Immobilon-P Millipore Corp., Bedford, MA, USA); complete transfer was assessed using prestained protein standards (Bio-Rad). After blocking with TBS-BSA (25 mM Tris, pH 7.4, 200 mM NaCl, 5% bovine serum albumin), the membrane was incubated with the primary antibody against UbcH10 (Boston Biochem Inc., Cambridge, MA, USA) for 60 min (at room temperature). Primary antibody against c-Fos protein (Santa Cruz Biotechnology Inc., Santa Cruz, CA, USA) was used to confirm the specificity of siRNAs against UbcH10 protein. To ascertain that equal amounts of protein were loaded, the Western blots were incubated with antibodies against the γ-tubulin protein (Sigma). Membranes were then incubated with the horseradish peroxidase-conjugated secondary antibody (1:3000) for 60 min (at room temperature) and the reaction was detected with a Western blotting detection system (ECL; Amersham Biosciences, UK).

Immunohistochemistry: tissue samples

UbcH10 protein cellular distribution was assessed by immunohistochemical analysis and compared to that of the standard cell proliferation marker Ki-67/MIB1. A series of surgical specimens from patients with thyroid diseases comprised of Hashimoto's thyroiditis-HT (six cases), nodular goiter (12 cases), follicular carcinoma (13 cases), papillary carcinoma (33 cases), poorly differentiated carcinoma (five cases) and anaplastic carcinoma (15 cases) was chosen to represent a wide range of thyroid pathology. As control, 10 areas of normal thyroid parenchyma were selected from the lobe controlateral to the tumour in surgical specimens of papillary carcinoma.

Immunostaining: technique, evaluation and statistical analysis

Xylene dewaxed and alcohol-rehydrated paraffin sections were placed in Coplin jars filled with a 0.01 M tri-sodium citrate solution, and heated for 3 min in a conventional pressure cooker (Troncone *et al*, 2003). After heating, slides were thoroughly rinsed in cold running water for 5 min. They were then washed in Tris-Buffered Saline (TBS) pH 7.4 before incubating overnight with the specific antibody, diluted as follows: rabbit polyclonal α -UbcH10 (Boston Biochem) 1:1000; α -MIB-1 (Novocastra, Newcastle upon Tyne, UK) 1:50. After incubation with the primary antibody, tissue sections were stained with biotinylated anti-rabbit or anti-mouse immunoglobulins, followed by peroxidase-labelled streptavidine (Dako, Carpinteria, CA, USA); the signal was developed by using diaminobenzidine (DAB) chromogen as substrate. Incubations both omitting the specific antibody, and including unrelated antibodies, were used as negative controls.

Individual cells were scored for expression of UbcH10 and Ki-67 in similar areas of adjacent sections by quantitative analysis performed with a computerised analyser system (Ibas 2000, Kontron, Zeiss), as already described (Troncone *et al*, 2003). In each case, the distribution of these proteins was evaluated in at least 500 epithelial follicular cells and expressed as a percentage of the total cell population. The statistical analysis was performed using SPSS Ver. 9.0.1 for Windows. Data are expressed as median value and range. The nonparametric Mann–Whitney *U*-test was used to compare differences in labelling indexes for UbcH10 and Ki-67 in thyroid carcinomas. The Spearman rank order correlation was used to verify the association between UbcH10 and Ki-67. A *P*-value less than 0.05 was considered statistically significant.

RNA interference

For small interfering RNA (siRNA) experiments, the following double-strand RNA oligo specific for UbcH10 coding region was used: 5'-AACCTGCAAGAAACCTACTCA-3' as previously described (Wagner *et al*, 2004). As negative control, we used a corresponding scrambled sequence as follows: 5'-AACTAACAC TAGCTCAAGACC-3'. All of the siRNA duplexes were purchased from Qiagen and were transfected using Oligofectamine (Invitrogen) according to the manufacturer's recommendations. Small interfering RNAs were used at a final concentration of 100 nM and 12×10^5 cells well^{-1} were plated in a six-well format plates. Proteins were extracted 48 h after siRNA treatment and the levels of the UbcH10 protein were evaluated by Western blot.

Assay of the transformed state

Tumorigenicity of the cell lines was tested by injecting 2×10^6 cells subcutaneously into athymic mice. Soft agar colony assay was performed as previously described (Macpherson and Montagnier, 1964).

RESULTS

Expression of UbcH10 gene in normal human thyroid cells and thyroid carcinoma cell lines

To search for candidate genes involved in the neoplastic transformation of thyroid gland, RNAs extracted from normal human thyroid primary cells and six human thyroid carcinoma cell lines of different origin (WRO cell line from a follicular carcinoma, TPC-1 and FB-2 cell lines, both deriving from papillary thyroid cancers, NPA cell line, which derives from a poorly differentiated papillary carcinoma, ARO and FRO cell lines originating from anaplastic carcinomas) were hybridised to U95Av2 Affymetrix oligonucleotide arrays (data not shown). We

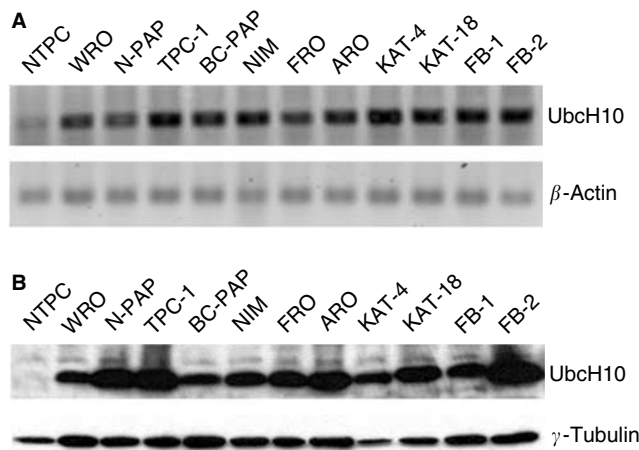


Figure 1 UbcH10 expression in human thyroid carcinoma cell lines. **(A)** UbcH10 gene expression analysis by RT–PCR in human thyroid carcinoma cell lines vs the normal human thyroid primary culture cells (NTPC). β -Actin gene expression was evaluated as control to normalise the amount of the used RNAs. **(B)** UbcH10 protein expression analysis by Western Blot in human thyroid carcinoma cell lines. Blot against γ -tubulin has been performed as control for equal protein loading.

concentrated our attention on the UbcH10 gene that was upregulated about 150-fold in all of the cell lines tested by the cDNA microarray. This result was confirmed by RT–PCR in a larger panel of thyroid carcinoma cell lines using as control normal thyroid primary culture (Figure 1A). Western blot analysis of UbcH10 expression, shown in Figure 1B, confirmed the RT–PCR data. In fact, the UbcH10 protein was abundantly expressed in all of the carcinoma cell lines, whereas it was barely detectable in normal thyroid cells.

Analysis of UbcH10 expression in normal and neoplastic thyroid tissues by immunohistochemistry, Western blot and RT–PCR

In order to evaluate whether the overexpression of UbcH10 is a feature of the thyroid tumours and not only of cultured thyroid carcinoma cell lines, we performed immunohistochemical analysis using a commercial antibody against UbcH10 protein. This methodology allows a rapid and sensitive screening of thyroid pathological tissues and is amenable to regular use as a routine diagnostic test. To find the best experimental conditions, ARO cell line and tumours, induced by injecting the ARO cell line into athymic mice, were used as positive controls (Cerutti *et al*, 1996). No staining was observed with normal human thyroid primary cell culture, whereas a positive staining was obtained with ARO cell line and ARO-induced tumours (data not shown). We found that normal thyroid, nodular goiter and Hashimoto's thyroiditis (HT) were almost always completely negative for UbcH10 expression. Only occasionally, single UbcH10-labelled thyroid epithelial cells showing mitotic figures could be observed by meticulous scrutiny (Figure 2A). In HT, there was a sharp contrast between the negative epithelial oxyphilic cells and the positive lymphoid germinal centers (Figure 2B). While a weak staining is detectable in follicular adenomas (Figure 2C), higher levels of UbcH10 were recorded in papillary (median value 2.2% of positive cells; range 0.9–4.1%), follicular (median value 2.8% of positive cells; range 1–6.1%) and poorly differentiated (median value 10.4% of positive cells; range 8–14.9%) carcinomas, signal being always easily detectable in the nuclei of scattered neoplastic cells (Figure 2D, E and F). UbcH10 staining pattern was somewhat different in

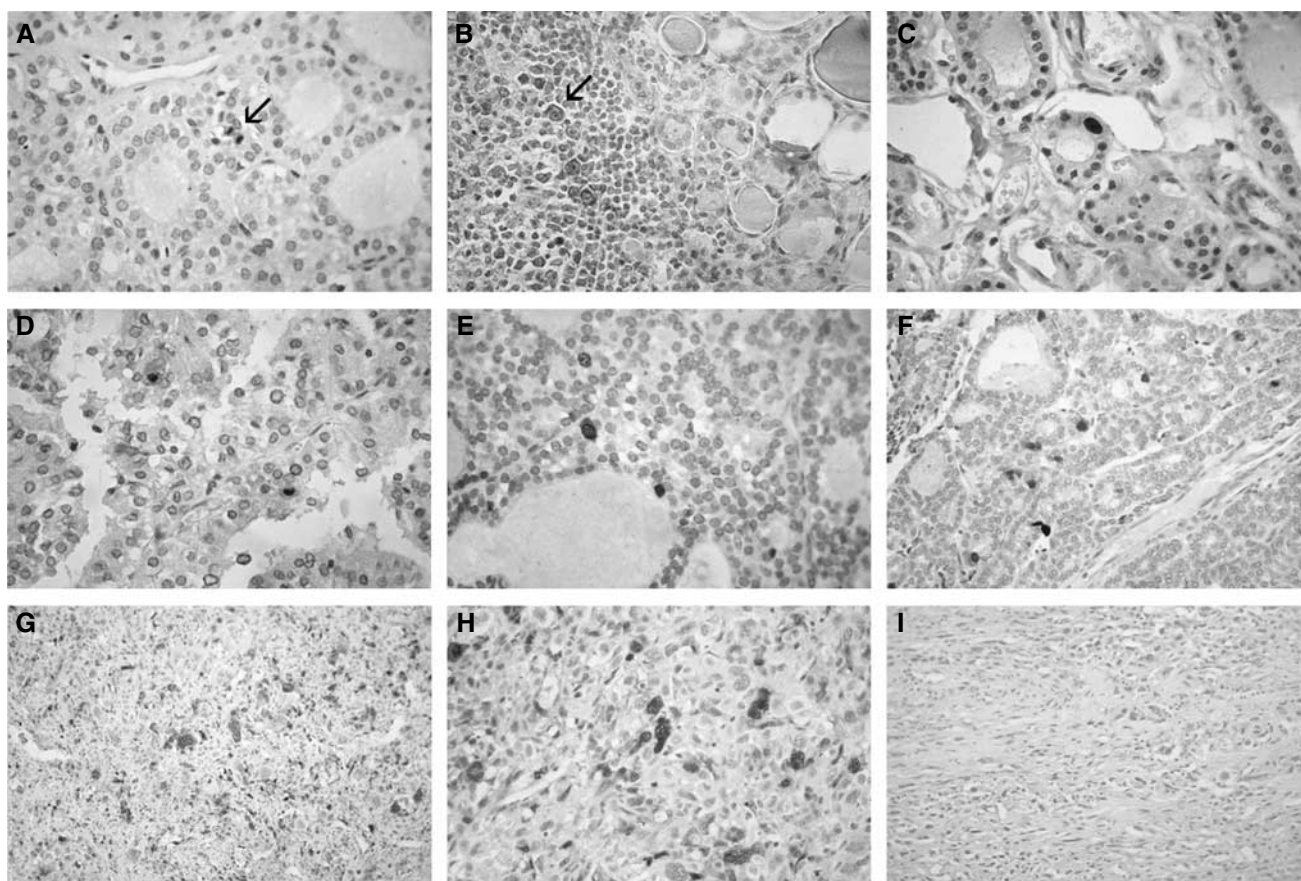


Figure 2 UbcH10 staining pattern in normal, inflammatory and neoplastic thyroid tissues. Follicular epithelial cells of normal thyroid (**A**) and oxyphilic cells of Hashimoto's thyroiditis (HT) (**B**) do not stain for UbcH10, with occasional mitotic figures (**A**, arrow) and lymphoid centroblasts of HT (**B**, arrow) providing the appropriate internal positive control. In neoplastic thyroid, UbcH10 staining pattern is strongly related to tumour grade, being weak in follicular adenoma (**C**), slightly more evident in well-differentiated papillary (**D**) and follicular (**E**) carcinomas, whereas stronger in poorly differentiated (**F**) and in anaplastic (**G**) carcinomas. In the latter, most of neoplastic cells show a very intense labelling, with intense nuclear staining (**H**), whereas signal disappeared by antigen incubation (**I**).

anaplastic carcinomas, the percentage (median value 45.8% of positive cells; range 38.8–56.2%) of stained cells being large and the intensity of the neoplastic cells being strong (Figure 2G and H).

No staining was observed when the same anaplastic carcinoma samples were stained with antibodies preincubated with UbcH10 recombinant protein (Figure 2I) or in the absence of the primary antibodies (data not shown). Therefore, as a general rule, UbcH10 expression is negligible in non-neoplastic thyroid, noticeable in well-differentiated carcinomas and conspicuous in less-differentiated tumours (Figure 3A).

To determine the relationship between UbcH10 expression and tissue proliferation, we correlated its expression in carcinomas with the proliferation rate of thyrocytes, as measured by Ki-67 staining; this latter showed the same tissue distribution of UbcH10, which was evident when adjacent (mirror) sections were stained. By using the Spearman rank order correlation, we determined that the association between UbcH10 and Ki-67 expression in thyroid cancer was statistically significant. In fact, the value of the Spearman R was 0.4 ($P < 0.001$) (Figure 3B).

Western blot analysis, performed on 30 surgically removed thyroid tumours, confirmed the immunohistochemical data. A representative Western blot is shown in Figure 4A. A strong band of 19.6 kDa corresponding to the UbcH10 protein was detected in anaplastic thyroid carcinomas and a weak one in poorly differentiated carcinomas, but not in papillary carcinomas and normal thyroids. These data strongly indicate that the expression

of UbcH10 is more abundant in thyroid carcinomas characterised by a highly malignant and aggressive phenotype. Equal amounts of total proteins were used for each sample as demonstrated by the same gel analysed with an antibody against γ -tubulin.

UbcH10 expression was also evaluated by RT-PCR analysis on a panel of matched tumour/normal tissues. This analysis confirmed the protein data. In fact, as shown in Figure 4B, an amplified band of 115 bp was clearly detected in the anaplastic and poorly differentiated carcinoma samples, but not in the papillary ones and in all the corresponding normal thyroid tissues. Finally, quantitative RT-PCR analysis confirmed a great increase of UbcH10 expression in thyroid anaplastic samples, whereas a light increase was observed in papillary carcinoma samples (Figure 4C).

UbcH10 expression in experimental models of thyroid carcinogenesis

Thyroid neoplasias developing in transgenic animal lines expressing TRK (Tg-TRK) (Russell *et al*, 2000), RET/PTC3 (Tg-RET/PTC3) (Powell *et al*, 1998) and large T SV40 (Tg-SV40) (Ledent *et al*, 1991) oncogenes under the transcriptional control of the thyroglobulin promoter have been analysed for UbcH10 expression by Western blot analysis. Transgenic mice carrying TRK and RET/PTC3 oncogenes develop thyroid papillary carcinomas (Powell *et al*, 1998; Russell *et al*, 2000); thyroid anaplastic carcinomas were, conversely, obtained in the Tg-SV40 mice

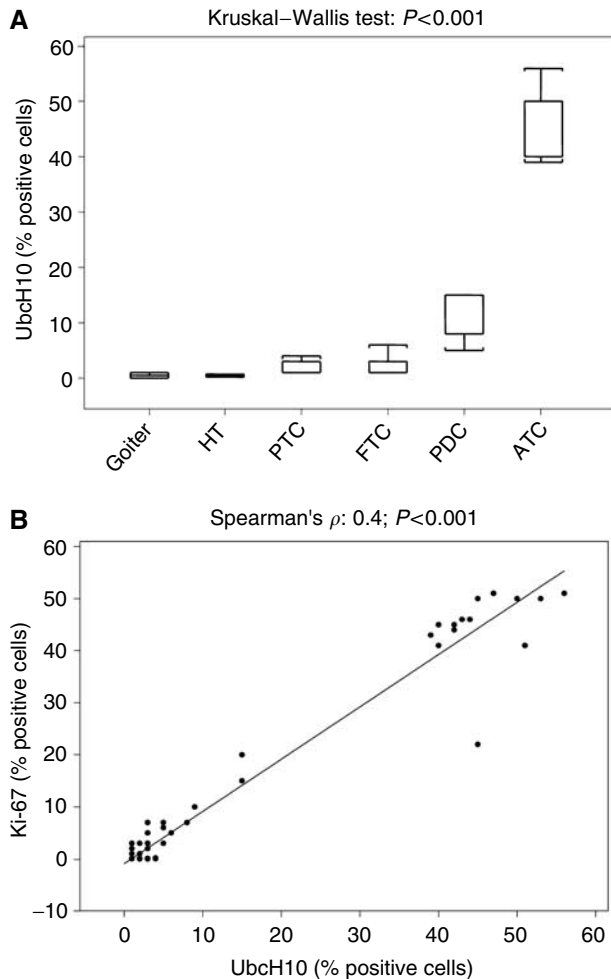


Figure 3 Statistical analysis of the immunohistochemical data. **(A)** Protein expression of UbcH10 (% positive cells) progressively increases in the several diagnostic categories from thyroid goiter to the thyroid anaplastic carcinomas. The analysis has been carried out using the Kruskal–Wallis test. HT, Hashimoto's thyroiditis; PTC, papillary thyroid carcinoma; FTC, follicular thyroid carcinoma; PDC, poorly differentiated thyroid carcinoma; ATC, anaplastic thyroid carcinoma. **(B)** Protein expression of UbcH10 (% positive cells) is correlated to that of Ki-67 (% positive cells) in the several diagnostic categories. The analysis has been carried out calculating the Spearman rank correlation coefficient.

(Ledent *et al*, 1991). As shown in Figure 5, elevated UbcH10 protein levels were observed in the thyroid anaplastic carcinomas derived from large TSV40 transgenic mice. Conversely, UbcH10 protein was absent in normal mouse thyroid tissue and in the papillary carcinomas originating from TRK and RET/PTC3 mice.

Therefore, the analysis of the experimental models of thyroid carcinogenesis seems to confirm that the UbcH10 overexpression is essentially restricted to the undifferentiated histotype.

Suppression of the UbcH10 synthesis inhibits thyroid carcinoma cell growth

We asked whether UbcH10 overexpression had a role in the process of thyroid carcinogenesis by evaluating the growth rate of two thyroid carcinoma cell lines, in which UbcH10 protein was suppressed by RNA interference. The NPA and TPC-1 cell lines were treated with siRNA duplexes targeting to the UbcH10 mRNA. After transfection, we observed an efficient knockdown of the UbcH10 protein levels at 48 h after treatment (Figure 6A). The

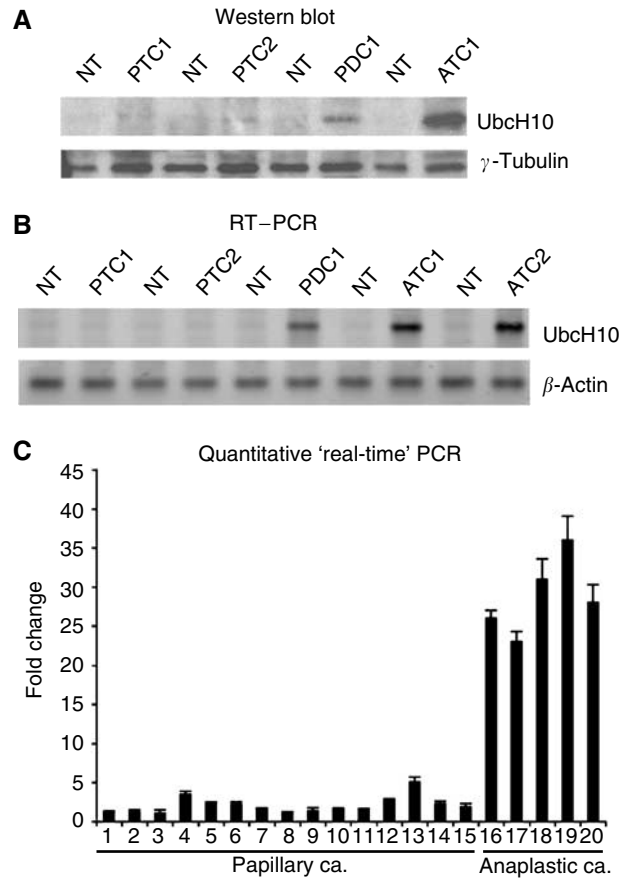


Figure 4 UbcH10 expression in human thyroid fresh tumour samples. **(A)** Western blot analysis of UbcH10 protein expression in a panel of thyroid neoplasias. The level of γ -tubulin has been used as loading control. NT, normal thyroid tissue; PTC1 and PTC2, papillary thyroid carcinomas from two different patients; PDC1, poorly differentiated carcinoma; ATC1, anaplastic thyroid carcinoma. **(B)** RT–PCR analysis of UbcH10 expression in human thyroid tumour samples vs their normal thyroid counterparts. β -Actin expression shows the same amount of RNAs used. NT, normal thyroid tissue; PTC1 and PTC2, papillary thyroid carcinomas from two different patients; PDC1, poorly differentiated carcinoma; ATC1 and ATC2, anaplastic thyroid carcinomas from two different patients. **(C)** Quantitative RT–PCR analysis was performed on human thyroid tumour samples of different histotype. The Fold Change values indicate the relative change in the expression levels between tumour samples and normal samples, assuming that the value of each normal sample is equal to 1.

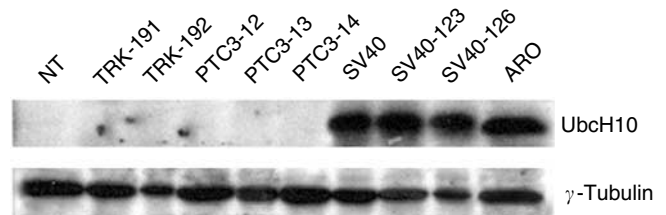


Figure 5 UbcH10 expression in experimental mouse thyroid tumours. Western blot analysis of experimental thyroid carcinomas developed in transgenic mice expressing TRK, RET-PTC-3 and large T SV40 oncogenes. ARO cell line was used as positive control. γ -Tubulin shows the same amount of protein level.

analysis of cell growth of these cell lines in the presence or absence of the UbcH10 siRNA duplexes revealed that the block of the UbcH10 protein synthesis significantly inhibits thyroid carcinoma

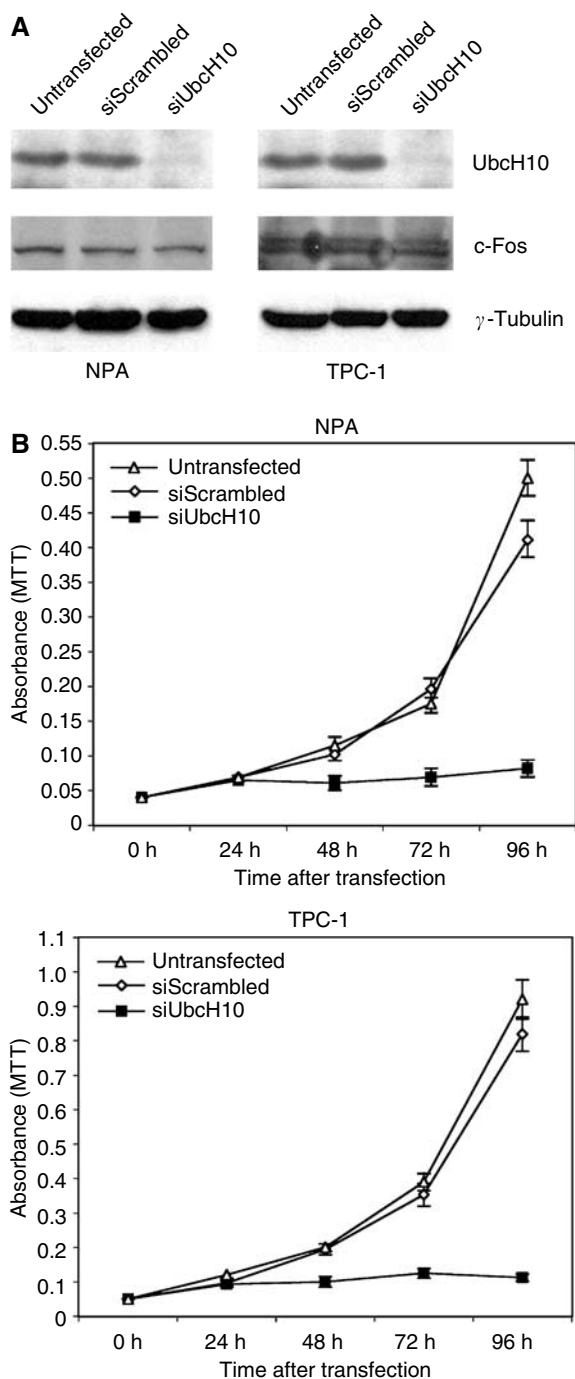


Figure 6 The block of UbcH10 protein synthesis by RNA interference inhibits the proliferation of thyroid carcinoma cells. **(A)** Inhibition of UbcH10 protein expression by RNAi in NPA and TPC-1 cell lines evaluated by Western blot analysis. At 48 h after siRNA transfection, total cell lysates were prepared and normalised for protein concentration. The expression of γ -tubulin was used to control equal protein loading (30 μ g). In this figure, we also show the expression of a fast turning-over gene like c-Fos to confirm the specific effect of siRNAs against UbcH10. **(B)** Growth curves of NPA and TPC-1 cell lines after siUbcH10 treatment. NPA and TPC-1 cells were transfected with siUbcH10 duplexes (siUbcH10) and the relative number of viable cells was determined by MTT assay. Cells transfected with a scrambled duplex (siScrambled) and untransfected cells (Untransfected) were used as negative controls. Absorbance was read at 570 nm and the data are the mean of triplicates.

Table 1 Analysis of the neoplastic phenotype of the UbcH10-transfected rat thyroid cell lines

Cell line	Doubling time (h)	Colony-forming efficiency ^a (%)	Tumour ^b incidence
PC CL 3	24	0	0/4
PC UbcH10 CL1	24	0	0/4
PC UbcH10 CL2	23	0	0/4
PC MPSV	18	70	4/4

^aColony-forming efficiency was calculated by the formula (number of colonies formed/number of plated cells) \times 100. ^bTumorigenicity was assayed by injecting 2×10^6 cells into athymic mice (4–6 weeks old).

cell growth. In fact, as shown in Figure 6B, a significant reduction in cell growth rate was observed in NPA and TPC-1 cell lines treated with UbcH10 siRNA in comparison to the untreated cells or those treated with the control scrambled siRNA.

These results indicate a role of UbcH10 in neoplastic thyroid cell proliferation.

UbcH10 overexpression is not sufficient to transform rat thyroid cells

To further characterise the role of UbcH10 in thyroid carcinogenesis, we transfected normal rat thyroid cells with an expression vector carrying the UbcH10 gene under the transcriptional control of the cytomegalovirus promoter. The selected clones were shown to express high UbcH10 protein levels (data not shown). We evaluated the growth rate of the UbcH10-transfected PC Cl 3 cells and the same cells transfected with a backbone vector: no differences were observed. Equally, the neoplastic phenotype of the UbcH10-transfected PC Cl 3 cells was evaluated by a soft agar colony assay and by injection into athymic mice. As reported in Table 1, the PC Cl 3 cells transfected with the UbcH10 expression vector were not able to give rise to colonies in soft agar and induce tumours in athymic mice. As a positive control, we used the PC Cl 3 cells transformed with the Myeloproliferative sarcoma virus (PC MPSV): these cells have a very highly malignant phenotype (Fusco *et al*, 1987).

These results indicate that UbcH10 overexpression is not able to transform rat thyroid cells *in vitro*.

DISCUSSION

Thyroid neoplasms represent an excellent model for studying the process of cell transformation since they include a broad spectrum of histotypes showing different degree of malignancy (Hedinger *et al*, 1989; Wynford-Thomas, 1997). From the Affymetrix microarray analysis, we found the UbcH10 gene that appeared greatly increased in all of the thyroid carcinoma cell lines. UbcH10 was previously identified as a human homologue of the cyclin-selective E2 (E2-c), which is required for the destruction of mitotic cyclins by the ubiquitination pathway. The UbcH10 gene belongs to the E2 gene family and codes for a protein of 19.6 kDa that is involved in the ubiquitin-dependent proteolysis. In this system, three distinct enzymes cooperate to process target proteins for degradation. More precisely, the ubiquitin-conjugating enzyme (E2) transfers activated ubiquitin by ubiquitin-activating enzyme (E1) to a lysine residue of the target proteins in cooperation with the ubiquitin-ligase (E3). Polyubiquitinated proteins are then recognised by the 26S proteasome and rapidly degraded (Hershko and Ciechanover, 1998; Joazeiro and Weissman, 2000).

In our study, we have evaluated the expression of UbcH10 in human thyroid neoplasias and in mouse experimental tumours. No

significant UbcH10 expression was observed in normal thyroids, goiters and adenomas, whereas a great induction of UbcH10 expression was observed in anaplastic human thyroid carcinomas and in experimental undifferentiated thyroid tumours. Just a weak expression of UbcH10 was observed in follicular and papillary human thyroid carcinomas. Therefore, these data strongly indicate that UbcH10 overexpression could be associated with the thyroid tumour progression since there is a good correlation with the late stage of thyroid neoplastic transformation. The low UbcH10 levels detected in the differentiated thyroid malignancies would appear in contrast with the data showing an abundant UbcH10 expression in the cell lines deriving from differentiated carcinomas. We retain this discrepancy only apparent since thyroid carcinoma cell lines, even deriving from differentiated tumours, cannot be completely compared to surgically removed tumours. In fact, these cell lines harbour p53 mutations that are rare in thyroid differentiated neoplasias (Tanaka *et al*, 1987; Estour *et al*, 1989; Pang *et al*, 1989; Ito *et al*, 1992; Dobashi *et al*, 1993; Donghi *et al*, 1993; Fagin *et al*, 1993; Zeki *et al*, 1993; Fabien *et al*, 1994; Matias-Guiu *et al*, 1994; Ain *et al*, 1997; Fiore *et al*, 1997; Basolo *et al*, 2002) and they have a high proliferation rate. However, this consideration does not exclude the validity of the use of the thyroid carcinoma cell lines as experimental model to draw new information that, however, need to be subsequently validated on fresh tumours.

Our results also indicate a correlation between UbcH10 overexpression and the proliferation status since there is a good association with the proliferation marker Ki-67/MIB1.

An aim of our work was to evaluate the possible causal role of UbcH10 overexpression in thyroid carcinogenesis. Indeed, the block of protein synthesis significantly inhibited the growth of several thyroid carcinoma cell lines, suggesting an important role of UbcH10 in thyroid cell proliferation, and then in the progression step of thyroid carcinogenesis.

Therefore, even though the mechanisms by which UbcH10 overproduction contributes to the neoplastic phenotype remains unclear, we can assume that it leads to a deregulation of cell growth. These results are quite consistent with previous published data showing that UbcH10 was expressed at high levels in primary tumours derived from the lung, stomach, uterus, and bladder as compared with their corresponding normal tissues, suggesting that UbcH10 is involved in tumorigenesis or cancer progression (Okamoto *et al*, 2003; Wagner *et al*, 2004). It has also been shown that UbcH10 is upregulated in NIH3T3 cell line transformed by

EWS/FLI1, but not in untransformed NIH3T3 cell clone expressing EWS/FLI1 (Arvand *et al*, 1998). Moreover, it has been shown that UbcH10 is required for override metaphase, likely degrading growth suppressor, and for destruction of mitotic cyclins, indicating a role of UbcH10 in cell cycle progression (Arvand *et al*, 1998).

However, overexpression of UbcH10 in normal rat thyroid cells did not affect cell growth neither induced a malignant phenotype, indicating that UbcH10 overexpression is not sufficient for malignant thyroid cell transformation. This result might appear in contrast with those showing that NIH3T3 stable transfectants overexpressing UbcH10 exhibited a malignant phenotype as compared with parental NIH3T3 cells (Okamoto *et al*, 2003). This discrepancy is, in our opinion, just apparent since we have to consider that NIH 3T3 cells are preneoplastic cells, whereas PC Cl 3 cells are much more resistant to express the neoplastic phenotype, since even the expression of several oncogenes (v-ras-Ki, v-ras-Ha, etc.) are not able to lead these cells to the fully malignant phenotype that is achieved only when there is a synergy of two different oncogenes (Fusco *et al*, 1987). In conclusion, our data propose the UbcH10 overexpression as a feature of the anaplastic carcinoma histotype. The block of UbcH10 expression significantly reduced the growth of thyroid carcinoma cell lines indicating an involvement of UbcH10 in the increased proliferation of these carcinoma cell lines. Therefore, these results open the perspective of a therapy of the anaplastic thyroid carcinoma, one of the most aggressive tumours in mankind, based on the suppression of the UbcH10 synthesis and/or function.

ACKNOWLEDGEMENTS

This work was supported by grants from the Associazione Italiana Ricerca sul Cancro (AIRC), Progetto Strategico Oncologia Consiglio Nazionale delle Ricerche, the Ministero dell'Università e della Ricerca Scientifica e Tecnologica (MIUR), and 'Piani di Potenziamento della Rete Scientifica e Tecnologica' CLUSTER C-04, the Programma Italia-USA sulla Terapia dei Tumori coordinated by Professor Cesare Peschle, and 'Ministero della Salute'. This work was supported from NOGEC-Naples Oncogenomic Center. We thank the Associazione Partenopea per le Ricerche Oncologiche (APRO) for its support. We are grateful to Jean Ann Gilder (Scientific Communication) for editing the text.

REFERENCES

- Ain KB, Taylor KD, Tofiq S, Venkataraman G (1997) Somatostatin receptor subtype expression in human thyroid and thyroid carcinoma cell lines. *J Clin Endocrinol Metab* **82**: 1857–1862
- Arvand A, Bastians H, Welford SM, Thompson AD, Ruderman JV, Denny CT (1998) EWS/FLI1 up regulates mE2-C, a cyclin-selective ubiquitin conjugating enzyme involved in cyclin B destruction. *Oncogene* **17**: 2039–2045
- Basolo F, Giannini R, Toniolo A, Casalone R, Nikiforova M, Pacini F, Elisei R, Miccoli P, Berti P, Faviana P, Fiore L, Monaco C, Pierantoni GM, Fedele M, Nikiforov YE, Santoro M, Fusco A (2002) Establishment of a non-tumorigenic papillary thyroid cell line (FB-2) carrying the RET/PTC1 rearrangement. *Int J Cancer* **97**: 608–614
- Cerutti J, Trapasso F, Battaglia C, Zhang L, Martelli ML, Visconti R, Berlingieri MT, Fagin JA, Santoro M, Fusco A (1996) Block of c-myc expression by antisense oligonucleotides inhibits proliferation of human thyroid carcinoma cell lines. *Clin Cancer Res* **2**: 119–126
- Curcio F, Ambesi-Impombato FS, Perrella G, Coon HG (1994) Long-term culture and functional characterization of follicular cells from adult normal human thyroids. *Proc Natl Acad Sci USA* **91**: 9004–9008
- Di Renzo MF, Olivero M, Ferro S, Prat M, Bongarzone I, Pilotti S, Belfiore A, Costantino A, Vigneri R, Pierotti MA (1992) Overexpression of the c-MET/HGF receptor gene in human thyroid carcinomas. *Oncogene* **7**: 2549–2553
- Dobashi Y, Sakamoto A, Sugimura H, Mernyei M, Mori M, Oyama T, Machinami R (1993) Overexpression of p53 as a possible prognostic factor in human thyroid carcinoma. *Am J Surg Pathol* **17**: 375–381
- Donghi R, Longoni A, Pilotti S, Michieli P, Della Porta G, Pierotti MA (1993) Gene p53 mutations are restricted to poorly differentiated and undifferentiated carcinomas of the thyroid gland. *J Clin Invest* **91**: 1753–1760
- El-Rifai W, Frierson Jr HF, Moskaluk CA, Harper JC, Petroni GR, Bissonette EA, Jones DR, Knuutila S, Powell SM (2001) Genetic differences between adenocarcinomas arising in Barrett's esophagus and gastric mucosa. *Gastroenterology* **121**: 592–598
- Estour B, Van Herle AJ, Juillard GJ, Totanes TL, Sparkes RS, Giuliano AE, Klandorf H (1989) Characterization of a human follicular thyroid carcinoma cell line (UCLA RO 82 W-1). *Virchows Arch B Cell Pathol Incl Mol Pathol* **57**: 167–174
- Fabien R, Fusco A, Santoro M, Barbier Y, Dubois PM, Paulin C (1994) Description of a human papillary thyroid carcinoma cell line. Morphologic study and expression of tumoral markers. *Cancer* **73**: 2206–2212
- Fagin JA, Matsuo K, Karmakar A, Chen DL, Tang SH, Koeffler HP (1993) High prevalence of mutations of p53 gene in poorly differentiated human thyroid carcinomas. *J Clin Invest* **91**: 179–184

- Fiore L, Pollina LE, Fontanini G, Casalone R, Berlingieri MT, Giannini R, Pacini F, Miccoli P, Toniolo A, Fusco A, Basolo F (1997) Cytokine production by a new undifferentiated human thyroid carcinoma cell line, FB-1. *J Clin Endocrinol Metab* **82**: 4094–4100
- Fukushima T, Suzuki S, Mashiko M, Ohtake T, Endo Y, Takebayashi Y, Sekikawa K, Hagiwara K, Takenoshita S (2003) BRAF mutations in papillary carcinomas of the thyroid. *Oncogene* **22**: 6455–6457
- Fusco A, Berlingieri MT, Di Fiore PP, Portella G, Grieco M, Vecchio G (1987) One- and two-step transformation of rat thyroid epithelial cells by retroviral oncogenes. *Mol Cell Biol* **7**: 3365–3370
- Grieco M, Santoro M, Berlingieri MT, Melillo RM, Donghi R, Bongarzone I, Pierotti MA, Della Porta G, Fusco A, Vecchio G (1990) PTC is a novel rearranged form of the RET proto-oncogene and is frequently detected *in vivo* in human thyroid papillary carcinomas. *Cell* **60**: 557–563
- Hedinger C, Williams D, Sobin LH (1989) The WHO histological classification of thyroid tumours: a commentary on the second edition. *Cancer* **63**: 908–911
- Hershko A, Ciechanover A (1998) The ubiquitin system. *Annu Rev Biochem* **67**: 425–479
- Ito T, Seyama T, Mizuno T, Tsuyama N, Hayashi T, Hayashi Y, Dohi K, Nakamura N, Akiyama M (1992) Unique association of p53 mutations with undifferentiated but not differentiated carcinomas of the thyroid gland. *Cancer Res* **52**: 1369–1371
- Joazeiro CA, Weissman AM (2000) RING finger proteins: mediators of ubiquitin ligase activity. *Cell* **102**: 549–552
- Kroll TG, Sarraf P, Pecciarini L, Chen CJ, Mueller E, Spiegelman BM, Fletcher JA (2000) PAX-8-PPARGamma1 fusion oncogene in human thyroid carcinoma. *Science* **289**: 1357–1360
- Ledent C, Dumont J, Vassart G, Parmentier M (1991) Thyroid adenocarcinomas secondary to tissue-specific expression of simian virus-40 large T-antigen in transgenic mice. *Endocrinology* **129**: 1391–1401
- Macpherson I, Montagnier I (1964) Agar suspension culture for the selective assay of cells transformed by polyoma virus. *Virology* **23**: 291–294
- Matias-Guiu X, Cuatrecasas M, Musulen E, Prat J (1994) p53 expression in anaplastic carcinomas arising from thyroid papillary carcinomas. *J Clin Pathol* **47**: 337–339
- Okamoto Y, Ozaki T, Miyazaki K, Aoyama M, Miyazaki M, Nakagawara A (2003) UbcH10 is the cancer-related E2 ubiquitin-conjugating enzyme. *Cancer Res* **63**: 4167–4173
- Pang XP, Hershman JM, Chung M, Pekary AE (1989) Characterization of tumor necrosis factor-alpha receptors in human and rat thyroid cells and regulation of the receptors by thyrotropin. *Endocrinology* **125**: 1783–1788
- Pierotti MA, Bongarzone I, Borrello MG, Mariani C, Miranda C, Sozzi G, Greco A (1995) Rearrangements of TRK proto-oncogene in papillary thyroid carcinomas. *J Endocrinol Invest* **18**: 130–133
- Powell Jr DJ, Russell J, Nibu K, Li G, Rhee E, Liao M, Goldstein M, Keane WM, Santoro M, Fusco A, Rothstein JL (1998) The RET/PTC3 oncogene: metastatic solid-type papillary carcinomas in murine thyroids. *Cancer Res* **58**: 5523–5528
- Russell JP, Powell DJ, Cunnane M, Greco A, Portella G, Santoro M, Fusco A, Rothstein JL (2000) The TRK-T1 fusion protein induces neoplastic transformation of thyroid epithelium. *Oncogene* **19**: 5729–5735
- Suarez HG, du Villard JA, Severino M, Caillou B, Schlumberger M, Tubiana M, Parmentier C, Monier R (1990) Presence of mutations in all three ras genes in human thyroid tumors. *Oncogene* **5**: 565–570
- Tallini G, Santoro M, Helie M, Carlomagno F, Salvatore G, Chiappetta G, Carcangiu ML, Fusco A (1998) RET/PTC oncogene activation defines a subset of papillary thyroid carcinomas lacking evidence of progression to poorly differentiated or undifferentiated tumor phenotypes. *Clin Cancer Res* **4**: 287–294
- Tanaka J, Ogura T, Sato H, Datano M (1987) Establishment and biological characterization of an *in vitro* human cytomegalovirus latency model. *Virology* **161**: 62–72
- Troncone G, Iaccarino A, Caleo A, Bifano D, Pettinato G, Palombini L (2003) p27 Kip1 protein expression in Hashimoto's thyroiditis. *J Clin Pathol* **56**: 587–591
- Wagner KW, Sapinoso LM, El-Rifai W, Frierson Jr HF, Butz N, Mestan J, Hofmann F, Deveraux QL, Hampton GM (2004) Overexpression, genomic amplification and therapeutic potential of inhibiting the UbcH10 ubiquitin conjugase in human carcinomas of diverse anatomic origin. *Oncogene* **23**: 6621–6629
- Wynford-Thomas D (1997) Origin and progression of thyroid epithelial tumours. Cellular and molecular mechanisms. *Horm Res* **47**: 145–157
- Zeki K, Nakano Y, Inokuchi N, Watanabe K, Morimoto I, Yamashita U, Eto S (1993) Autocrine stimulation of interleukin-1 in the growth of human thyroid carcinoma cell line NIM 1. *J Clin Endocrinol Metab* **76**: 127–133

Loss of the *CBX7* Gene Expression Correlates with a Highly Malignant Phenotype in Thyroid Cancer

Pierlorenzo Pallante,^{1,2} Antonella Federico,² Maria Teresa Berlingieri,¹ Mimma Bianco,¹ Angelo Ferraro,² Floriana Forzati,¹ Antonino Iaccarino,³ Maria Russo,³ Giovanna Maria Pierantoni,¹ Vincenza Leone,² Silvana Sacchetti,² Giancarlo Troncone,^{2,3} Massimo Santoro,^{1,2} and Alfredo Fusco^{1,2}

¹Istituto di Endocrinologia ed Oncologia Sperimentale del CNR c/o Dipartimento di Biologia e Patologia Cellulare e Molecolare, Facoltà di Medicina e Chirurgia, Università degli Studi di Napoli "Federico II"; ²NOGEC (Naples Oncogenomic Center)-CEINGE, Biotecnologie Avanzate-Napoli and SEMM-European School of Molecular Medicine-Naples Site; and ³Dipartimento di Scienze Biomorfologiche e Funzionali, Facoltà di Medicina e Chirurgia, Università di Napoli "Federico II," Naples, Italy

Abstract

Using gene expression profiling, we found that the *CBX7* gene was drastically down-regulated in six thyroid carcinoma cell lines versus control cells. The aims of this study were to determine whether *CBX7* is related to the thyroid cancer phenotype and to try to identify new tools for the diagnosis and prognosis of thyroid cancer. We thus evaluated *CBX7* expression in various snap-frozen and paraffin-embedded thyroid carcinoma tissues of different degrees of malignancy by quantitative reverse transcription-PCR and immunohistochemistry, respectively. *CBX7* expression progressively decreased with malignancy grade and neoplasia stage. Indeed, it decreased in an increasing percentage of cases going from benign adenomas to papillary (PTC), follicular, and anaplastic (ATC) thyroid carcinomas. This finding coincides with results obtained in rat and mouse models of thyroid carcinogenesis. *CBX7* loss of heterozygosity occurred in 36.8% of PTC and in 68.7% of ATC. Restoration of *CBX7* expression in thyroid cancer cells reduced growth rate, with a retention in the G₁ phase of the cell cycle, suggesting that *CBX7* can contribute to the proliferation of the transformed thyroid cells. In conclusion, loss of *CBX7* expression correlates with a highly malignant phenotype in thyroid cancer patients. [Cancer Res 2008;68(16):6770–8]

Introduction

Thyroid tumors originating from follicular cells are a good model with which to investigate the events involved in carcinogenesis because they differ in malignant potential from differentiated to undifferentiated phenotypes (1, 2). Papillary thyroid carcinoma (PTC), which is differentiated and has a good prognosis, is the most frequent malignancy of the thyroid gland (2). The tall-cell variant (TCV) of PTC has a worse prognosis than conventional PTC (3). Poorly differentiated carcinomas (PDC) have a less differentiated phenotype and a poor 5-year survival rate (2). Finally, anaplastic carcinomas (ATC) are completely undifferentiated, very

aggressive, and always fatal (2). In PTC, activation of the *RET/PTC* oncogene, caused by rearrangements of the *RET* proto-oncogene, occurs in about 20% of cases (2), whereas the *B-RAF* gene is mutated in about 40% of cases (4). These tumors have also been associated with *TRK* gene rearrangements (5) and *MET* gene overexpression (6). *RAS* gene mutations (7) and *PAX8-PPAR-γ* rearrangements (8) are frequent in follicular thyroid carcinomas (FTC), whereas impaired function of the p53 tumor suppressor gene is a feature of ATC (9). Although critical molecular mechanisms of thyroid carcinogenesis have been clarified, other molecular steps of thyroid neoplastic progression need to be investigated.

Therefore, within the context of a microarray study, we found that the *CBX7* gene was down-regulated in thyroid carcinoma-derived cell lines and in surgically removed tumors. *CBX7*, which is located on chromosome 22q13.1, encodes a novel Polycomb protein (Pc) of 28.4 kDa and 251 amino acids that contains a "chromodomain" between amino acids 10 and 46. The chromodomain was originally defined as a 37-amino-acid region of homology shared by heterochromatin protein 1 (HP1) and Pc proteins from *Drosophila melanogaster* (10, 11). The *CBX7* protein seems to be involved in the control of normal cell growth (11, 12). Moreover, mouse *CBX7* associates with facultative heterochromatin and with the inactive X chromosome, which indicates that *CBX7* is involved in the repression of gene transcription (13).

Thyroid cancer is the most prevalent endocrine neoplasia. About 20,000 new cases are diagnosed in the United States each year, and >1,500 patients die of thyroid cancer annually. Given the poor prognosis associated with the less differentiated histologic types, namely TCV-PTC and Hurthle variants, and the undifferentiated ATC, there is a need for molecular markers that can help to predict prognosis, so that patients with a dismal prognosis can be offered a different, perhaps, innovative therapy.

In an attempt to determine whether *CBX7* is related to thyroid cancer phenotype, and to find new tools for the diagnosis and prognosis of thyroid cancer, we have evaluated its expression in a large number of thyroid carcinoma tissues and in rat and mouse models of thyroid carcinogenesis. This analysis revealed a decreased *CBX7* expression in an increasing percentage of cases going through from benign adenomas (FTA) to PTC, FTC, and ATC. Taken together, these results indicate a correlation of the loss of *CBX7* expression with a highly malignant phenotype in thyroid cancer patients. Because restoration of *CBX7* expression in thyroid cancer cells reduced growth rate, a role of the loss of *CBX7* gene expression in thyroid carcinogenesis may be envisaged.

Note: Supplementary data for this article are available at Cancer Research Online (<http://cancerres.aacrjournals.org/>).

Requests for reprints: Alfredo Fusco, Dipartimento di Biologia e Patologia Cellulare e Molecolare, Università di Napoli Federico II and Naples Oncogenomic Center (NOGEC)-CEINGE-Biotecnologie Avanzate, Napoli, and European School of Molecular Medicine (SEMM), via Pansini 5, 80131 Naples, Italy. Phone: 39-081-3737857; Fax: 39-081-3737808; E-mail: afusco@napoli.com or afusco@unina.it

©2008 American Association for Cancer Research.

doi:10.1158/0008-5472.CAN-08-0695

Materials and Methods

Cell culture and transfections. We used the following human thyroid carcinoma cell lines in this study: TPC-1, WRO, NPA, ARO, FRO, NIM 1, B-CPAP, FB-1, FB-2, Kat-4, and Kat-18, which are described elsewhere (14). They were grown in DMEM (Gibco Laboratories) containing 10% FCS (Gibco Laboratories), glutamine (Gibco Laboratories), and ampicillin/streptomycin (Gibco Laboratories) in a 5% CO₂ atmosphere. Normal human thyroid primary culture cells have been established and grown as already described (15). PC CL 3 (16) and FRTL-5 (17) cell lines were cultured in modified F12 medium supplemented with 5% calf serum (Gibco Laboratories) and six growth factors (thyrotropic hormone, hydrocortisone, insulin, transferrin, somatostatin, and glycyl-histidyl-lysine; Sigma). PC CL 3 and FRTL-5 infected with several oncogenes PC KiMSV, PC HaMSV, PC *v-raf*, PC MPSV (16), PC PyMLV (18), PC E1A, PC E1A+*v-raf* (19), PC RET/PTC, PC HaMSV+RET/PTC1 (20), PC MPSV-HMGA2 (21), FRTL-5 KiMSV (22), and FRTL-5 KiMSV-HMGA1 (23) cells were cultured in the same medium as PC CL 3 and FRTL-5 cells but without the six growth factors. Thyroid cells were transfected using Lipofectamine reagent (Invitrogen) according to the manufacturer's instructions. The transfected cells were selected in a medium containing geneticin (G418; Life Technologies). For each transfection, several G418-resistant clones and the mass cell population were isolated and expanded for further analysis.

Human thyroid tissue samples. Neoplastic human thyroid tissues and normal adjacent tissue or the contralateral normal thyroid lobe were obtained from surgical specimens and immediately frozen in liquid nitrogen. Thyroid tumors were collected at the Service d'Anatomopathologie, Centre Hospitalier Lyon Sud, Pierre Bénite, France. The tumor samples were stored frozen until required for RNA or protein extraction.

This study has been approved by the institutional review board of the Dipartimento di Biologia e Patologia Cellulare e Molecolare, Università degli Studi di Napoli "Federico II".

RNA isolation. Total RNA was extracted from tissues and cell cultures using the RNeasy Mini Kit (Qiagen) according to the manufacturer's instructions. The integrity of the RNA was assessed by denaturing agarose gel electrophoresis.

Reverse transcription and PCR analysis. One microgram of total RNA from each sample was reverse-transcribed with QuantiTect Reverse Transcription Kit (Qiagen) using an optimized blend of oligo-dT and random primers according to the manufacturer's instructions. PCR was carried out on cDNA as previously described (14). Primer sequences are available as Supplementary Materials and Methods. To design a quantitative reverse transcription-PCR (qRT-PCR) assay, we used the Human ProbeLibrary system (Exiqon). Detailed procedure and primer sequences, as well as qRT-PCR experiments, are available as Supplementary Materials and Methods.

Protein extraction, Western blotting, and antibodies. Protein extraction and Western blotting procedure were carried out as reported elsewhere (14). Membranes were incubated with a primary antibody raised against the COOH terminus of the human CBX7 protein (Neosystem) for 60 min (at room temperature). To ascertain that equal amounts of protein were loaded, the Western blots were incubated with antibodies against the α -tubulin protein (Sigma). Membranes were then incubated with the horseradish peroxidase-conjugated secondary antibody (1:3,000) for 60 min (at room temperature) and the reaction was detected with a Western blotting detection system (enhanced chemiluminescence; GE Healthcare).

Histologic analyses. The cell distribution of the CBX7 protein was assessed by immunostaining formalin-fixed, paraffin-embedded thyroid tumor blocks retrieved from the files of the Dipartimento di Scienze Biomorfologiche e Funzionali at the Università di Napoli "Federico II" and selected to represent a wide range of thyroid neoplastic diseases. Briefly, xylene-dewaxed and alcohol-rehydrated paraffin sections were placed in Coplin jars filled with a 0.01 mol/L trisodium citrate solution and heated for 3 min in a conventional pressure cooker (14). After heating, slides were thoroughly rinsed in cool running water for 5 min. They were washed in TBS (pH 7.4) and then incubated overnight with the specific rabbit polyclonal primary antibody. Subsequently, tissue sections were stained

with biotinylated anti-rabbit immunoglobulins and then with peroxidase-labeled streptavidin (Dako). The signal was developed by using diaminobenzidine chromogen as substrate. Incubations both omitting and preadsorbing the specific antibody were used as negative controls.

To ensure that we evaluated CBX7 expression only on technically adequate slides, we discarded slides that lacked a convincing internal control, namely labeling of stromal, endothelial, or lymphoid cell, shown to be positive in a preliminary normal tissue microarray analysis (data not shown). Based on these criteria, we scored paraffin-embedded stained slides from 20 cases of FTA, 30 cases of classic PTC, 6 cases of TCV PTC, 32 cases of FTC, 12 cases of PDC, and 12 cases of ATC. As controls, we selected areas of normal thyroid parenchyma from the lobe contralateral to the tumor in 20 surgical specimens of PTC. Individual cells were scored for the expression of CBX7 by quantitative analysis performed with a computerized analyzer system (Ibas 2000, Kontron, Zeiss), as described previously (14), and tumors were subdivided into low expressors (<50% of positive cells) and high expressors (>50% of positive cells).

Thyroid fine-needle aspiration biopsies. The fine-needle aspiration biopsies (FNAB) were carried out at the Cytopathology Section of the Dipartimento di Scienze Biomorfologiche e Funzionali (Università di Napoli "Federico II") as described elsewhere (24, 25). To evaluate whether CBX7 gene expression analysis is also feasible on cytologic samples, we selected cell-block specimens obtained from 15 FNAB diagnosed as PTC and histologically confirmed. Five-micrometer paraffin-embedded sections were cut from each cell block and were examined for the presence of neoplastic cells by H&E staining, before CBX7 immunocytochemistry and qRT-PCR had been carried out. Nonneoplastic cytologic specimens, used as controls, were obtained from the cell block corresponding to FNAB taken from goiter nodules. FNAB samples were processed for RNA extraction using the procedure described in a previous section.

Loss of heterozygosity analysis. We used several single nucleotide polymorphism (SNP) markers to evaluate the loss of heterozygosity (LOH) at the CBX7 locus on chromosome 22q13.1. We selected the SNP markers⁴ that showed high average heterozygosity levels to obtain the highest number of informative cases. Briefly, genomic DNA was PCR amplified in a region spanning about 200 bp around the SNP analyzed, then the purified PCR product was sequenced. We measured the height of the two peaks on the chromatogram and calculated the ratio of the two alleles in the matched tumor/normal samples: LOH was defined if the ratio in the carcinoma sample was <50%. SNPs and relative primer sequences are available as Supplementary Materials and Methods.

Plasmid constructs and cell colony-forming assay. CBX7 expression plasmid was constructed by cloning the human cDNA sequence in a pCRII TA Cloning vector (Invitrogen). The primers used were as follows: CBX7 forward 5'-ATGGAGCTGTCAGCCATC-3' and CBX7 reverse 5'-TCA-GAACTTCCCCTGCG-3'. The inserted cDNA was then subcloned into the *Bam*HI/*Xho*I sites of the mammalian expression vector pcDNA 3.1 (Invitrogen). The expression of CBX7 was assessed by Western blotting. Cells, plated at a density of 90% in 100-mm dishes, were transfected with 5 μ g pcDNA3.1 or pCBX7 and supplemented with geneticin (G418) 24 h later. Two weeks after the onset of drug selection, the cells were fixed and stained with crystal violet (0.1% crystal violet in 20% methanol).

Cell cycle analysis. Cells were harvested in PBS containing 2 mmol/L EDTA, washed once with PBS, and treated for 30 min in cold ethanol (70%). Cells were washed once in PBS and permeabilized with 0.2% Tween 20 and 1 mg/mL RNase A for 30 min, and washed and stained with 50 μ g/mL propidium iodide. Stained cells were analyzed with a FACSCalibur (Becton Dickinson), and the data were analyzed using a Mod-Fit cell cycle analysis program.

Preparation of recombinant adenovirus and infection protocol. The recombinant adenovirus was constructed using the AdEasy Vector System (Quantum Biotechnologies). The cDNA fragment was inserted in the sense orientation into the *Not*I and *Hind*III sites of the pShuttle-CMV vector to

⁴ <http://www.ncbi.nih.gov/SNP/>

generate the recombinant pShuttle-CBX7-CMV construct. It was linearized and cotransformed through electroporation with pAdEasy-1, which carries the adenovirus genome, in BJ5183 electrocompetent cells. After homologous recombination, a recombinant AdEasy-CMV-CBX7 plasmid was generated (Ad-CBX7), which was then extracted and linearized. QBI-293A cells were

transfected with different clones to produce different viral particles, and the infectivity of each clone was tested. Viral stocks were expanded in QBI-293A cells, which were harvested 36 to 40 h after infection and lysed. The virus titer of the 293 cells was determined. The adenovirus AdCMV-GFP (Quantum Biotechnologies) was used as control. Cells (5×10^4) were

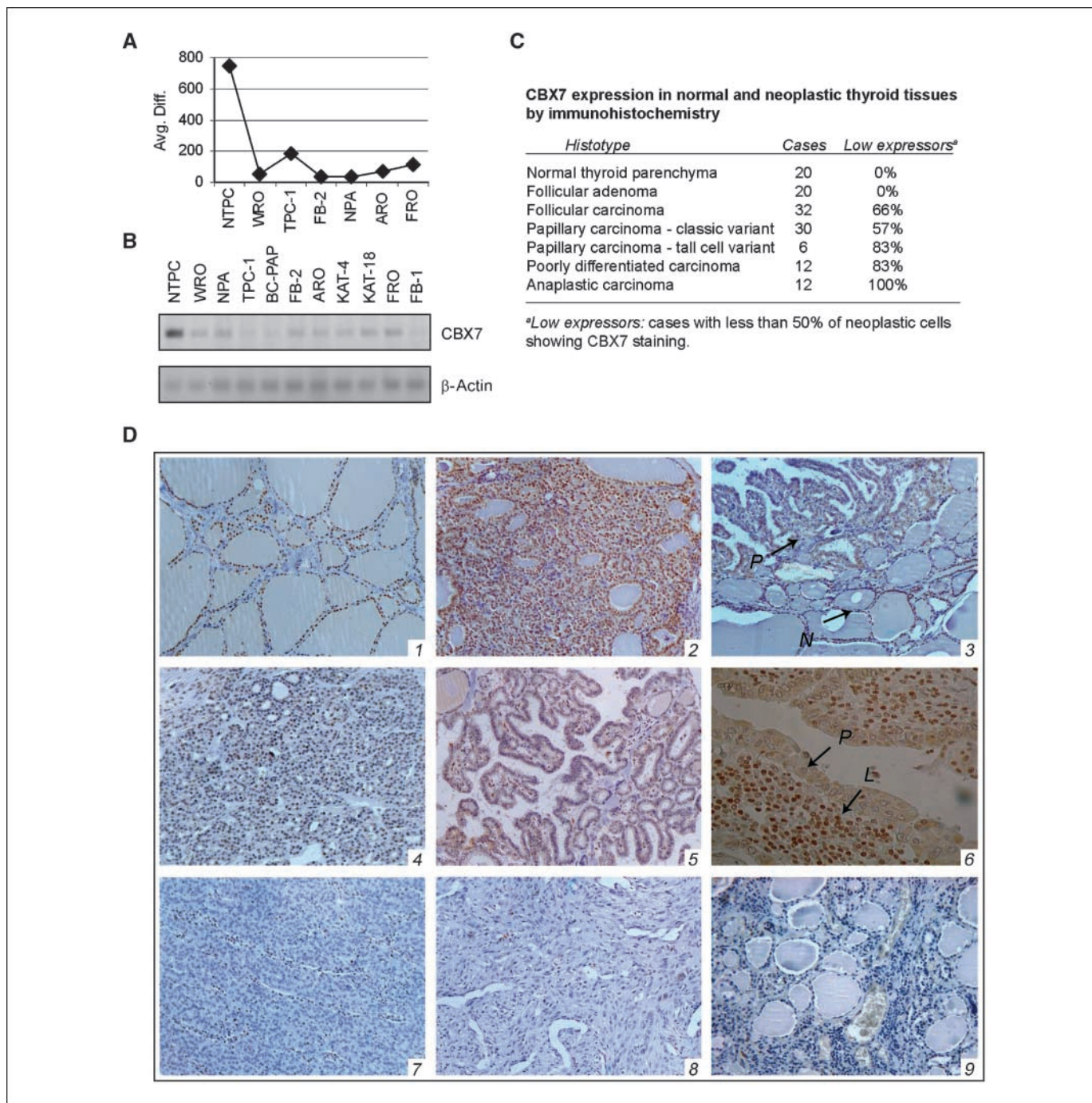
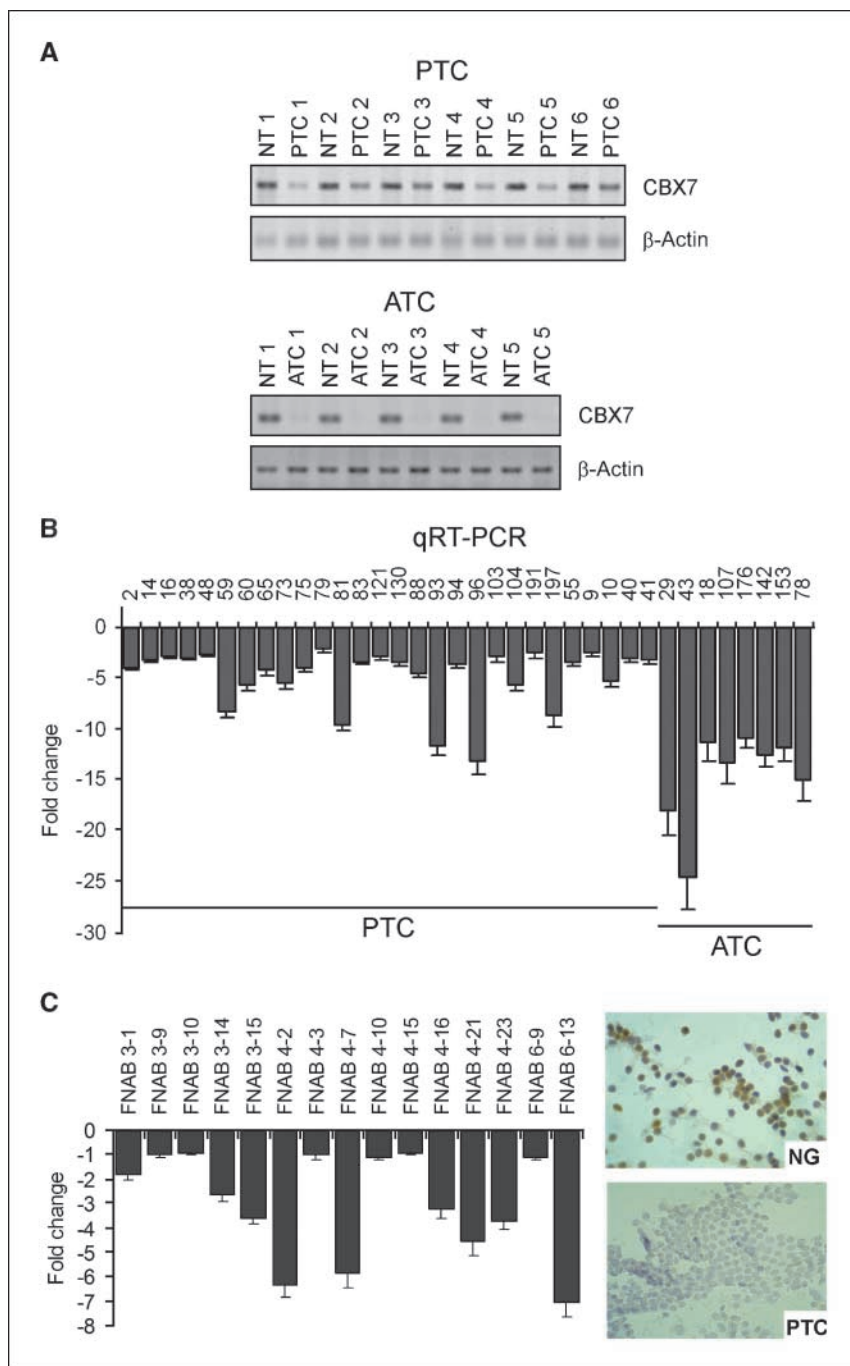


Figure 1. CBX7 expression in human thyroid carcinoma cell lines and neoplastic thyroid tissues. **A**, CBX7 gene expression by microarray analysis in human thyroid carcinoma cell lines versus human normal thyroid primary culture cells (NTPC). The average difference (Avg. Diff) is a quantitative relative indicator of a transcript expression level [$\sum(PM-MM) / \text{pairs on average}$]. **B**, CBX7 gene expression analysis by RT-PCR in human thyroid carcinoma cell lines versus normal thyroid primary culture cells. β -Actin gene expression served as loading control. **C**, normal and neoplastic thyroid tissues analyzed for CBX7 protein expression by immunohistochemistry. **D**, CBX7 nuclear staining was intense in benign follicular epithelial cells of normal thyroid (1) and follicular adenoma (2), whereas it was weaker in malignant lesions (3), where normal thyroid and papillary carcinoma are adjacent. The decrease of CBX7 in neoplastic lesions was progressive going from well-differentiated cancer, such as minimally invasive follicular carcinoma (4) and "classic variant" papillary carcinomas (PTC; 5) to the "tall cell variant" of PTC (6), whose nuclei are magnified to better show lack of signal, to poorly differentiated (7) and anaplastic (8) carcinomas. The signal disappeared after incubation of the sample with antigen (9). Arrows with letters indicate the following sample features: P→, nuclei showing cytologic features of PTC negative for CBX7 expression; N→, normal thyroid adjacent to papillary cancer; L→, lymphocyte showing CBX7 expression and providing positive internal control.

Figure 2. CBX7 expression in fresh thyroid tumor samples from patients. **A**, RT-PCR analysis of CBX7 expression in human thyroid tumor samples versus their normal thyroid counterparts. β -Actin expression served as loading control. *NT*, normal thyroid tissue; *PTC1* to *PTC6*, papillary thyroid carcinomas from different patients; *ATC1* to *ATC5*, anaplastic thyroid carcinomas from different patients. **B**, qRT-PCR analysis of human thyroid tumor samples of different histotypes. The fold change indicates the relative change in expression levels between tumor samples and normal samples, assuming that the value of each normal sample is equal to 1. **C**, qRT-PCR and immunocytochemical analyses of FNAB, whose PTC preoperative cytologic diagnosis was histologically proven. FNAB goiter samples were used as controls. The fold change indicates the relative change in expression levels between tumor and goiter samples, assuming that the value of the goiter sample was equal to 1. *NG*, nodular goiter.



seeded in a six-well plate. After 24 h, cells were infected at a multiplicity of infection (MOI) of 100 with Ad-CBX7 or Ad-GFP for 90 min using 500 μ L of infection medium (DMEM supplemented with 2% fetal bovine serum) at 37°C in a 5% CO₂ incubator. Pilot experiments with Ad-GFP were carried out to determine the optimal MOI for each cell line. At MOI 100, the cell lines became GFP positive without manifesting toxicity. Infected cells were harvested and counted daily in a hemacytometric chamber.

Results

CBX7 gene expression is down-regulated in human thyroid carcinoma cell lines. To look for genes potentially involved in the neoplastic transformation of the thyroid gland, we extracted RNAs

from normal human thyroid primary cells and six human thyroid carcinoma cell lines (WRO cell line from FTC, TPC-1 and FB-2 cell lines from PTC, NPA cell line from a poorly differentiated PTC, and ARO and FRO cell lines from ATC) and hybridized them to U95Av2 Affymetrix oligonucleotide arrays (Affymetrix) containing 12,625 transcripts (14). We looked for genes whose expression was drastically (at least 10-fold) up- or down-regulated in all the six thyroid carcinoma cell lines versus normal thyroid primary cell culture, on the assumption that genes whose expression was altered in all carcinoma cell lines could be involved in thyroid cell transformation. Thus, genes that were decreased in all the carcinoma cell lines were considered candidate tumor suppressor

genes. Among these genes, we decided to concentrate our studies on *CBX7*. The reasons of this choice were that *CBX7* was one of the genes with the highest down-regulation in all the carcinoma cell lines, according to the data of the cDNA microarray analysis (Fig. 1A), and that previous studies suggested its involvement in the repression of gene transcription (13), and then, a possible tumor suppressor function. This result was confirmed by RT-PCR analysis in a large panel of thyroid carcinoma cell lines with normal thyroid primary culture cells as control (Fig. 1B).

The loss of *CBX7* expression correlates with a more aggressive phenotype of thyroid carcinomas. Because thyroid carcinoma cell lines have a relative validity (26), we decided to carry out an immunohistochemical analysis of paraffin-embedded tissues using polyclonal antibodies raised against the carboxyl-terminal region of the human *CBX7* protein. As shown in Fig. 1C, all 20 samples of normal thyroid parenchyma expressed *CBX7* at a high level, which coincides with the strong *CBX7* staining in all follicles (Fig. 1D, subpanel 1). The intensity of nuclear labeling of epithelial thyroid cells in FTA (Fig. 1D, subpanel 2) and in goiters (not shown) was similar to that of normal thyroids and of the internal control represented by lymphoid cells. Conversely, *CBX7* expression was reduced in malignant lesions, as it was evident when neoplastic and normal tissue areas were adjacent (Fig. 1D, subpanel 3). The percentage of low expressors was high in well-differentiated tumors, namely FTC (66%, 21 of 32 samples; Fig. 1C and D, subpanel 4) and PTC (57%, 17 of 30 samples; Fig. 1C and D, subpanel 5). It was even higher in the less differentiated tumors, namely PDC (83%, 10 of 12 samples; Fig. 1C and D, subpanel 7) and TCV PTC (83%, 5 of 6 samples; Fig. 1C and D, subpanel 6). In the latter, neoplastic cells were almost devoid of *CBX7* expression, which sharply contrasted with the intense staining of the infiltrating lymphocytes and stromal cells. Similarly, *CBX7* expression was completely lost in the neoplastic cells in all cases of ATC (100%, 12 of 12; Fig. 1C and D, subpanel 8). No staining was observed when normal thyroid gland samples were stained with antibodies preincubated with the peptide against which the antibodies were raised (Fig. 1D, subpanel 9) or in the absence of the primary antibodies (data not shown). Therefore, *CBX7* was expressed in normal thyroid and in benign neoplastic lesions, decreased in well-differentiated carcinomas, and drastically reduced in aggressive thyroid tumors.

Analysis of *CBX7* expression in normal and neoplastic thyroid tissues by RT-PCR and quantitative real-time PCR.

We also evaluated *CBX7* expression by RT-PCR in a panel of matched normal/tumor tissues. The results confirmed the immunohistochemical data. In fact, there was an amplified band corresponding to *CBX7* in normal thyroid tissues (Fig. 2A). The amplified band decreased in PTC samples (Fig. 2A, top) and almost disappeared in ATC (Fig. 2A, bottom). Quantitative qRT-PCR analysis of a large number of human thyroid carcinoma samples of different histotypes confirmed a correlation between the reduction of *CBX7* expression and a more malignant phenotype of thyroid neoplasias. In fact, as reported in Fig. 2B, there was a negative fold change in *CBX7* expression from -2.1 to -13 (average -4.8) in the PTC samples versus the normal counterpart tissues. The reduction was even more pronounced in the ATC samples, with a fold change ranging from -10.8 to -24.5 (average -14.6). These data are well correlated with the immunohistochemical data and suggest that *CBX7* expression is controlled at the transcriptional level.

Analysis of human thyroid FNAB. FNAB has become an integral part of the preoperative evaluation of thyroid nodules. To evaluate whether *CBX7* gene expression analysis is also feasible preoperatively, immunocytochemistry and qRT-PCR were carried out on cell block specimens obtained from 15 FNAB diagnosed as PTC and histologically confirmed. In 8 cases of 15, *CBX7* expression was lower in PTC cell blocks than in specimen from thyroid goiter as evaluated by immunocytochemistry and qRT-PCR (Fig. 2C). This percentage was quite similar to that obtained by analyzing paraffin-embedded tissues diagnosed as PTC by immunohistochemistry.

LOH at *CBX7* locus. In some types of cancers, LOH of tumor suppressor genes at region 22q is believed to be a key step in carcinogenesis (27, 28). We therefore used several SNP markers to evaluate LOH at the *CBX7* locus on chromosome 22q13.1 in 77 cases of thyroid carcinomas of different histotypes. As shown in Table 1, LOH at the *CBX7* locus occurred in 36.8% of the informative PTC (7 of 19 cases) and in 68.7% (11 of 16 cases) of informative ATC. No LOH was observed in FTA (0 of 6 cases).

***CBX7* expression in rat thyroid cells transformed by viral oncogenes and in experimental mouse models of thyroid carcinogenesis.** The infection of two rat thyroid differentiated cell lines, PC Cl 3 and FRTL-5, with several murine retroviruses, induces different effects on the differentiated and transformed phenotype (16–23). PC MPSV cells are dedifferentiated and tumorigenic, whereas PC *v-raf*, PC KiMSV, and PC E1A cells are dedifferentiated but not tumorigenic when injected into nude mice. PC E1A cells are transformed to an irrefutable neoplastic phenotype after introducing a second oncogene such as the polyoma middle-T antigen or *v-raf* genes. Conversely, FRTL-5 cells become tumorigenic after infection with the Kirsten murine sarcoma virus carrying the *v-ras-Ki* oncogene. We evaluated the *CBX7* expression in these cell lines. As shown Fig. 3A, the gene was abundantly expressed in normal thyroid cells and in all cells that did not show the malignant phenotype, whereas its expression was abolished in the malignant transformed cells FRTL-5 KiMSV and PC MPSV, and in PC E1A *v-raf* oncogene. This result was also confirmed by Western blot analysis on representative cell lines (Supplementary Fig. S2). Interestingly, *CBX7* expression was retained in FRTL-5 KiMSV-HMGA1 and in PC MPSV-HMGA2, cells previously transfected with a vector carrying the *HMGA1* and *HMGA2* genes, respectively, in an antisense orientation, able to prevent the malignant transformation of FRTL-5 and PC Cl 3 cells (21, 23), and then with the relative oncogene. In fact, although these cells

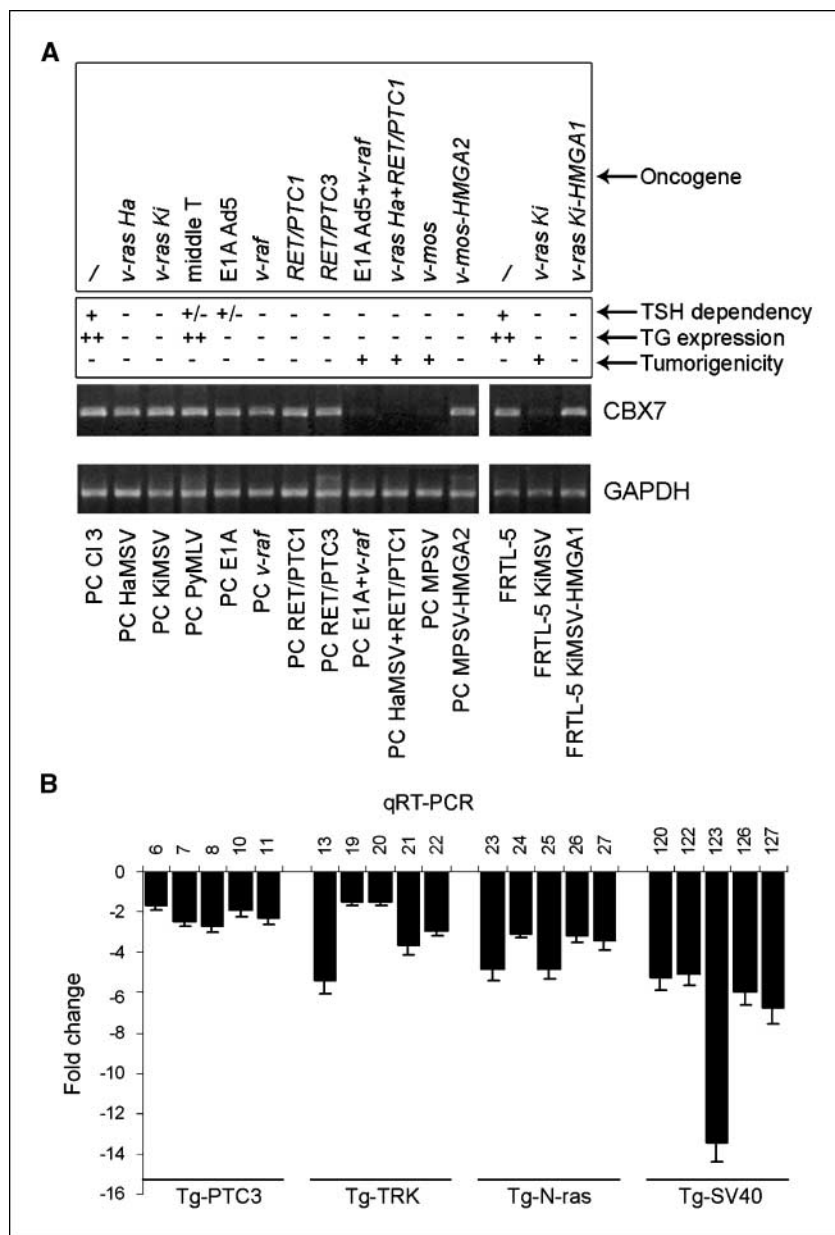
Table 1. LOH frequency statistics at the *CBX7* locus (22q13.1) by SNP sequencing method

Histotype	Cases (Inf)*	LOH [†]
Follicular adenoma	10 (6)	0% (0/6)
Follicular carcinoma	5 (3)	66.6% (2/3)
Papillary carcinoma—classic variant	36 (19)	36.8% (7/19)
Papillary carcinoma—tall cell variant	6 (4)	75% (3/4)
Anaplastic carcinoma	20 (16)	68.7% (11/16)

*Informative cases (Inf) are samples showing SNP heterozygosity corresponding to two peaks (two alleles) on the sequencing chromatogram.

[†] The LOH frequency is equal to the ratio between allelic loss and informative cases.

Figure 3. CBX7 expression in experimental models of thyroid carcinogenesis. *A*, CBX7 expression by RT-PCR in rat thyroid cells transformed by several oncogenes. *GAPDH* gene expression was evaluated as control to normalize the amount of the used RNAs. *B*, CBX7 expression by qRT-PCR in thyroid carcinomas developing in transgenic mice expressing RET-PTC-3, TRK, N-ras, and large T SV40 oncogenes. The fold change indicates the relative change in expression levels between tumor samples and normal samples, assuming that the value of normal sample is equal to 1.



undergo morphologic changes and lose the thyroid differentiation markers, they are unable to grow in soft agar and to induce tumors after injection into athymic mice (21, 23). Therefore, the analysis of rat thyroid cells transformed *in vitro* also confirms that the loss of CBX7 expression is associated with the expression of a highly malignant phenotype.

In addition, we used qRT-PCR analysis to evaluate CBX7 expression in thyroid neoplasias developing in transgenic animal lines expressing some oncogenes under the transcriptional control of the thyroglobulin promoter. Transgenic mice carrying *TRK* and *RET/PTC3* oncogenes develop PTC (29, 30), whereas N-ras mice develop thyroid follicular neoplasms that undergo dedifferentiation, predominantly FTC (31). ATCs were obtained from mice carrying SV40 large T antigen (32). As shown in Fig. 3B, CBX7 expression was much lower in ATC from large T SV40 transgenic mice compared with mouse normal thyroid tissue. CBX7 mRNA expression was significantly, albeit not greatly, reduced in PTC

from TRK and RET/PTC3 mice. CBX7 expression was also reduced in the FTC from N-ras mice.

Restoration of CBX7 gene expression inhibits the growth of thyroid carcinoma cell lines. To determine whether the loss of CBX7 gene expression affects thyroid carcinogenesis, we evaluated the growth rate of three thyroid carcinoma cell lines in which CBX7 expression had been restored. To this aim, we carried out a colony-forming assay with three human thyroid carcinoma cell lines (ARO, NPA, TPC-1) after transfection with the vector carrying the CBX7 gene or the backbone vector. As shown in Fig. 4A, cells transfected with the CBX7 gene generated a lower number of colonies than cells transfected with the backbone vector did.

Moreover, we have analyzed the growth potential of CBX7 stably expressing ARO cells by a 2,3-bis[2-methoxy-4-nitro-5-sulfophenyl]-2H-tetrazolium-5-carboxanilide inner salt (XTT) assay at different times after plating. As shown in Fig. 4B, the ARO cells expressing the CBX7 gene grew at a significantly slower rate

compared with the untransfected and backbone vector-transfected ARO cells.

We then investigated the cell cycle phase distribution of these CBX7 stably transfected ARO cells through flow cytometric analysis. As shown in Fig. 4C, ARO cells expressing CBX7 had a significant increase in the G₁-phase population (ARO CBX7-1, 66%; ARO CBX7-8, 64%), compared with empty vector-transfected cells (ARO HA-3, 49%; ARO HA-4, 51%) and parental cells (ARO, 48%). Therefore, these results suggest that CBX7 negatively regulates thyroid carcinoma cell proliferation.

Generation of an adenovirus carrying the CBX7 gene. We generated a replication-defective adenovirus carrying the CBX7 gene in the sense (Ad-CBX7) orientation. We then infected thyroid carcinoma cell lines with the Ad-CBX7 virus and measured protein

levels in cell lysates collected at different time points after adenovirus infection. No CBX7 protein was detected in carcinoma cells infected with the control virus (Ad-GFP). We then constructed growth curves of cells infected with Ad-CBX7 and control adenovirus (Ad-GFP). As shown in Fig. 4D, cell growth rate was significantly lower in ARO and NPA cell lines infected with Ad-CBX7 than in the same cells infected with the control virus. The percentage of growth inhibition 5 days after infection was 38.5% in ARO cells and 54% in NPA cells.

Expression of CDKN2A/p16 in human thyroid tumor samples. It has been reported that a target of CBX7 would be the *CDKN2A/p16* tumor suppressor gene (11, 12, 33), suggesting that overexpression of CBX7 could enable cells to evade oncogene-induced senescence; we then evaluated CDKN2A/p16 expression in

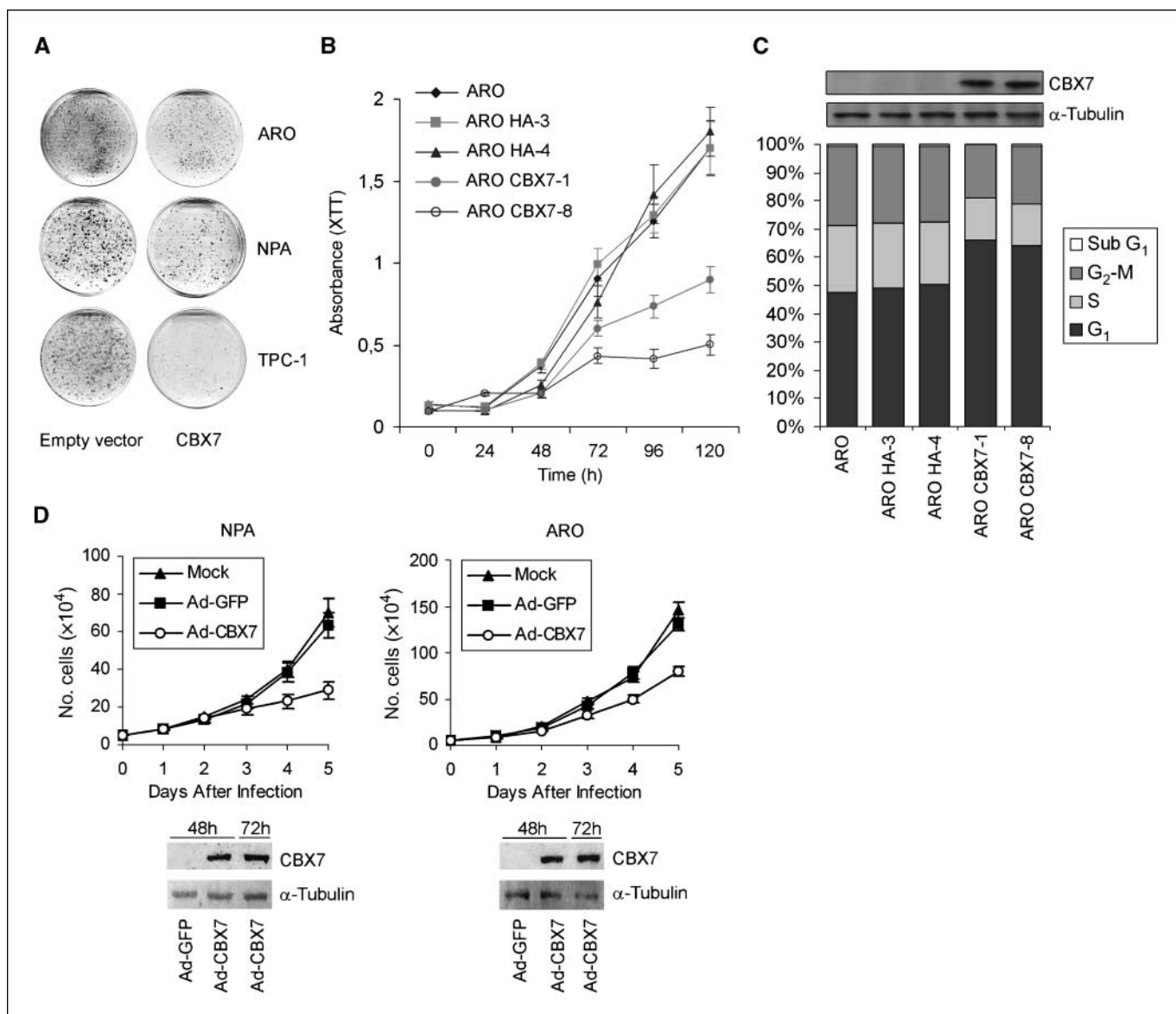


Figure 4. Effect of CBX7 restoration on thyroid carcinoma cell lines. *A*, colony-forming assay with CBX7 transfection in several thyroid carcinoma cell lines (ARO, NPA, and TPC-1). *B*, growth curve of ARO cells and ARO cells stably carrying a vector expressing CBX7 (ARO CBX7-1 and ARO CBX7-8) or the backbone vector (ARO HA-3 and ARO HA-4). The relative number of viable cells was determined by the XTT assay. Absorbance was read at 450 nm and the data are the mean of triplicates. *C*, CBX7 expression affects the cell cycle distribution of ARO cells as assessed by flow cytometric analysis. The expression of the CBX7 protein in ARO CBX7-1 and ARO CBX7-8 was confirmed by Western blot. *D*, top, inhibitory effects of Ad-CBX7 infection on the growth of human thyroid carcinoma cell lines. Representative curves of three independent experiments are reported. Bottom, CBX7 expression by Western blot analysis. Blot against α -tubulin is to show an equal protein loading.

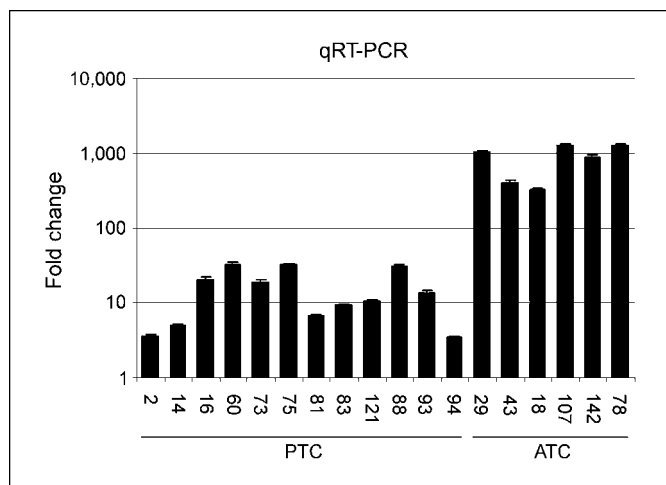


Figure 5. qRT-PCR analysis of CDKN2A/p16 expression in human thyroid tumor samples of different histotypes. The fold change indicates the relative change in expression levels between tumor samples and normal samples, assuming that the value of each normal sample is equal to 1.

a panel of thyroid tumors. Consistent with already published results (34, 35), we show that CDKN2A/p16 is moderately overexpressed in PTCs and highly overexpressed in ATCs compared with normal thyroid tissues (Fig. 5). These results seem to confirm that CDKN2A/p16 is negatively regulated by CBX7. However, they also suggest that CDKN2A/p16 is not effective in thyroid carcinoma cells because ATCs are fast-growing highly malignant tumors (2). Because recent evidence shows that senescence acts as a barrier to tumorigenesis in response to oncogene activation (36), it is reasonable to retain that this result may represent an effect of the activated oncogenes. However, further studies are required to elucidate this paradoxical result. Therefore, other molecular mechanisms must be envisaged to explain the negative role exerted by CBX7 restoration in thyroid carcinoma cells.

Discussion

Microarray studies are widely used to define diagnostic and prognostic signatures in cancers and they have led to the identification of a large list of carcinoma-regulated genes also in thyroid cancers (37). Just within the context of a microarray study, we found that the *CBX7* gene was drastically down-regulated in all the thyroid carcinoma-derived cell lines analyzed.

The results of this study show that CBX7 expression decreased with malignancy grade and neoplasia stage. In fact, CBX7 expression was comparable with normal thyroid tissue in FTA, which is benign; slightly reduced in PTC displaying the classic histotype; and drastically reduced, and in most cases absent, in FTC, TCV PTC, PDC, and ATC. Our finding of a decrease in CBX7 levels in relation to malignancy was supported by our model of rat thyroid cells transformed by several oncogenes and in transgenic mice carrying thyroglobulin promoter-driven oncogenes. CBX7 expression was absent in rat thyroid cells that show a highly malignant phenotype and in ATC that develop in large T SV40 transgenic mice. Differently, CBX7 expression was retained, albeit at a low level, in transformed rat thyroid cells that are not yet tumorigenic and in PTC developing in RET/PTC and TRK mice. Therefore, our data indicate that loss of CBX7 expression correlates with a more aggressive phenotype of thyroid carcinomas and,

likely, with a worse prognosis. Interestingly, a recent article concerning the cytogenetics of Chernobyl thyroid tumors identified a correlation between the deletion of the chromosomal region 22q13.1, where the *CBX7* gene is located, and a worse prognosis (38). Our preliminary finding shows a correlation between low CBX7 expression and reduced survival in colon carcinoma.⁵ Moreover, the association between lack of CBX7 expression and a more aggressive histotype seems to apply also to breast, ovary, and lung carcinomas.⁶

To determine whether CBX7 may contribute to thyroid carcinogenesis, we restored the CBX7 function in human thyroid cancer cell lines and examined cell growth rate. Restoration of CBX7 expression reduced cell growth rate, indicating that the loss of CBX7 expression may play a role in thyroid carcinogenesis.

In the attempt to unravel the mechanism underlying the loss of *CBX7* gene expression in malignant thyroid neoplasias, we analyzed LOH at the *CBX7* locus (22q13.1). We detected LOH in 36.8% and 68.7% of the PTC and ATC, respectively, but not in FTA. However, no mutations were found in thyroid carcinomas; moreover, no hypermethylation status was observed in ATC (data not shown), which are practically devoid of CBX7 expression. Therefore, we suggest that other epigenetic mechanisms associated with an allelic loss might account for the reduced CBX7 expression in thyroid carcinomas. Consistent with this hypothesis, our preliminary data indicate that the HMGAI proteins, also overexpressed in highly malignant neoplasias (39), are able to directly down-regulate the CBX7 expression.

The data reported here seem to propose *CBX7* as a tumor suppressor gene. However, recent publications (11, 12, 33) seem to attribute oncogenic functions to CBX7. In fact, it has been shown, by the generation of transgenic mice overexpressing CBX7, that CBX7 can initiate T-cell lymphomagenesis and cooperate with c-Myc to produce highly aggressive B-cell lymphomas (33). Moreover, it has been also shown that CBX7 expression facilitates the survival of the mouse embryonic fibroblasts (11), consistently with a CBX7 oncogenic role. These contrasting results are, in our opinion, not mutually exclusive at all. The cellular context can account for the opposite functions attributed to CBX7. We retain that this can occur with a certain frequency with chromatin proteins: the cellular partners, which may vary from cell to cell, can modify the action exerted by them. This hypothesis is supported by the studies on the HMGAI proteins that are overexpressed in most of the malignant tumors, and *in vitro* and *in vivo* studies showed the oncogenic activity of overexpressed HMGAI proteins (40–42). However, the phenotype of the null mice revealed that the *HMGAI* gene plays a hitherto unsuspected tumor suppressor role because they developed, even at the heterozygous state, B-cell lymphomas and myeloid malignancies (43). There are also evidence that some E2F family members are able to act as both oncogene and tumor suppressor gene depending on the context (44). In fact, E2F1 expression can either promote or inhibit tumorigenesis depending on the nature of the other oncogenic mutations that are present (44). The dual role of the *CBX7* gene as an oncogene or a tumor suppressor is also suggested by the loss of CBX7 expression in pediatric ependymomas (45), and also by our recent data showing a correlation between CBX7 overexpression and a high malignant

⁵ P. Pallante and L. Terracciano, in preparation.

⁶ P. Pallante and G. Troncone, in preparation.

phenotype in head and neck tumors, although an inverse correlation has been found in ovary, lung, and colon carcinomas.⁷ Moreover, mouse embryonic fibroblasts (MEF) null for CBX7 (generated in our laboratory) have a higher proliferation rate than the wild-type MEFs, whereas the CBX7^{+/-} MEFs show an intermediate behavior, suggesting a negative role of the CBX7 protein in the growth of these cells (Supplementary Fig. S1).

In conclusion, our data indicate that a reduced *CBX7* gene expression is associated with a malignant phenotype of thyroid

neoplasias and suggest that the loss of CBX7 could contribute to thyroid cancer progression.

Disclosure of Potential Conflicts of Interest

No potential conflicts of interest were disclosed.

Acknowledgments

Received 2/25/2008; revised 6/5/2008; accepted 6/5/2008.

Grant support: Associazione Italiana per la Ricerca sul Cancro, P. Pallante was supported by a fellowship from Fondazione Italiana per la Ricerca sul Cancro.

The costs of publication of this article were defrayed in part by the payment of page charges. This article must therefore be hereby marked *advertisement* in accordance with 18 U.S.C. Section 1734 solely to indicate this fact.

⁷ P. Pallante and L. Terracciano, in preparation.

References

- Hedinger C, Williams ED, Sobin LH. The WHO histological classification of thyroid tumours: a commentary on the second edition. *Cancer* 1989;63:908–11.
- Kondo T, Ezzat S, Asa SL. Pathogenetic mechanisms in thyroid follicular-cell neoplasia. *Nat Rev Cancer* 2006;6:292–306.
- Nardone HC, Ziober AF, LiVolsi VA, et al. c-Met expression in tall cell variant papillary carcinoma of the thyroid. *Cancer* 2003;98:1386–93.
- Xing M. BRAF mutation in thyroid cancer. *Endocr Relat Cancer* 2005;12:245–62.
- Pierotti MA, Greco A. Oncogenic rearrangements of the NTRK1/NGF receptor. *Cancer Lett* 2006;232:90–8.
- Di Renzo MF, Olivero M, Ferro S, et al. Overexpression of the c-MET/HGF receptor gene in human thyroid carcinomas. *Oncogene* 1992;7:2549–53.
- Suarez HG, du Villard JA, Severino M, et al. Presence of thyroids in all three ras genes in human thyroid tumors. *Oncogene* 1990;5:565–70.
- Kroll TG, Sarraf P, Pecciarini L, et al. PAX-8-PPAR γ 1 fusion oncogene in human thyroid carcinoma. *Science* 2000;289:1357–60.
- Fagin JA, Matsuo K, Karmakar A, Chen DL, Tang SH, Koefler HP. High prevalence of mutations of p53 gene in poorly differentiated human thyroid carcinomas. *J Clin Invest* 1993;91:179–84.
- Paro R, Hogness DS. The Polycomb protein shares a homologous domain with a heterochromatin-associated protein of *Drosophila*. *Proc Natl Acad Sci U S A* 1991;88:263–67.
- Gil J, Bernard D, Martinez D, Beach D. Polycomb CBX7 has a unifying role in cellular lifespan. *Nat Cell Biol* 2004;6:67–72.
- Bernard D, Martinez-Leal JF, Rizzo S, et al. CBX7 controls the growth of normal and tumor-derived prostate cells by repressing the Ink4a/Arf locus. *Oncogene* 2005;24:5543–51.
- Bernstein E, Duncan EM, Masui O, Gil J, Heard E, Allis CD. Mouse polycomb proteins bind differentially to methylated histone H3 and RNA and are enriched in facultative heterochromatin. *Mol Cell Biol* 2006;26:2560–69.
- Pallante P, Berlingieri MT, Troncone G, et al. Ubch10 overexpression may represent a marker of anaplastic thyroid carcinomas. *Br J Cancer* 2005;93:464–71.
- Curcio F, Ambesi-Impombato FS, Perrella G, Coon HG. Long-term culture and functional characterization of follicular cells from adult normal human thyroids. *Proc Natl Acad Sci U S A* 1994;91:9004–8.
- Fusco A, Berlingieri MT, Di Fiore PP, Portella G, Greco M, Vecchio G. One- and two-step transformations of rat thyroid epithelial cells by retroviral oncogenes. *Mol Cell Biol* 1987;7:3365–70.
- Ambesi-Impombato FS, Parks LA, Coon HG. Culture of hormone dependent functional epithelial cells from rat thyroids. *Proc Natl Acad Sci U S A* 1980;77:3455–9.
- Berlingieri MT, Portella G, Greco M, Santoro M, Fusco A. Cooperation between the polyomavirus middle-T-antigen gene and the human c-myc oncogene in a rat thyroid epithelial differentiated cell line: model of *in vitro* progression. *Mol Cell Biol* 1988;8:2261–6.
- Berlingieri MT, Santoro M, Battaglia C, Greco M, Fusco A. The Adenovirus E1A gene blocks the differentiation of a thyroid epithelial cell line, however the neoplastic phenotype is achieved only after cooperation with other oncogenes. *Oncogene* 1993;8:249–55.
- Santoro M, Melillo RM, Grieco M, Berlingieri MT, Vecchio G, Fusco A. The TRK and RET tyrosine kinase oncogenes cooperate with ras in the neoplastic transformation of a rat thyroid epithelial cell line. *Cell Growth Differ* 1993;4:77–84.
- Berlingieri MT, Manfoletti G, Santoro M, et al. Inhibition of HMGI-C protein synthesis suppresses retrovirally induced neoplastic transformation of rat thyroid cells. *Mol Cell Biol* 1995;15:1545–53.
- Fusco A, Portella G, Di Fiore PP, et al. A mos oncogene-containing retrovirus, myeloproliferative sarcoma virus, transforms rat thyroid epithelial cells and irreversibly blocks their differentiation pattern. *J Virol* 1985;56:284–92.
- Berlingieri MT, Pierantoni GM, Giancotti V, Santoro M, Fusco A. Thyroid cell transformation requires the expression of the HMGA1 proteins. *Oncogene* 2002;21:2971–80.
- Zeppa P, Vetrani A, Marino M, et al. Fine needle aspiration of medullary thyroid carcinoma: a review of 18 cases. *Cytopathology* 1990;1:35–44.
- Troncone G, Fulciniti F, Zeppa P, Vetrani A, Caleo A, Palombini L. Cyclin-dependent kinase inhibitor p27(Kip1) expression in thyroid cells obtained by fine needle aspiration biopsy: a preliminary report. *Diagn Cytopathol* 2000;23:77–81.
- Van Staveren WC, Solis DW, Delys L, et al. Human thyroid tumor cell lines derived from different tumor types present a common dedifferentiated phenotype. *Cancer Res* 2007;67:8113–20.
- Wild A, Langer P, Celik I, Chaloupka B, Bartsch DK. Chromosome 22q in pancreatic endocrine tumors: identification of a homozygous deletion and potential prognostic associations of allelic deletions. *Eur J Endocrinol* 2002;147:507–13.
- Iida A, Kurose K, Isobe R, et al. Mapping of a new target region of allelic loss to a 2-cM interval at 22q13.1 in primary breast cancer. *Genes Chromosomes Cancer* 1998;21:108–12.
- Russell JP, Powell DJ, Cunnane M, et al. The TRK-T1 fusion protein induces neoplastic transformation of thyroid epithelium. *Oncogene* 2000;19:5729–35.
- Powell DJ, Jr., Russell J, Nibu K, et al. The RET/PTC3 oncogene: metastatic solid-type papillary carcinomas in murine thyroids. *Cancer Res* 1998;58:5523–8.
- Vitagliano D, Portella G, Troncone G, et al. Thyroid targeting of the N-ras(Gln61Lys) oncogene in transgenic mice results in follicular tumors that progress to poorly differentiated carcinomas. *Oncogene* 2006;25:5467–74.
- Ledent C, Dumont J, Vassart G, Parmentier M. Thyroid adenocarcinomas secondary to tissue-specific expression of simian virus-40 large T-antigen in transgenic mice. *Endocrinology* 1991;129:1391–401.
- Scott CL, Gil J, Hernando E, et al. Role of the chromobox protein CBX7 in lymphomagenesis. *Proc Natl Acad Sci U S A* 2007;104:5389–94.
- Barroeta JE, Baloch ZW, Lal P, Pasha TL, Zhang PJ, LiVolsi VA. Diagnostic value of differential expression of CK19, Galectin-3, HBME-1, ERK, RET, and p16 in benign and malignant follicular-derived lesions of the thyroid: an immunohistochemical tissue microarray analysis. *Endocr Pathol* 2006;17:225–34.
- Ferru A, Fromont G, Gibelin H, et al. The status of CDKN2A α (p16INK4A) and β (p14ARF) transcripts in thyroid tumour progression. *Br J Cancer* 2006;95:1670–7.
- Swarbrick A, Roy E, Allen T, Bishop JM. Id1 cooperates with oncogenic Ras to induce metastatic mammary carcinoma by subversion of the cellular senescence response. *Proc Natl Acad Sci U S A* 2008;105:5402–7.
- Delys L, Detours V, Franc B, et al. Gene expression and the biological phenotype of papillary thyroid carcinomas. *Oncogene* 2007;26:7894–903.
- Richter H, Braselmann H, Hieber L, et al. Chromosomal imbalances in post-Chernobyl thyroid tumors. *Thyroid* 2004;14:1061–4.
- Fusco A, Fedele M. Roles of HMGA proteins in cancer. *Nat Rev Cancer* 2007;7:899–910.
- Wood LJ, Maher JF, Bunton TE, Resar LM. The oncogenic properties of the HMG-I gene family. *Cancer Res* 2000;60:4256–61.
- Baldassarre G, Fedele M, Battista S, et al. Onset of natural killer cell lymphomas in transgenic mice carrying a truncated HMGA1 gene by the chronic stimulation of the IL-2 and IL-15 pathway. *Proc Natl Acad Sci U S A* 2001;98:7970–5.
- Fedele M, Pentimalli F, Baldassarre G, et al. Transgenic mice overexpressing the wild-type form of the HMGA1 gene develop mixed growth hormone/prolactin cell pituitary adenomas and natural killer cell lymphomas. *Oncogene* 2005;24:3427–35.
- Fedele M, Fidanza V, Battista S, et al. Haploinsufficiency of the Hmga1 gene causes cardiac hypertrophy and myelo-lymphoproliferative disorders in mice. *Cancer Res* 2006;66:2536–43.
- Johnson DG, Degregori J. Putting the oncogenic and tumor suppressive activities of E2F into context. *Curr Mol Med* 2006;6:731–8.
- Suarez-Merino B, Hubank M, Revesz T, et al. Microarray analysis of pediatric ependymoma identifies a cluster of 112 candidate genes including four transcripts at 22q12.1-q13.3. *Neuro-oncol* 2005;7:20–31.

Chromobox Protein Homologue 7 Protein, with Decreased Expression in Human Carcinomas, Positively Regulates E-Cadherin Expression by Interacting with the Histone Deacetylase 2 Protein

Antonella Federico,^{1,3} Pierlorenzo Pallante,^{1,3} Mimma Bianco,¹ Angelo Ferraro,³ Francesco Esposito,¹ Maria Monti,⁴ Marianna Cozzolino,⁴ Simona Keller,^{1,3} Monica Fedele,¹ Vincenza Leone,^{1,3} Giancarlo Troncone,^{2,3} Lorenzo Chiariotti,^{1,3} Piero Pucci,⁴ and Alfredo Fusco^{1,3}

¹Istituto di Endocrinologia ed Oncologia Sperimentale del CNR c/o Dipartimento di Biologia e Patologia Cellulare e Molecolare and ²Dipartimento di Anatomia Patologica e Citopatologia, Facoltà di Medicina e Chirurgia di Napoli, Università degli studi di Napoli "Federico II"; ³Naples Oncogenomic Center-CEINGE, Biotecnologie Avanzate-Napoli, and European School of Molecular Medicine-Naples Site; ⁴CEINGE, Biotecnologie Avanzate-Napoli and Dipartimento di Chimica Organica e Biochimica, Università degli studi di Napoli "Federico II," Naples, Italy

Abstract

Chromobox protein homologue 7 (CBX7) is a chromobox family protein encoding a novel polycomb protein, the expression of which shows a progressive reduction, well related with the malignant grade of the thyroid neoplasias. Indeed, CBX7 protein levels decreased in an increasing percentage of cases going from benign adenomas to papillary, follicular, and anaplastic thyroid carcinomas. To elucidate the function of CBX7 in carcinogenesis, we searched for CBX7 interacting proteins by a proteomic analysis. By this approach, we identified several proteins. Among these proteins, we selected histone deacetylase 2 (HDAC2), which is well known to play a key role in neoplastic cell transformation and down-regulation of E-cadherin expression, the loss of which is a critical event in the epithelial-to-mesenchymal transition. We confirmed by coimmunoprecipitation that CBX7 physically interacts with the HDAC2 protein and is able to inhibit its activity. Then, we showed that both these proteins bind the *E-cadherin* promoter and that CBX7 up-regulates E-cadherin expression. Consistent with these data, we found a positive statistical correlation between CBX7 and E-cadherin expression in human thyroid carcinomas. Finally, we showed that the expression of CBX7 increases the acetylation status of the histones H3 and H4 on the *E-cadherin* promoter. Therefore, the ability of CBX7 to positively regulate E-cadherin expression by interacting with HDAC2 and inhibiting its activity on the *E-cadherin* promoter would account for the correlation between the loss of CBX7 expression and a highly malignant phenotype. [Cancer Res 2009;69(17):7079–87]

Introduction

Chromobox protein homologue 7 (*CBX7*) gene encodes a novel polycomb protein of 28.4 kDa and 251 amino acids, which contains a "chromodomains" between amino acids 10 and 46 (1, 2). *CBX7* is a chromobox family protein and a member of the polycomb

repressive complex 1, which, together with the polycomb repressive complex 2, maintains developmental regulatory genes in a silenced state (3–5). Mouse *Cbx7* associates with facultative heterochromatin and with the inactive X chromosome, suggesting a role of the *Cbx7* protein in the repression of gene transcription (6, 7). We have found previously that the *CBX7* gene was drastically down-regulated in six thyroid carcinoma cell lines versus normal thyroid cells. Subsequently, the analysis of *CBX7* expression in a large number of thyroid carcinoma samples revealed a progressive reduction of *CBX7* levels that was well related with the malignant grade of the thyroid neoplasias (8). Indeed, it decreased in an increasing percentage of cases going from benign adenomas to papillary, follicular, and anaplastic thyroid carcinomas (9, 10). The analysis of rat and mouse models of thyroid carcinogenesis gave rise to very similar results (8). More recent results confirmed a correlation between low *CBX7* expression and a reduced survival in colon carcinoma patients.⁵ Moreover, the association between lack of *CBX7* expression and a more aggressive histotype has also been shown by our group in breast, ovary, and prostate carcinomas.⁶ Restoration of *CBX7* expression in thyroid cancer cells reduced their growth rate, indicating that *CBX7* plays a critical role in the regulation of transformed thyroid cell proliferation (8).

The aim of the present work has been to elucidate the mechanisms by which the loss of *CBX7* is involved in carcinogenesis, attempting to identify the *CBX7* protein partners by performing a functional proteomic experiment. Here, we show that *CBX7* interacts with histone deacetylase 2 (HDAC2) and inhibits its activity. Moreover, both HDAC2 and *CBX7* bind the *E-cadherin* (*CDH1*) promoter, and *CBX7* contrasts the inhibiting effect of HDAC2 on *E-cadherin* expression.

Therefore, the ability of *CBX7* to positively regulate *E-cadherin* expression might account for the correlation of the loss of *CBX7* expression with a highly malignant phenotype in cancer patients.

Materials and Methods

Cell culture and transfections. TPC1 and NPA (derived from thyroid papillary carcinomas) and PC Cl3, HEK 293, and HeLa cells were grown as described previously (8, 11). PC Cl3 cells are differentiated thyroid cells of 18-month-old rat Fischer origin depending on thyrotropine for the growth (12). For the inhibition of *CBX7* expression, rat *Cbx7* small interfering RNA

Note: Supplementary data for this article are available at Cancer Research Online (<http://cancerres.aacrjournals.org/>).

Requests for reprints: Alfredo Fusco, Istituto di Endocrinologia ed Oncologia Sperimentale del CNR, via Pansini 5, 80131 Napoli, Italy. Phone: 39-81-7463602; Fax: 39-81-2296674; E-mail: afusco@napoli.com or alfusco@unina.it.

©2009 American Association for Cancer Research.
doi:10.1158/0008-5472.CAN-09-1542

⁵ Pallante et al., submitted for publication.

⁶ Pallante, Terracciano, and Troncone, manuscript in preparation.

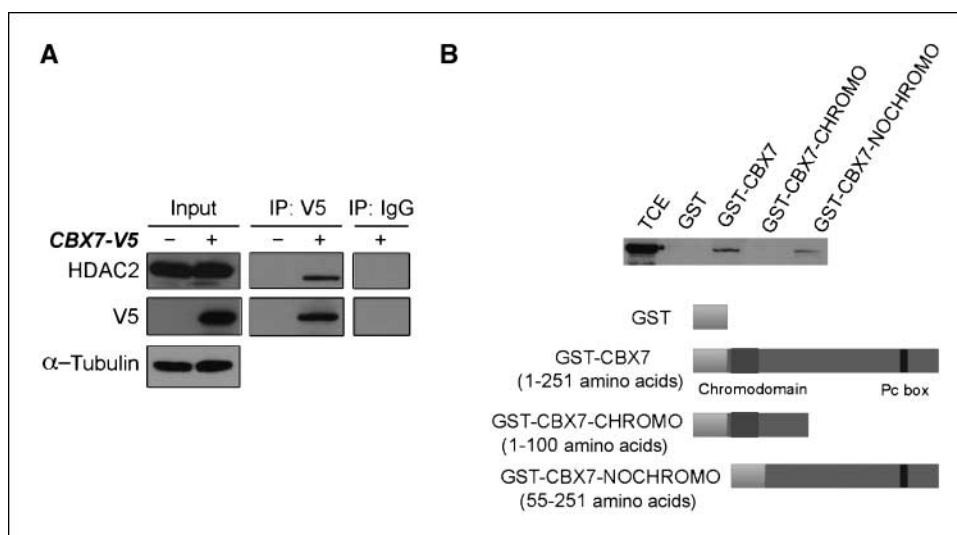


Figure 1. CBX7 interacts with HDAC2. **A**, HEK 293 cells were transiently transfected with V5-tagged CBX7 or empty vector and total cell extracts (TCE) were coimmunoprecipitated using anti-V5 antibodies. Immunocomplexes were analyzed by Western blot with either anti-V5 or anti-HDAC2 antibodies. IgG indicates the negative control of immunoprecipitation using an unrelated antibody. **B**, GST pull-down assay with GST or recombinant GST-CBX7 proteins (wild-type and mutants as schematically reported below). The filter was incubated with an anti-HDAC2 antibody.

(SI01495795 and SI01495802; Qiagen) and nonsilencing control small interfering RNA (1022076; Qiagen) were transfected using Oligofectamine (Invitrogen) according to the manufacturer's recommendations. CBX7-inducible NPA cells were generated by transfecting NPA cells with the pcDNA6/TR regulatory vector (Invitrogen). Trichostatin A (Sigma) treatments were done for 24 h after transfection.

Plasmids. V5-tagged CBX7 expression plasmid was generated by the insertion of the PCR product CBX7 cDNA into pcDNA-DEST-40 Gateway Vector (Invitrogen). HA-tagged CBX7 expression plasmid was obtained by PCR amplification and subcloned into the pCefl-HA expression vector. CBX7-deletion mutants were cloned in pCefl-HA as well.

Protein extraction, Western blotting, and immunoprecipitation assays. Protein extraction, Western blotting, and coimmunoprecipitation procedures were carried out as reported elsewhere (13). The antibodies used for immunoprecipitation and Western blotting were anti-CBX7 (8), anti-HA (Roche), anti-V5 (Sigma), anti-pan-cadherin (Sigma), and anti- α -tubulin (Sigma).

GST pull-down experiments. GST fusion proteins were constructed by cloning the human cDNA sequence in a pGEX4T-1 vector (Promega). GST pull-down experiments were carried out as reported elsewhere (14).

HDAC activity assay. Cells were transfected with increasing amount of CBX7 expression vector and were used to assay the HDAC activity according to the manufacturer's instructions of Histone Deacetylase Assay Kit (Upstate).

Fresh human thyroid tissue samples. Neoplastic human thyroid tissues and normal adjacent tissue or the normal contralateral thyroid lobe were obtained as described previously (8).

RNA extraction, reverse transcription, and PCR analysis. Total RNA isolation and reverse transcription-PCR (RT-PCR) from human tissues were done as described previously (8, 15). Each reaction was carried out in duplicate. We used the $2^{-\Delta\Delta CT}$ method to calculate relative expression levels (16, 17). Detailed primer sequences are available as Supplementary Materials and Methods.

Immunohistochemistry. Immunohistochemical analysis were done as described previously (8).

Electrophoretic mobility shift assay. For gel shift analysis, nuclear extracts were prepared as described elsewhere (18) and electrophoretic mobility shift assay was done as described previously (19). The double-strand oligonucleotides covered a region spanning from nucleotide -70 to +54 of the human *E-cadherin* promoter with respect to the transcription start site (TSS).

Chromatin immunoprecipitation and re-chromatin immunoprecipitation assays. After transfection, chromatin samples were processed for chromatin immunoprecipitation and re-chromatin immunoprecipitation experiments as reported elsewhere (19). Samples were subjected to immunoprecipitation with the following specific antibodies: anti-HA

(Roche) and anti-HDAC2, anti-H3K4m2, anti-H3K4m3, anti-H3K9me, anti-H3K9m3, and anti-H4K20 (Upstate). The sequences of the used primers are available as Supplementary Materials and Methods.

Transactivation assay. Cells were transiently transfected with the reporter construct in which the luciferase gene was driven by described fragments of *E-cadherin* promoter (20, 21) and normalized with the use of a cotransfected β -galactosidase construct. Luciferase activity was analyzed by Dual-Light System (Applied Biosystems).

DNA extraction and methylation analysis. DNA was prepared using QIAamp DNA Mini Kit (Qiagen) following the instruction manual. PCR primers to analyze *E-cadherin* promoter were designed by using Methprimer (22). The MassCLEAVE biochemistry was done as described previously (23). Mass spectra were acquired by using a MassARRAY Compact matrix-assisted laser desorption/ionization—time-of-flight (Sequenom) and spectra methylation ratios were generated by the Epityper software version 1.0 (Sequenom).

Statistical analysis. For the comparison between two groups of experiments, Student's *t* test was used. The statistical significant difference was considered when $P < 0.05$. A Pearson correlation coefficient (R^2) close to 1 was considered indicative of a significant direct correlation. All experiments were done in triplicate and the data are mean \pm SD of three independent experiments.

Results

CBX7 physically interacts with HDAC2 protein. To investigate the mechanisms by which the loss of CBX7 expression correlates with the highly malignant phenotype, we searched for CBX7 interacting proteins by performing a functional proteomic analysis. Therefore, we transiently transfected the HEK 293 cells with a V5-tagged CBX7 expression vector, immunoprecipitated the nuclear protein lysates with anti-V5 antibodies (Supplementary Fig. S1A), and fractionated the immunoprecipitated material on a 12% one-dimensional gel and stained with colloidal Coomassie (Supplementary Fig. S1B). After SDS-PAGE, single components of the immunoprecipitated complexes were analyzed by mass spectrometry (24). In Supplementary Table S1, we report some representative CBX7 interacting proteins. Among them, we focused our attention on HDAC2 because of its relevance in tumor biology (25). HDACs catalyze the removal of acetyl groups from core histones and, because of their ability to induce local condensation of chromatin, are generally considered repressors of transcription.

To verify the CBX7/HDAC2 interaction *in vivo*, HEK 293 cells were transiently transfected with the V5-tagged CBX7 expression

vector. Protein lysates were immunoprecipitated with either anti-V5 or anti-HDAC2 antibodies and immunoblotted with both anti-V5 and anti-HDAC2 antibodies (Fig. 1A; Supplementary Fig. S1C). As shown in Fig. 1A, we detected the association between CBX7 and the endogenous HDAC2 protein, confirming that CBX7 and HDAC2 form complexes *in vivo*.

To further examine the specificity of this interaction, and to map the regions of CBX7 protein required for the binding to HDAC2, pull-down assays were done incubating total cell extracts deriving from HEK 293 cells, with the CBX7 recombinant protein fused to GST (GST-CBX7) and with two deletion mutants of CBX7: GST-CBX7-CHROMO (1-100 amino acids) and GST-CBX7-NOCHROMO (55-251 amino acids). As shown in Fig. 1B, HDAC2 interacts with both GST-CBX7 and GST-CBX7-NOCHROMO mutants but not with the GST alone or the GST-CBX7-CHROMO mutant. These results clearly show that the CBX7 chromodomain is not required for the interaction between CBX7 and HDCA2.

CBX7 inhibits HDAC activity. To evaluate the effects of the CBX7/HDAC2 interaction on the HDAC2 activity, nuclear extracts from HeLa and NPA cells were prepared and the ability of increasing amount of transfected CBX7 to modulate HDAC activity was tested using a HDAC activity assay. CBX7 expression significantly inhibited HDAC activity in a dose-dependent manner (the percentage of inhibition was 65.15% and 42.55% in HeLa and NPA cells, respectively, after the transfection of 10 μ g CBX7 expression vector; Fig. 2A and B). As positive control for HDAC inhibition, we used 250 mmol/L sodium butyrate, a strong HDAC inhibitory compound (26, 27). Nuclear extracts from NPA transfected with CBX7 were immunoprecipitated with anti-HDAC2 antibodies. Then, immunoprecipitated material was tested using a HDAC activity assay. As shown in Fig. 2C, CBX7 specifically inhibited HDAC2 activity.

CBX7 binds to the *E-cadherin* gene promoter. It has been recently shown that HDAC2 is involved in the repressive complex that silences the *E-cadherin* gene expression during tumor progression (28). *E-cadherin* is emerging as one of the caretakers of the epithelial phenotype because the loss of its expression has been shown to be a critical event of epithelial-to-mesenchymal transition (29, 30). Therefore, to evaluate whether CBX7 was able to bind the *E-cadherin* promoter *in vitro*, we performed an electrophoretic mobility shift assay. Nuclear extracts from HEK 293

cells transiently transfected with either V5-tagged CBX7 or empty vectors were incubated with a radiolabeled oligonucleotide corresponding to the *E-cadherin* promoter. As shown in Fig. 3A, the *E-cadherin* oligonucleotide forms a specific complex (indicated in the figure as A) with nuclear proteins of cells transfected with V5-tagged CBX7, which was not present in mock-transfected cells (compare lanes 1 and 2). Binding specificity was shown by incubating the nuclear extract with a 100-fold molar excess of unlabeled *E-cadherin* oligonucleotide (lanes 3 and 4).

Then, HEK 293 and HeLa cells were transiently transfected with HA-tagged CBX7 expression vector, tested by Western blotting for protein expression (Fig. 3B), crosslinked, and immunoprecipitated with anti-HA or IgG antibodies. Immunoprecipitation of chromatin was subsequently analyzed by semiquantitative PCR using primers spanning the region of the *E-cadherin* promoter (-300 bp upstream to +40 bp downstream to the TSS). Anti-HA antibodies precipitated this *E-cadherin* promoter region from HEK 293 and HeLa cells transfected with HA-tagged CBX7 protein. No immunoprecipitation was observed with IgG precipitates, and when primers for the control promoter *GAPDH* were used (Fig. 3B), indicating that the binding is specific for the *E-cadherin* promoter. Similar results were obtained when NPA cells were used (data not shown). These results indicate that CBX7 binds the *E-cadherin* promoter region *in vivo*.

Then, to investigate whether the physical interaction between CBX7 and HDAC2 takes place on the human *E-cadherin* promoter, we performed re-chromatin immunoprecipitation analysis. HEK 293 cells transiently transfected with HA-tagged CBX7 were crosslinked and immunoprecipitated with anti-HDAC2 antibodies. The anti-HDAC2 complexes were released, re-immunoprecipitated with anti-HA antibodies, and then analyzed by PCR. The results shown in Fig. 3C reveal that the antibodies against HA precipitate the *E-cadherin* promoter after their release from anti-HDAC2, indicating that CBX7 occupies this promoter region together with HDAC2. The reciprocal experiment provided comparable results (Fig. 3D). Taken together, these results indicate that CBX7 binds the human *E-cadherin* promoter *in vivo* and participates in the same DNA-bound complexes that contain HDAC2.

CBX7 positively regulates the *E-cadherin* promoter. To evaluate the effect of CBX7 expression on *E-cadherin* transcription, HEK 293 cells were transiently cotransfected with an expression

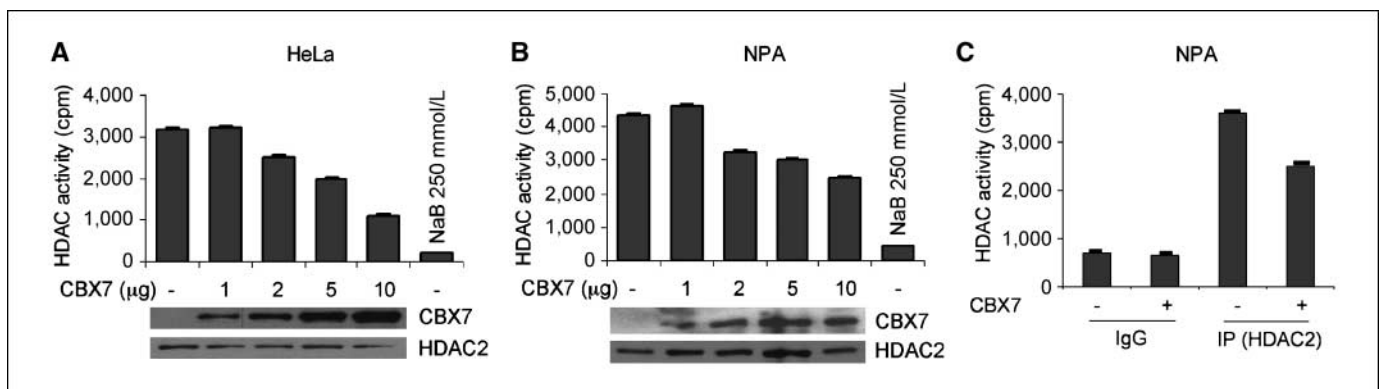


Figure 2. CBX7 inhibits HDAC activity. HeLa and NPA cells (A and B, respectively), transiently transfected with increasing amounts of CBX7 expression vector, were assayed for HDAC activity. Samples treated with sodium butyrate (NaB) were used as positive control of HDAC activity inhibition. Aliquots of the same lysates were immunoblotted with the indicated antibodies (bottom). C, NPA cells were transiently transfected with the CBX7 expression vector or the empty vector. Nuclear extracts were immunoprecipitated using anti-HDAC2 antibodies and assayed for HDAC activity. Mean \pm SD of three independent experiments.

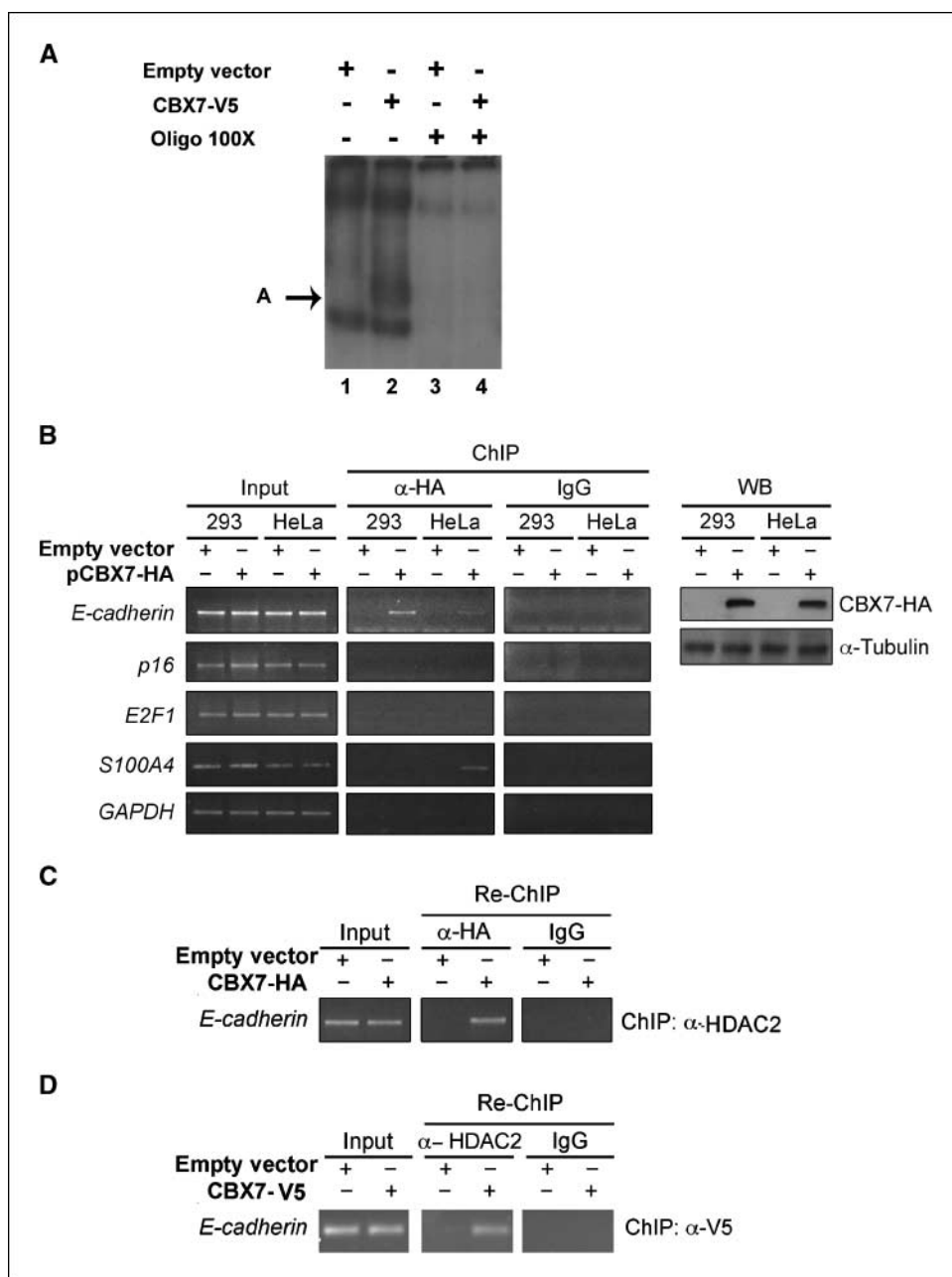


Figure 3. CBX7 binds to the *E-cadherin* gene promoter. **A**, electrophoretic mobility shift assay with nuclear extracts from HEK 293 cells transiently transfected with the V5-tagged CBX7 expression vector or the empty vector using the oligonucleotide spanning from nucleotide -70 to +54 of the human *E-cadherin* promoter as a probe. To assess the specificity of the binding, nuclear extracts were incubated in the presence of a 100-fold excess of unlabeled oligonucleotide used as competitor. **B**, chromatin immunoprecipitation (ChIP) assay using anti-HA antibodies in HEK 293 and HeLa cells transiently transfected with HA-tagged CBX7 or the empty vector. The associated DNA was amplified by PCR using primers specific for the human *E-cadherin* promoter, a region spanning from nucleotide -300 to +40 of the gene with respect to the TSS was used. IgGs were used as an immunoprecipitation control. **C**, re-chromatin immunoprecipitation experiments in which soluble chromatin immunoprecipitated with anti-HDAC2 was re-immunoprecipitated with anti-HA. IgG control refers to re-chromatin immunoprecipitation with anti-HA. **D**, re-chromatin immunoprecipitation experiments in which soluble chromatin immunoprecipitated with anti-V5 was re-immunoprecipitated with anti-HDAC2. IgG control refers to re-chromatin immunoprecipitation with anti-HDAC2.

vector encoding *CBX7* and with a reporter vector carrying the luciferase gene under the control of the *E-cadherin* promoter. As shown in Fig. 4A (top), CBX7 increases the transcriptional activity of the *E-cadherin* promoter in a dose-dependent manner. The same results were obtained on the NPA and TPC1 cell lines (Supplementary Fig. S2A). The treatment of cells with trichostatin A, a potent inhibitor of HDAC activity (31), cooperates with CBX7 to induce *E-cadherin* gene transcription (Fig. 4A, bottom). These results strongly suggest that CBX7 protein is involved in the *E-cadherin* gene transcription likely counteracting with the already known inhibitory effect of HDAC2 on this gene promoter.

To identify the region of CBX7 required for *E-cadherin* promoter activation, we constructed two CBX7 deletion mutants in the expression vector pCefl-HA: pCefl-HA-CBX7-CHROMO (1-100 amino acids) and pCefl-HA-CBX7-NOCHROMO (55-251 amino

acids). Transfection of the mutant pCefl-HA-CBX7-CHROMO, containing only the chromodomain, did not induce transcriptional activation of the *E-cadherin* promoter. Conversely, the mutant lacking the chromodomain, pCefl-HA-CBX7-NOCHROMO, induced a moderate activation of the *E-cadherin* promoter. Thus, these data indicate that chromodomain is not essential for the CBX7 transcriptional activity on the *E-cadherin* promoter (Fig. 4B).

Moreover, to show that the expression of *E-cadherin* is directly regulated by CBX7, we generated some clones of NPA cells (NPA 4-11 and NPA 5-11) in which *CBX7* cDNA was under the control of a tetracycline-regulated promoter. Western blot analysis (Fig. 4C, top) and quantitative RT-PCR experiment (Fig. 4C, bottom) show that the expression of CBX7 increases the levels of *E-cadherin* only after treatment with tetracycline.

To further confirm the role of CBX7 in the modulation of the *E-cadherin* gene, we evaluated the expression of the *E-cadherin* gene in the normal rat thyroid cell line PC Cl3 in which the synthesis of Cbx7 was suppressed by RNA interference. The knockdown of the *Cbx7* mRNA levels, observed at 48 h after treatment, resulted in the reduction of *E-cadherin* mRNA levels in comparison with the untreated cells or those treated with the nonsilencing control small interfering RNA (Fig. 4D).

To identify the regulatory elements essential for the activity of CBX7 on the *E-cadherin* promoter, we also tested some deletion mutants of the *E-cadherin* promoter: E-cadherin 601 and E-cadherin 211 (20, 21). Activation of *E-cadherin* promoter by CBX7 protein was maintained on full-length and -601 mutants of *E-cadherin* promoter. Conversely, the -211 mutant, which lacks a portion of -70/+54 sequence (able to bind CBX7), was not activated by CBX7 protein (Supplementary Fig. S2B).

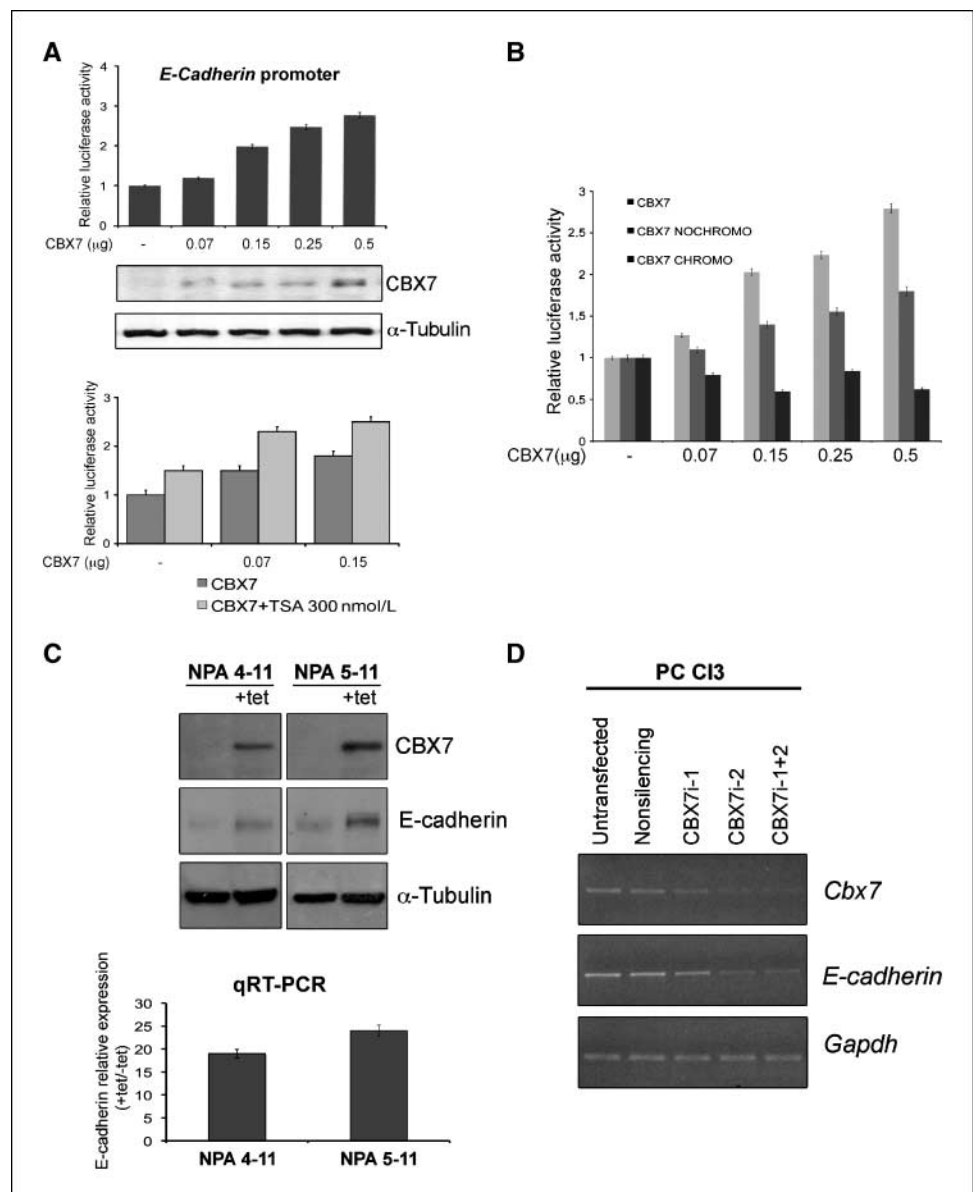
CBX7 expression results in increased histone acetylation of the *E-cadherin* promoter. During the last years, chromatin

remodeling and histone modifications have emerged as the main mechanisms in the control of gene expression and the connection between DNA methylation and histone deacetylation in the silencing of genes has been established (32–37).

Because we have shown previously that CBX7 (a) interacts with HDAC2 on the human *E-cadherin* promoter, (b) increases the transcriptional activity of the *E-cadherin* promoter in a dose-dependent manner, and (c) reduces the activity of HDACs, we hypothesized that the positive effect on *E-cadherin* activation by CBX7 may be due to its ability to reduce the HDAC activity on the *E-cadherin* promoter. Therefore, we have evaluated the lysine acetylation of histone tails at the *E-cadherin* promoter.

HEK 293 cells were transiently transfected with V5-tagged CBX7 expression vector or empty vector. Then, the cells were crosslinked and DNA-chromatin was immunoprecipitated with anti-H3 or anti-H4 acetylated or IgG antibodies. The immunoprecipitated chromatin was subsequently analyzed by quantitative PCR using primers spanning the region of the *E-cadherin* promoter

Figure 4. CBX7 enhances *E-cadherin* promoter activity. *A, top*, dose-response analysis of increasing amounts of CBX7 on the *E-cadherin* luciferase-reporter vector transiently transfected into HEK 293 cells. Western blot analysis confirmed the increasing amounts of CBX7 expression. α -Tubulin expression served as a control of equal protein loading. *Bottom*, dose-response analysis of increasing amounts of CBX7 on the *E-cadherin* luciferase-reporter vector transiently transfected into HEK 293 cells treated or not with 300 nmol/L of HDAC inhibitor trichostatin A (TSA). *B*, dose-response analysis of increasing amounts of CBX7 and the two CBX7-deletion mutants (schematically illustrated in Fig. 1B) on the *E-cadherin* luciferase-reporter vector transiently transfected into HEK 293 cells. *C, top*, Western blot analysis of CBX7 and E-cadherin expression in the NPA cell clones 4-11 and 5-11 treated or not with tetracycline. The treatment with tetracycline (+tet) was indicated on the top. α -Tubulin expression served as a control of equal protein loading. *Bottom*, quantitative RT-PCR (qRT-PCR) analysis of E-cadherin expression in the same NPA cell clones. The relative expression indicates the relative change in E-cadherin expression levels between treated cells versus the untreated ones, assuming that the value of E-cadherin expression in the untreated cells is equal to 1. *D*, *Cbx7* and *E-cadherin* gene expression was evaluated by RT-PCR in rat PC Cl3 cells after treatment with small interfering RNA against rat *Cbx7*. The expression of *GAPDH* was used to normalize the amounts of RNAs used in the experiment.



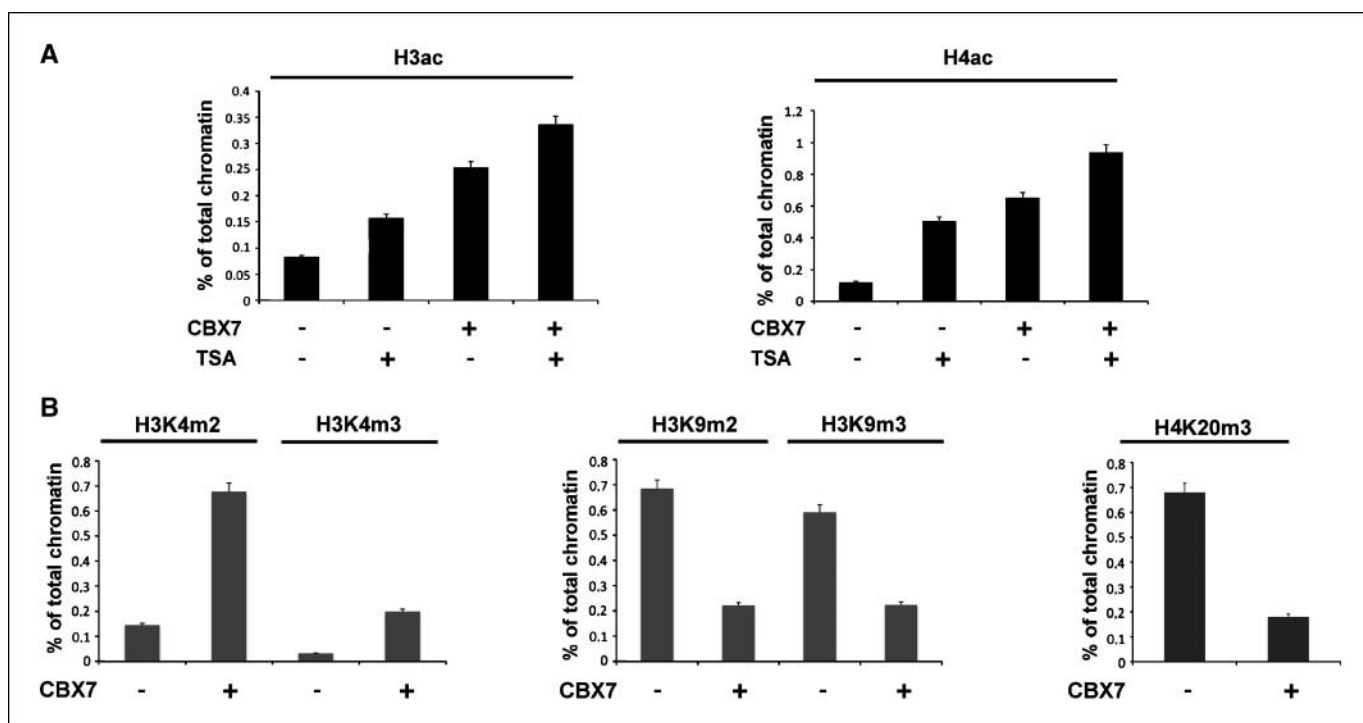


Figure 5. Analysis of the histone code modifications of the human *E-cadherin* promoter. *A*, HEK 293 cells transiently transfected with V5-tagged CBX7 expression or empty vectors, and treated or not with trichostatin A for 24 h, were subjected to chromatin immunoprecipitation using anti-acetyl histone H3 (*H3ac*; left) and anti-acetyl histone H4 (*H4ac*; right) and analyzed by quantitative RT-PCR for the *E-cadherin* promoter. *B*, HEK 293 cells transiently transfected with V5-tagged CBX7 expression or empty vectors were subjected to chromatin immunoprecipitation using anti-H3K4m2 and anti-H3K4m3 (left), anti-H3K9m2 and anti-H3K9m3 (middle), and anti-H4K20m3 (right) and analyzed by quantitative RT-PCR for the *E-cadherin* promoter.

(-70 bp upstream to +54 bp downstream to the TSS; ref. 38). As shown in Fig. 5A, higher amounts of H3 and H4 acetylated tails were detected in the *E-cadherin* promoter in the cells transfected with CBX7, with respect to those detected in mock-transfected cells, indicating an increased histone acetylation in CBX7-transfected cells, likely due to the ability of CBX7 to reduce HDAC activity. We also treated the cells, transfected or not with CBX7, with trichostatin A to verify the HDAC activity on H3 and H4 tails. As shown in the same figure, there were higher amounts of H3 and H4 acetylated tails in CBX7-transfected samples treated with trichostatin A than in untreated cells. These results indicate that CBX7 protein regulates the *E-cadherin* expression by modifying histone acetylation at its promoter, likely reducing HDAC activity.

Increased methylation of H3K4 and decreased methylation of H3K9 and H4K20 in CBX7-transfected cells. Lysine methylation can have different effects depending on which residue is modified: methylation of H3K4 and H3K36 is generally associated with transcribed chromatin; in contrast, methylation of H3K9, H3K27, and H4K20 generally correlates with gene repression (38). Therefore, we have evaluated the lysine methylation status of histone tails of *E-cadherin* promoter in presence or absence of CBX7.

HEK 293 cells were transiently transfected with V5-tagged CBX7 or empty vectors and crosslinked, and DNA-chromatin was immunoprecipitated with anti-H3K4m2, anti-H3K4m3, anti-H3K9m2, anti-H3K9m3, and anti-H4K20m3 or IgG antibodies. The immunoprecipitated chromatin was subjected to PCR with specific primers for the *E-cadherin* promoter region (-70/+54).

Higher amounts of chromatin immunoprecipitated for H3K4m2 and H3K4m3 were observed in the CBX7-transfected cells

compared with the control ones, indicating that this lysine is methylated in a higher proportion in CBX7-transfected cells with respect to that observed in control cells. Conversely, in the case of chromatin immunoprecipitated for the H3K9m2, H3K9m3, and H4K20m3, higher amounts of chromatin were detected in control cells, indicating that these sites were methylated at a higher level in the control cells versus CBX7-transfected cells (Fig. 5B). These data indicate that CBX7 is able to alter the methylation status of specific lysines of *E-cadherin* promoter, promoting the transcriptional activity of *E-cadherin* promoter.

CBX7 and *E-cadherin* expression levels are correlated in human thyroid carcinomas. *E-cadherin* down-regulation, due to epigenetic mechanisms, including transcriptional repression, also mediated by HDAC activity, and promoter hypermethylation is a frequent event during human cancer progression (39, 40). Because previous experiments showed that CBX7 expression was lost in most advanced thyroid cancers, we hypothesized the down-regulation of *E-cadherin* as a possible mechanism by which loss of CBX7 is involved in advanced stages of thyroid carcinogenesis. This hypothesis was also supported by recent results showing a role of polycomb repressive complex 1/2 in the regulation of *E-cadherin* expression (41).

Therefore, we analyzed *CBX7* and *E-cadherin* mRNA levels in human thyroid carcinomas of different histotypes (Fig. 6A). *CBX7* and *E-cadherin* mRNA levels were drastically reduced in anaplastic thyroid carcinoma, whereas just a weak decrease was observed for both genes in papillary thyroid carcinoma. The epithelial-to-mesenchymal transition in our tumor samples was also confirmed by the increased N-cadherin expression (Fig. 6A).

We found a positive statistical correlation between CBX7 and E-cadherin expression in human thyroid carcinomas as shown in Fig. 6B. We also compared CBX7 and E-cadherin at protein level, by immunohistochemical analysis, confirming that E-cadherin protein expression parallels that of CBX7 (Fig. 6C).

Because hypermethylation of the *E-cadherin* promoter has been postulated to play a critical role in the loss of E-cadherin expression and has been reported previously in other cancers, we decided to investigate the DNA methylation status of *E-cadherin* promoter (42). We analyzed DNA methylation status

of 26 CpG sites located in a 368-bp region spanning the *E-cadherin* gene TSS (Fig. 6D, inset) on 16 papillary thyroid carcinomas, 15 follicular variants of papillary thyroid carcinomas, 4 anaplastic thyroid carcinomas, and 4 normal thyroid tissue samples. A very low level of methylation was present in both normal and tumor samples, with the exception of only one anaplastic thyroid carcinoma sample in which a high degree of methylation was detected (Fig. 6D).

Therefore, epigenetic mechanisms, other than hypermethylation of the *E-cadherin* promoter, have a critical role in the down-regulation of E-cadherin expression.

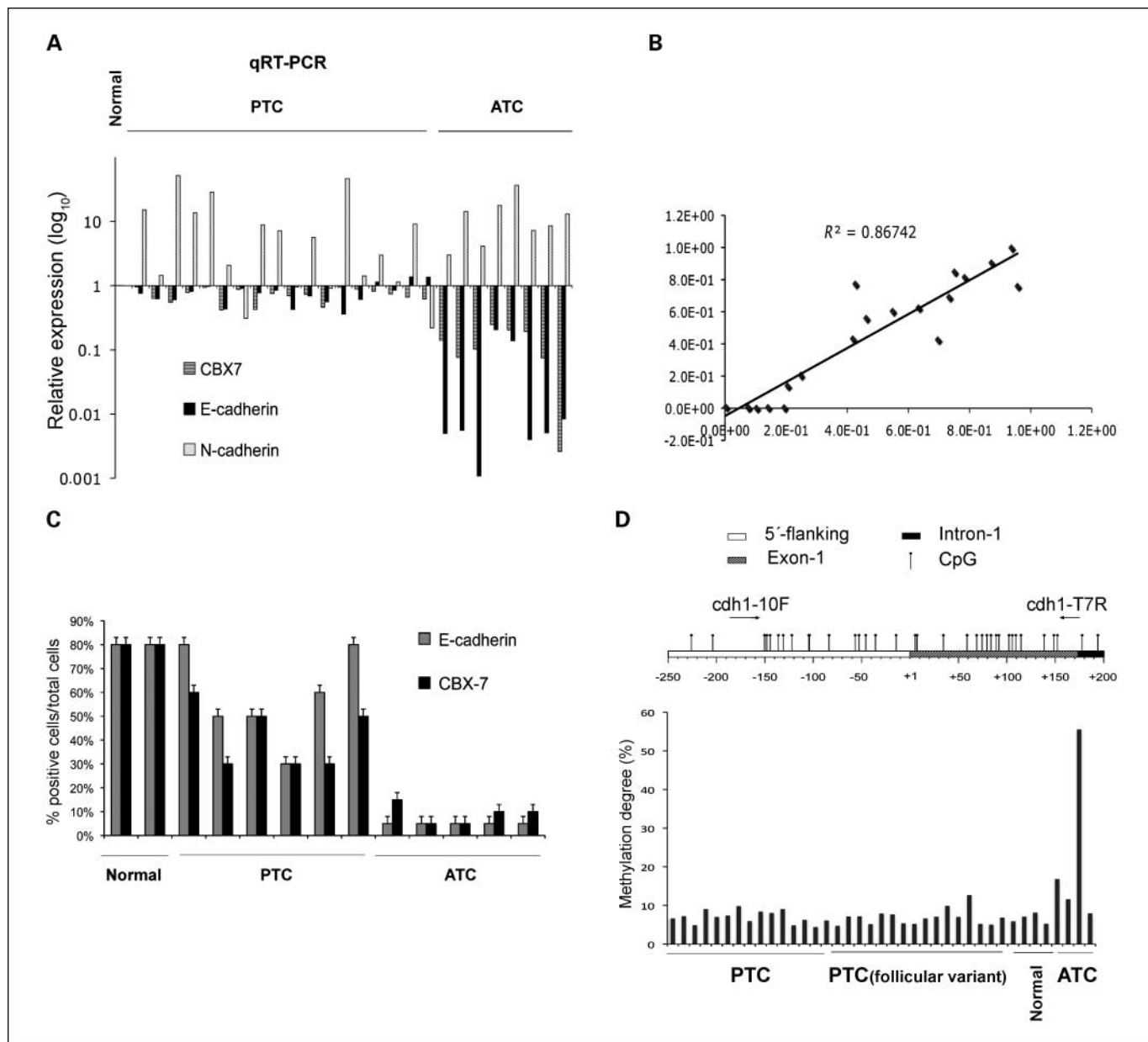


Figure 6. *CBX7* and *E-cadherin* gene expression levels are correlated in human thyroid carcinomas. *A*, *CBX7*, *E-cadherin*, and *N-cadherin* gene expression in thyroid tumor samples was analyzed by quantitative RT-PCR. Relative expression indicates the change in expression levels between tumor and normal samples, assuming that the value of each normal sample is equal to 1. *B*, positive statistical correlation between *CBX7* and *E-cadherin* expression in human thyroid carcinomas analyzed in *A*. R^2 , Pearson correlation coefficient. *C*, immunohistochemical analysis of normal and tumor samples stained with anti-*CBX7* and anti-*E-cadherin* antibodies. The percentage of positive cells for the staining/total number of cells was reported. *D*, top, positions of the primers used for amplifications of the region spanning from nucleotide -200 to +200 of *E-cadherin* with respect to the TSS; bottom, average methylation degree of 26 CpG sites at *E-cadherin* promoter in human thyroid carcinomas. *PTC*, papillary thyroid carcinoma; *ATC*, anaplastic thyroid carcinoma.

Discussion

Our group has reported previously that *CBX7* gene is drastically down-regulated in thyroid carcinomas and its expression progressively decreases with malignant grade and neoplastic stage (8). These data suggest that the loss of *CBX7* expression may be strictly correlated with the acquisition of invasiveness accompanied by the loss of the epithelial features and the gain of a mesenchymal phenotype, a process known as epithelial-to-mesenchymal transition. E-cadherin is a main component of the cell-cell adhesion junctions that plays a principal role in maintaining normal epithelial cell morphology, therefore emerging as one of the caretakers of the epithelial phenotype. In most cancers, E-cadherin down-regulation during neoplastic progression occurs by epigenetic mechanisms, including transcriptional repression, in some cases mediated by HDAC activity (40), and hypermethylation of the promoter (42). Only in a few cases mutations have been found in the *E-cadherin* gene leading to the absence or the expression of a nonfunctional protein (29). For this reason, we evaluated E-cadherin expression in human thyroid carcinomas of different histotypes: an evident correlation was found between *CBX7* and E-cadherin expression levels in human thyroid carcinomas, both being drastically down-regulated in anaplastic thyroid carcinomas in comparison with the normal thyroid tissue. Interestingly, no hypermethylation of *E-cadherin* promoter was observed in thyroid carcinomas. Therefore, we have hypothesized a role for *CBX7* as a transcriptional repressor of E-cadherin. We have shown that *CBX7* binds to *E-cadherin* gene promoter *in vitro* by electrophoretic mobility shift assay and *in vivo* by chromatin immunoprecipitation and is able to positively regulate the activity of *E-cadherin* promoter. At the same time, a proteomic approach, aimed to unravel the mechanism by which the loss of *CBX7* expression is involved in cancer progression, has identified HDAC2 among the *CBX7* interacting proteins. HDACs regulate the expression and activity of numerous proteins involved in both cancer initiation and cancer progression, inducing a nonpermissive chromatin conformation that prevents the transcription of genes encoding proteins involved in tumorigenesis. HDACs are often overexpressed in many tumors (25).

Here, we show that *CBX7* physically interacts with HDAC2 protein inhibiting its activity. Chromatin immunoprecipitation shows that both HDAC2 and *CBX7* bind the *E-cadherin* promoter. We also show the ability of *CBX7* to positively regulate E-cadherin expression by interacting with HDAC2 and inhibiting its activity on the *E-cadherin* promoter. Further, we show that, in the presence of the *CBX7* protein, there is an increased histone acetylation of the *E-cadherin* promoter, validating our hypothesis that *CBX7* recruits HDAC2 on the *E-cadherin* promoter. Moreover, we showed modifications in the histone methylation state on the *E-cadherin* promoter in the cells transfected with *CBX7* confirming a relationship between acetylation and DNA methylation (36).

It is noteworthy that, among *CBX7* interacting proteins, we have also identified an arginine methylation protein that can have a regulator effect on HDACs activity, because a cross-talk between histone acetylation and arginine methylation has also been observed (43). In fact, histone deacetylation is a prerequisite for PRMT5-mediated H3 and H4 arginine methylation, whereas histone acetylation enhances H3R17 methylation by PRMT4 (44–46).

In conclusion, here we propose a novel pathway regulating the progression step of carcinogenesis in which the *CBX7* protein, the loss of expression of which correlates with a highly malignant phenotype, is a key molecule. Indeed, our results indicate that the loss of *CBX7* expression contributes to cancer progression by down-regulating E-cadherin expression because of the lack of its inhibitory effect on HDAC activity on the *E-cadherin* promoter.

Disclosure of Potential Conflicts of Interest

No potential conflicts of interest were disclosed.

Acknowledgments

Received 4/27/09; revised 6/23/09; accepted 6/25/09; published OnlineFirst 8/25/09.

Grant support: Associazione Italiana Ricerca sul Cancro.

The costs of publication of this article were defrayed in part by the payment of page charges. This article must therefore be hereby marked *advertisement* in accordance with 18 U.S.C. Section 1734 solely to indicate this fact.

We thank Dr. E.R. Fearon for the *E-cadherin*-luciferase reporter construct and Konstantina Vergadou (Scientific Communication) for editing the text.

References

- Gil J, Bernard D, Martinez D, Beach D. Polycomb CBX7 has a unifying role in cellular lifespan. *Nat Cell Biol* 2004; 6:67–72.
- Bernard D, Martinez-Leal JF, Rizzo S, et al. CBX7 controls the growth of normal and tumor-derived prostate cells by repressing the *Ink4a/Arf* locus. *Oncogene* 2005;24:5543–51.
- Scott CL, Gil J, Hernando E, et al. Role of the chromobox protein CBX7 in lymphomagenesis. *Proc Natl Acad Sci U S A* 2007;104:5389–94.
- Schuettengruber B, Chourrout D, Vervoort M, Leblanc B, Cavalli G. Genome regulation by polycomb and trithorax proteins. *Cell* 2007;128:735–45.
- Wu JI, Lessard J, Crabtree GR. Understanding the words of chromatin regulation. *Cell* 2009;136:200–6.
- Bernstein E, Duncan EM, Masui O, Gil J, Heard E, Allis CD. Mouse polycomb proteins bind differentially to methylated histone H3 and RNA and are enriched in facultative heterochromatin. *Mol Cell Biol* 2006;26:2560–9.
- Lund AH, van Lohuizen M. Polycomb complexes and silencing mechanisms. *Curr Opin Cell Biol* 2004; 16:239–46.
- Pallante P, Federico A, Berlingieri MT, et al. Loss of the *CBX7* gene expression correlates with a highly malignant phenotype in thyroid cancer. *Cancer Res* 2008;68: 6770–8.
- Hedinger C, Williams ED, Sobin LH. The WHO histological classification of thyroid tumours: a commentary on the second edition. *Cancer* 1989;63:908–11.
- Kondo T, Ezat S, Asa SL. Pathogenetic mechanisms in thyroid follicular-cell neoplasia. *Nat Rev Cancer* 2006; 6:292–306.
- Pallante P, Berlingieri MT, Troncone G, et al. UbcH10 overexpression may represent a marker of anaplastic thyroid carcinomas. *Br J Cancer* 2005;93:464–71.
- Fusco A, Berlingieri M, Di Fiore PP, Portella G, Grieco M, Vecchio G. One- and two-step transformations of rat thyroid epithelial cells by retroviral oncogenes. *Mol Cell Biol* 1987;7:3365–70.
- Fedele M, Visone R, De Martino I, et al. HMGA2 induces pituitary tumorigenesis by enhancing E2F1 activity. *Cancer Cell* 2006;9:459–71.
- Pierantoni GM, Esposito F, Giraud S, Bienvenut WV, Diaz JJ, Fusco A. Identification of new high mobility group A1 associated proteins. *Proteomics* 2007;7:3735–42.
- Fedele M, Fidanza V, Battista S, et al. Haploinsufficiency of the *Hmga1* gene causes cardiac hypertrophy and myelo-lymphoproliferative disorders in mice. *Cancer Res* 2006;66:2536–43.
- Livak KJ, Schmittgen T. Analysis of relative gene expression data using real-time quantitative PCR and the 2^{-ΔΔC(T)}. *Method Methods* 2001;25:402–8.
- Frank SR, Schroeder M, Fernandez P, Taubert S, Amati B. Binding of c-Myc to chromatin mediates mitogen-induced acetylation of histone H4 and gene activation. *Genes Dev* 2001;15:2069–82.
- Dignam JD, Lebovitz RM, Roeder RG. Accurate transcription initiation by RNA polymerase II in a soluble extract from isolated mammalian nuclei. *Nucleic Acids Res* 1983;11:1475–89.
- Pierantoni GM, Rinaldo C, Esposito F, Mottolise M, Soddu S, Fusco A. High mobility group A1 (HMGA1) proteins interact with p53 and inhibit its apoptotic activity. *Cell Death Differ* 2006;13:1554–63.
- Ji X, Woodard AS, Rimm DL, Fearon ER. Transcriptional defects underlie loss of E-cadherin expression in breast cancer. *Cell Growth Differ* 1997;8:773–8.
- Hajra KM, Ji X, Fearon ER. Extinction of E-cadherin expression in breast cancer via a dominant repression pathway acting on proximal promoter elements. *Oncogene* 1999;18:7274–9.
- Li LC, Dahiya R. MethPrimer: designing primers for methylation PCRs. *Bioinformatics* 2002;18:1427–31.
- Ehrlich M, Nelson M, Stanssens P, et al. Quantitative high-throughput analysis of DNA methylation patterns

- by base-specific cleavage and mass spectrometry. *Proc Natl Acad Sci U S A* 2005;102:15785–90.
24. Shevchenko A, Keller P, Scheffele P, Mann M, Simons K. Identification of components of trans-Golgi network-derived transport vesicles and detergent-insoluble complexes by nano-electrospray tandem mass spectrometry. *Electrophoresis* 1997;18:2591–600.
 25. Glozak MA, Seto E. Histone deacetylases and cancer. *Oncogene* 2007;26:5420–32.
 26. Kruh J. Effects of sodium butyrate, a new pharmacological agent, on cells in culture. *Mol Cell Biochem* 1982;42:65–82.
 27. Rada-Iglesias A, Enroth S, Ameur A, et al. Butyrate mediates decrease of histone acetylation centered on transcription start sites and down-regulation of associated genes. *Genome Res* 2007;17:708–19.
 28. Peinado H, Ballestar E, Esteller M, Cano A. Snail mediates E-cadherin repression by the recruitment of the Sin3A/histone deacetylase 1 (HDAC1)/HDAC2 complex. *Mol Cell Biol* 2004;24:306–19.
 29. Thiery JP. Epithelial-mesenchymal transitions in tumour progression. *Nat Rev Cancer* 2002;2:442–54.
 30. Thiery JP, Sleeman J. Complex networks orchestrate epithelial-mesenchymal transitions. *Nat Rev Mol Cell Biol* 2006;7:131–42.
 31. Ou JN, Torrisani J, Unterberger A, et al. Histone deacetylase inhibitor trichostatin A induces global and gene-specific DNA demethylation in human cancer cell lines. *Biochem Pharmacol* 2007;73:1297–307.
 32. Marks P, Rifkind RA, Richon VM, et al. Histone deacetylases and cancer: causes and therapies. *Nat Rev Cancer* 2001;1:194–202.
 33. Bolden JE, Peart M, Johnstone RW. Anticancer activities of histone deacetylase inhibitors. *Nat Rev Drug Discov* 2006;5:769–84.
 34. Minucci S, Pelicci PG. Histone deacetylase inhibitors and the promise of epigenetic (and more) treatments for cancer. *Nat Rev Cancer* 2006;6:38–51.
 35. Smith CL. A shifting paradigm: histone deacetylases and transcriptional activation. *Bioessays* 2008;30:15–24.
 36. Kouzarides T. Chromatin modifications and their function. *Cell* 2007;128:693–705.
 37. van Leeuwen F, van Steensel B. Histone modifications: from genome-wide maps to functional insights. *Genome Biol* 2005;6:113.
 38. Li B, Gogol M, Carey M, Lee D, Seidel C, Workman JL. The role of chromatin during transcription. *Science* 2007;316:1050–4.
 39. Koizume S, Tachibana K, Sekiya T, Hirohashi S, Shiraiishi M. Heterogeneity in the modification and involvement of chromatin components of the CpG island of the silenced human *CDH1* gene in cancer cells. *Nucleic Acids Res* 2002;30:4770–80.
 40. Peinado H, Portillo F, Cano A. Transcriptional regulation of cadherins during development and carcinogenesis. *Int J Dev Biol* 2004;48:365–75.
 41. Cao Q, Yu J, Dhanasekaran SM, et al. Repression of E-cadherin by the polycomb group protein EZH2 in cancer. *Oncogene* 2008;27:7274–84.
 42. Hajra KM, Fearon E. Cadherin and catenin alterations in human cancer. *Genes Chromosomes Cancer* 2002;34:255–68.
 43. Huang S, Litt M, Felsenfeld G. Methylation of histone H4 by arginine methyltransferase PRMT1 is essential *in vivo* for many subsequent histone modifications. *Genes Dev* 2005;19:1885–93.
 44. Pal S, Vishwanath S, Erdjument-Bromage H, Tempst P, Sif S. Human SWI/SNF-associated PRMT5 methylates histone H3 arginine 8 and negatively regulates expression of ST7 and NM23 tumor suppressor genes. *Mol Cell Biol* 2004;24:9630–45.
 45. Pal S, Yun R, Datta A, et al. mSin3A/histone deacetylase 2- and PRMT5-containing Brg1 complex is involved in transcriptional repression of the Myc target gene *cad*. *Mol Cell Biol* 2003;23:7475–87.
 46. Kirmizis A, Santos-Rosa H, Penkett CJ, et al. Arginine methylation at histone H3R2 controls deposition of H3K4 trimethylation. *Nature* 2007;449:928–32.